Pressuremeter testing in Ruritania

A compilation of the results of ten tests in a variety of materials, selected to show what can be derived from careful pressuremeter testing

Reference: CIR 2001/11

Part 3 Appendices

CAMBRIDGE INSITU Ltd.
Little Eversden
Cambridge
ENGLAND
CB23 1HE

Tel:- (01223) 262361 Fax:- (01223) 263947 Email:- caminsitu@aol.com
Web site:- www.cambridge-insitu.com

PART 3 APPENDICES:

A. DESCRIPTION OF THE EQUIPMENT

1. The Mk VIIID Self Boring Pressuremeter
2. The Mk XD Self Boring Pressuremeter
3. The Weak Rock Self Boring Pressuremeter
4. The High Pressure Dilatometer
5. Electronics Interface Unit
6. Strain Control Unit
7. Pressure Control Panel
8. Data Logging / Analysis Software
9. Boring Equipment

B. THE CALIBRATION PROCEDURE

1. Scale Factors
2. Reference ('zero') outputs
3. Membrane stiffness
4. Instrument compliance
5. Membrane thinning
6. Displacement compliance
7. Instrument straightness
8. Repeatability
9. Table of measured scalar values
10. Table of membrane corrections

C. THE TEST PROCEDURE

1. Installing the probe
2. The expansion test
3. Logging rate
4. A typical test curve

D. INTERPRETATION OF PRESSUREMETER TESTS

1. Introduction
2. Analyses for expansion
3. Shear modulus
4. Creep
5. Analyses for the contraction

E. THE HOLDING TEST

1. The generation of excess pore pressures
2. The decay of excess pore pressures
3. Consolidation and Permeability
4. Practical considerations
5. Analysis procedure
6. The 'New method'

F. THE SELF BORING PERMEAMETER

1. Background
2. Comments

G. CONVERTING RAW DATA TO ENGINEERING UNITS

H. REFERENCES

APPENDIX A DESCRIPTION OF THE EQUIPMENT

1. The Mk VIIID Self Boring Pressuremeter

It is a probe about 83 millimetres in diameter and 1.2 metres long. Approximately 0.5m can be expanded by dry nitrogen or compressed air and a typical test will expand the instrument by 10%.

The expansion is monitored by three followers, conventionally referred to as 'strain arms' or more usually 'arms'. These are positioned at 120 degree intervals around the middle of the expanding test section. The arms are forced to follow the movements of the membrane by strain gauged leaf springs, and hence radial expansion is converted to an electrical output.

The Self Boring Pressuremeter without a Chinese lantern

The internal pressure is measured by a strain gauged cell within the instrument. A further two cells are attached to the membrane, 180 degrees apart, and these measure the changes in pore water pressure during the test.

The membrane covering the expanding portion of the instrument is in two parts. The inner layer, which is sealed, is made of polyurethane and is about 1.25mm thick. This inner skin is then covered by an outer layer, which because of its appearance when the instrument is inflated is known as a 'Chinese Lantern' (CHL). The CHL is made up of stainless steel strips bonded to a thin rubber skin; it has two main tasks - to take the frictional forces that occur when the instrument is being bored into the ground, and to provide some protection from inclusions that might otherwise puncture the inner membrane.

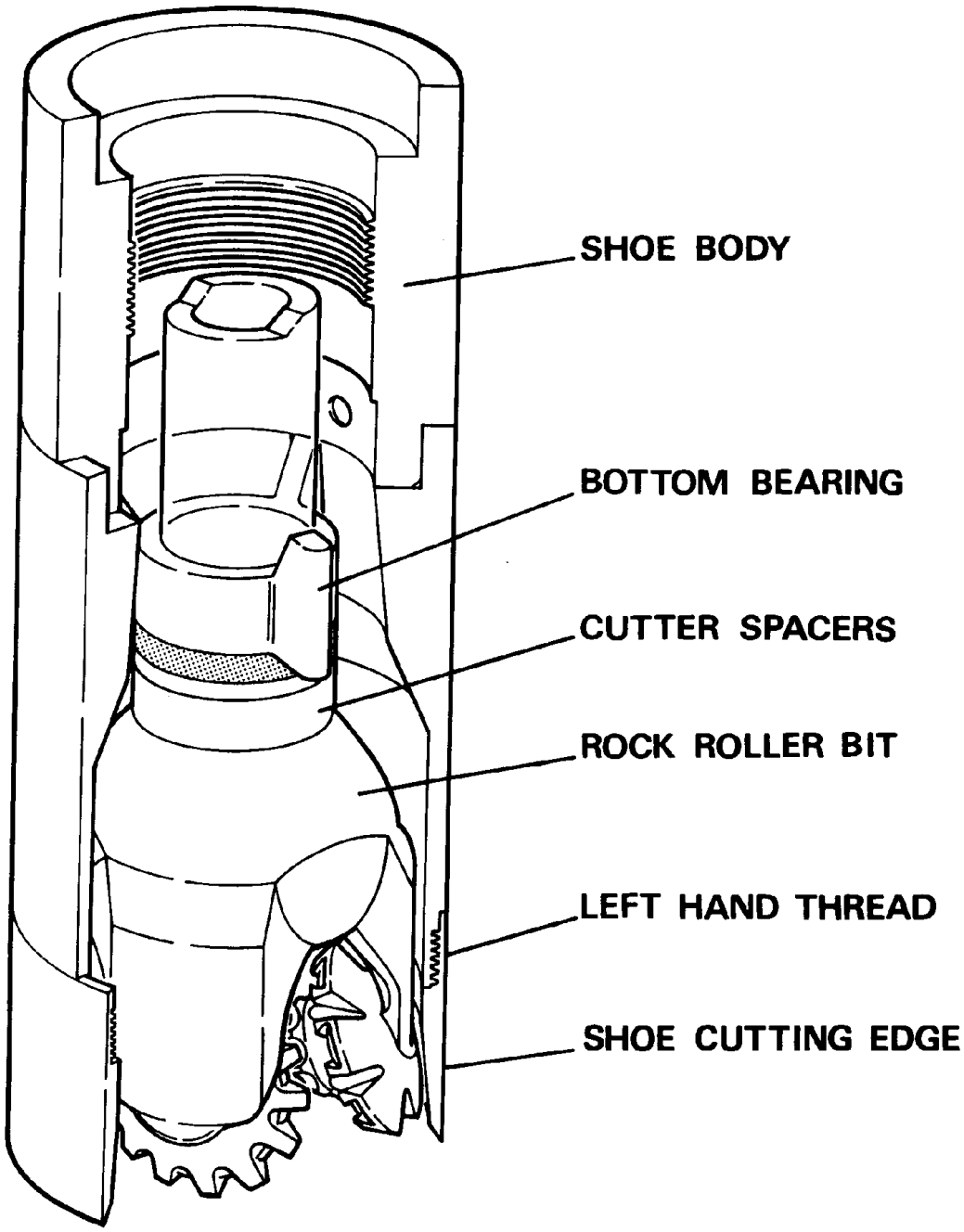

The foot of the instrument is fitted with a sharp edged internally tapered cutting shoe. When boring, the instrument is jacked into the ground, and the material being cut by the shoe is sliced into small pieces by a rotating cutting device.

The distance between the leading edge of the shoe and the start of the cutter is important and can be optimised for a particular material. If too close to the cutting edge the soil experiences some stress relief before being sheared. If the cutter is too far behind the shoe edge then the

instrument begins to resemble a close ended pile. In stiff materials the usual setting is flush with the cutting shoe edge. The cutting device takes many forms. In soft clays it is generally a small drag bit, in more brittle material a rock roller is often used. (see diagram on page 2)

The instrument is connected to the jacking system by a drill string. This is in two parts, an outer casing to transmit the jacking force and an inner rod which is rotated to drive the cutter device. The casing is smaller than the maximum instrument diameter and the drill string is extended in one metre lengths as necessary to allow continuous boring to take place.

The cut material is flushed back to the surface through the instrument annulus. Normally water is used but air and drilling muds can also be used if appropriate.

The self boring method has been well documented and a complete description of the instrument and its test can be found in the references.

There is a watertight compartment at the lower end of the probe which contains analogue and digital circuitry. All transducers in the probe are read once every five seconds, and the result is output as digital numbers in ASCII format via an RS232 compatible serial output. All the signal conditioning is carried out in the probe itself, so that the pressuremeter is unaffected by changes to external equipment including the cable.

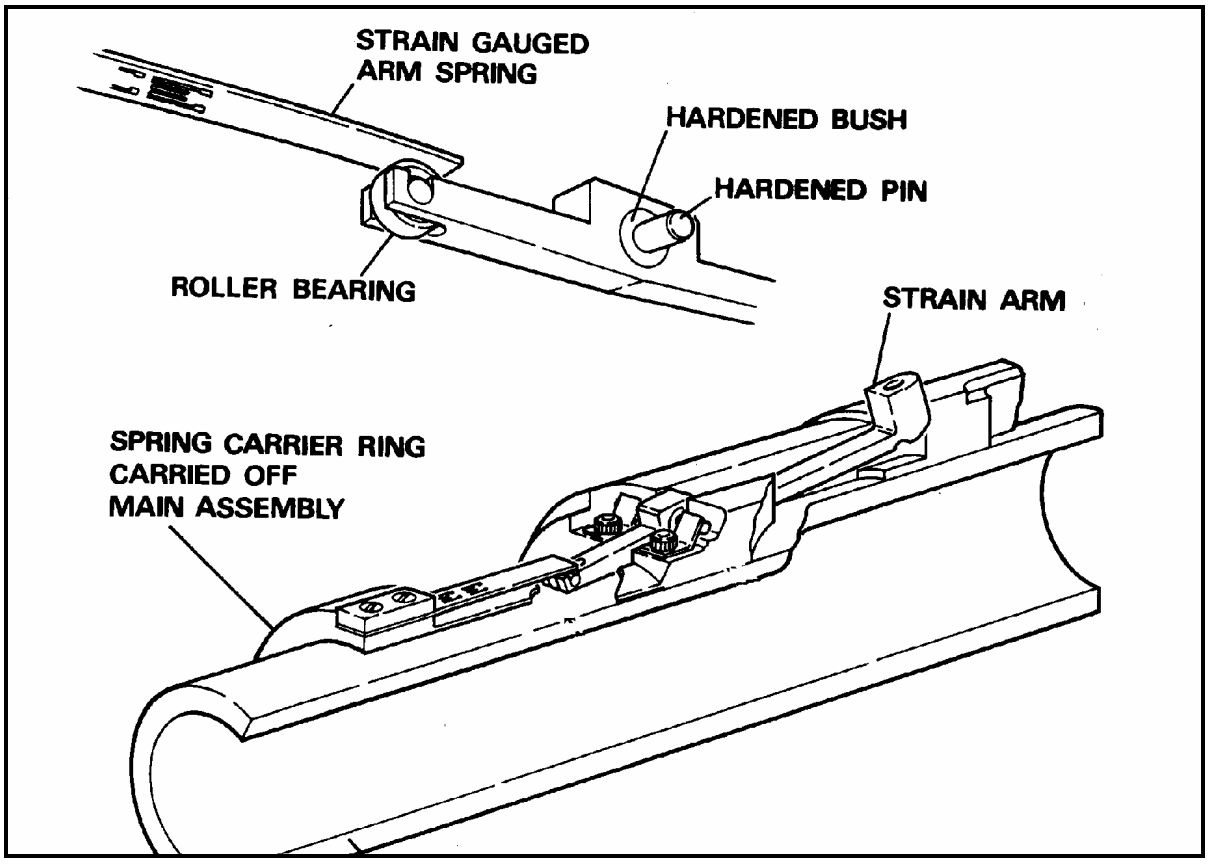

Strain arm configuration - a detailed view

2. The Mk XD Self Boring Pressuremeter

This is identical to the Mk VIIID, except it has six strain arms. As a direct consequence of having to read an extra three sensors on each dataline, its scan rate is slightly slower.

3. The Weak Rock Self Boring Pressuremeter

This is not a separate instrument but a conversion of the soft ground self boring pressuremeter – of either variety. The Chinese lantern and membrane are removed together with all associated parts. In their place is substituted a nitrile rubber membrane about 4mm thick which is a composite; the central part is plain rubber, but the ends are reinforced with kevlar strands so that the membrane is resistant to axial extrusion.

The rock machine uses a tougher Chinese lantern made from 0.5mm thick stainless steel strips curved to the form of the membrane but not bonded to a separate rubber sleeve as in the soft ground SBP. The new CHL is very effective at easing the skin friction associated with shearing heavily dilatant material, it also allows the pressuremeter to be used in gravelly materials that would wreck the standard instrument.

For most soft rock tests the cutting arrangement is very similar to the soft ground machine, but with the dimensions increased so that the cutting shoe shears a hole about 1% greater than the diameter over the expanding section.

This oversize is likely to be within the elastic range of the material, so that the effect is to introduce recoverable stress relief into the boring. The amount of relief is enough to minimise skin friction, and greatly increases the types of material which can be self bored. The system is especially effective at drilling into dense sand.

The crucial advantage of this arrangement is that at the foot of the instrument the machine is self boring in exactly the same manner as the soft ground probe. No flushing fluid comes into contact with the borehole wall. This gives a very high quality pre-bored type test. Allowance has to be made in the analysis for the stress relief, but the stiffness of the initial loading is similar to the slopes of unload/reload loops.

The disadvantage is that the point where the membrane first moves no longer necessarily indicates the insitu lateral stress. The analysis is therefore dependent on appropriate models of soil behaviour. The other major disadvantage used to be that there was no measurement made of excess pore water pressure; but it has now become possible to fit the cell caps in the usual way – even with the thicker membrane.

3. The High Pressure Dilatometer

The 95mm High Pressure Dilatometer (95HPD) is a pre-bored hole pressuremeter for testing a nominal 101mm diameter pocket. The instrument has an overall length of about 2 metres. The central third of the instrument is covered by a tough rubber membrane about 6mm thick and a 0.5mm thick Chinese Lantern – similar to that used on the weak rock SBP. The radial displacement of the inside boundary of the membrane is measured at six points equally distributed around the centre of the expanding section.

Figure 1 The basic HPD-MPX kit

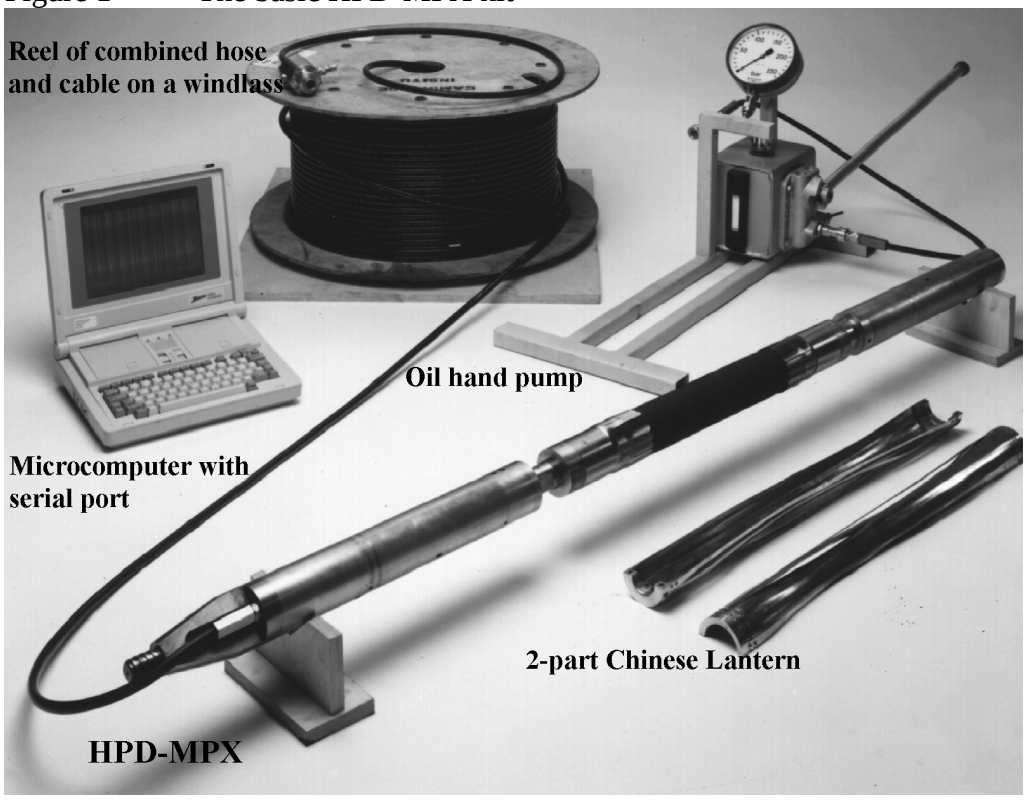

This displacement, and the pressure necessary to cause the movement, are continously monitored by strain gauged transducers contained within the instrument. Also within the instrument is the analogue and digital electronic circuitry necessary to condition the signals from the transducers. Every ten seconds a set of readings from all the measuring circuits are transmitted to the surface as an RS232 data stream which may be connected directly to the serial port of a microcomputer. Plotting these readings of displacement against pressure produces a loading curve for the material being tested. A number of mathematical analyses are available for translating this loading curve to fundamental strength and stiffness parameters for the ground.

Because the instrument has six strain arms there is some redundancy in the measurement of strain, and this enables the user to carry out a successful test even if one of the arms are defective. In order to give a similar level of reliability to the pressure measuring system a second pressure cell is included in the HPD-MPX, and its readings provide a check of the performance of the first transducer.

The HPD can apply up to 30MPa of pressure to the ground, and can expand from an initial diameter of 95mm to nearly 150mm. It will resolve movements of less than 1 micron and pressure changes of less than 1kPa. Hence although it was developed to test weak rock it can make a test at two extremes of ground conditions - stiff clays, which yield at pressures below 1MPa, and weak rock with a shear modulus greater than 4GPa.

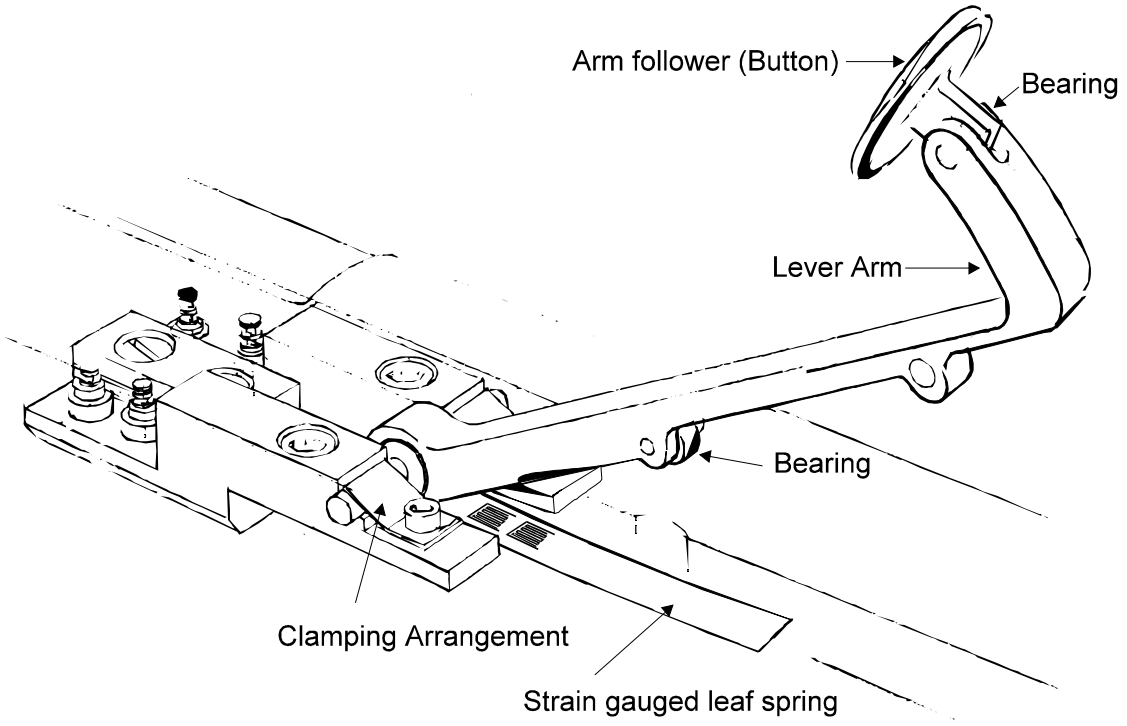

Figure 2 Displacement sensor of the 95mm HPD

The instrument is based on a smaller device (the 73mm HPD) that has had a long and successful history of site work and has been used worldwide. It is a development of an instrument invented by Dr J.M.O. Hughes in 1978. Although internally complex by the standards normally applied to instrumentation of this kind, it is reliable and robust, and the routine maintenance is straightforward. Because all the signal conditioning electronics is contained in the probe itself , the instrument is unaffected by external changes such as replacing the cable.

4. Electronic Interface Unit (EIU)

All the pressuremeter hardware is powered by a single 12 volt vehicle battery. The battery is connected to the EIU, which introduces some protection and distributes the power to a number of outlets, including one for the pressuremeter. The returning signals from the pressuremeter connect to the same socket. The digital signals pass through an opto-isolation circuit and are then made available on two identical sockets for connection to the serial port of a computer. There is also an analogue signal which represents the mean output of all the arms.
The unit has a panel meter which can be switched either to read the battery volts or to read the analogue signal.

5. Strain Control Unit

The Strain Control Unit (SCU) is a box of electronics that controls the rate at which gas is supplied to the self boring pressuremeter. It can be arranged to inflate the pressuremeter at a constant rate of strain (rather than the more usual constant rate of stress). From a soil mechanics point of view tests carried out at a constant rate of expansion are more desirable,

in that significant details of the shear stress/shear strain curve are suppressed or distorted during a stress controlled expansion.

The SCU uses specially modified magnetic valves which are controlled so as to operate in response to the strain signals returning from the instrument in the ground. Ten constant rates of strain are available between 0.1% per hour and 2% per minute, increasing and decreasing. In addition, the unit is able to hold the strain to a constant value for an indefinite period. This is useful when carrying out tests to determine the horizontal consolidation characteristics of clay. If at the end of a normal quick undrained expansion the strain is fixed whilst the excess pore water pressures are allowed to dissipate then a simple closed form solution leads to the derivation of C_h.

6. Pressure Control Panel

The Pressure Control Panel (PCP) consists of a hand operated regulator, two gauges and a number of valves.
It is used to monitor, and if necessary control, the gas supply to the Pressuremeter.
In general the panel is used to replace the Strain Control Unit in the event of a breakdown, but may be used instead of the SCU to give as smooth as possible a curve.

7. Data Logging / Analysis Software

Software developed by Cambridge Insitu is used to log the data during the test, and for analysing the results subsequently.
The logging software stores the incoming data, displays the pressure/expansion curve in real time, and provides a text file output of the test data in engineering units. This file is read directly by the analysis program, but can also be read by any of the common spreadsheet programs.
The analysis software provides routines which implement a number of standard analyses. The analyses are graphically driven, meaning that the analyst identifies and marks significant parts of the curve, either for slope or breakpoints. The final screen for the analysis is then output as hardcopy backup for the decisions made. For these tests, additional analysis work was implemented, using Microsoft Excel.

8. Boring Equipment

The SBPM is bored into its test positions using a rotary drill rig together with special equipment designed and manufactured by Cambridge Insitu. Reaction for the drilling is provided by the rotary rig. For shallow tests in soft ground a proprietary self-contained system may be used, normally relying on the casing for reaction.
The drilling is assisted by water flush passing down the rotating inner rods and returning between these and the stationary outer rods. Mud may be used, but it can affect the pore pressure cell response. In exceptional circumstances, air flush may be used – sometimes with larger diameter drill rods.
The drill rig is used to lower the SBPM down the hole and retrieve it after the test. The same rig is used to prepare the hole before self-boring, and deepen it afterwards.
For the HPD tests the drill rig cores ‘H’ size pockets, into which the probe is lowered – normally on the same rods used for the coring.

APPENDIX B THE CALIBRATION PROCEDURE

INTRODUCTION

There are eight aspects to the calibration of the self-boring pressuremeter:

1. Scale factors
2. Reference (‘zero’) outputs
3. Membrane stiffness
4. Instrument compliance
5. Membrane thinning
6. Displacement compliance
7. Instrument straightness
8. Repeatability (or how much effort should be devoted to calibrations)

After presenting the background to the calibration procedures the actual calibrations used on this contract are summarised, with plots presented of the more significant calibrations.

1 Scale Factors

The transducers in the pressuremeters are based on full bridge strain gauge circuits. Any such transducer produces an output dependent on the voltage being applied to it, the stress that is deflecting it and the amplification or buffering between it and the recording system.

The instrument contains electronic devices that provide a regulated voltage to the transducers and amplification of the resulting output signals. Because this electronic conditioning is a fixed part of the system it is not mentioned when presenting calibrations. The electrical output of the transducer, in volts, is quoted only as a function of the deflecting stress. This function is termed 'sensitivity' and gives the scale factor for deriving pressure or displacement from the transducer electrical output.

Although the output of the transducers is quoted in volts, the true output of the system is a digital data stream of ASCII encoded numbers which represent volts. This signal can be connected directly to the serial port of a small computer. All variables associated with producing the final digital output from the strain gauge signals are a function of the pressuremeter itself, and are independent of external changes such as replacing the cable.

When using the sensitivity calibrations to convert readings from volts into engineering units we make two important assumptions about this output; that it is linear and that the hysteresis is negligible. The calibration procedure needs to provide evidence that these assumptions are reasonable.

The displacement measuring system is often referred to as 'the arms'. The arms are calibrated by mounting a micrometer above each in turn and recording the output for a given deflection. When calibrating the instrument it is necessary to plot these readings for both an increasing and reducing deflection. The difference at a given point between increasing readings and reducing readings is a measure of the hysteresis. The worst case figure is noted, and steps are taken to reduce the friction in the system if the hysteresis is outside an acceptable limit - normally 0.5% of the sensitivity.

The slope of the best fit straight line through all the points is used to quote the arm sensitivity - as an output for a given deflection in units of millivolts per millimetre (mV/mm).

There is an additional output signal from the self boring probes which is an analogue representation of the average displacement signal. This is used in conjunction with a Strain Control Unit to control the gas pressure supplied to the instrument during a test. The average strain signal is separate from the pressuremeter digital outputs and is set to give a 0 to 600 millivolts change for a 0 to 10% increase in the instrument diameter. This implies that the sensitivities of the arms be broadly similar, within 5% of each other.

Positions for trimming resistors are provided in the instrument so that the sensitivity of the arm signals can be set. This is done by soldering high quality fixed resistors across the strain gauge bridge circuit. It is the only occasion when the absolute sensitivity of the strain gauge circuits is important.

For the pressure measuring circuits the maximum possible sensitivity is desirable, the only requirement is that the sensitivity be known and be linear and stable.

The sensitivity of the internal pressure cell is determined by placing a large metal cylinder over the membrane, and applying a known gas pressure to the inside of the instrument. The gas pressure being applied is measured by a standard test gauge.

As with the arms, the readings are plotted, the hysteresis noted, and the best fit straight line drawn through the plotted points.

The pore water pressure transducers are calibrated using a special calibration cylinder. This seals to the outside of the membrane and permits external pressure to be applied to the instrument. The output of the two transducers is then recorded and plotted as described above for the total pressure cell.

Pressure sensitivities are quoted in units of millivolts per MegaPascal.

2 Reference (‘zero’) outputs

The other parameter that the transducers have is a known output for an 'at rest' position. For the pressuremeter this is the value of the outputs produced by the circuits with atmospheric pressure on the inside of the instrument, and the displacement measuring system at the initial radius position. This is called a little misleadingly ‘zero’.

The absolute value of this figure is unimportant - it is not necessary or desirable that the figure be zero volts for the zero stress position, just that it be known. For practical purposes, as the analogue to digital converter can only output a number between -3.2767 and +3.2767, the ‘at rest’ readings tend be about minus one volt to allow the largest possibly range. There is one exception to this - the SBP requires that the average zero outputs of the arms be within plus or minus 50 millivolts of zero volts. This comes from the need to use a Strain Control Unit to carry out a test. The SCU uses the mean displacement signal from the instrument, and can only accommodate a limited offset from zero volts. Instruments which do not use an SCU to drive the expansion can ignore this restriction.

Adjustment positions are provided in the instrument for setting this 'zero' output.

It is normal to take zero readings both at ground level and also immediately prior to carrying out a test. A significant change between zero readings must be investigated. 'Significant' would mean a change of 30 millivolts from the last set of zero readings. It is not unusual for shifts of a few millivolts to occur from day to day. It is important that the zero readings be stable when viewed over a period of a few minutes.

3 Membrane stiffness

The membrane that is expanded by the instrument has its own initial tension requiring a finite pressure to move it. The readings measured by the stress cells need to be reduced by this pressure in order to determine the net stress being applied to the ground.

The term 'membrane' is used here to mean both the sealed elastic sleeve over the instrument that contains the pressure, and the rubber and stainless steel protective sheath that sometimes covers this. The sheath is known as the 'Chinese Lantern'.

The membrane correction has two components - the pressure to move the membrane from its position at rest on the instrument, and a second component that depends on the radial expansion.

The technique for obtaining the correction data is to pressurise the instrument in free air, using the same rate of expansion as would be applied during a test. The slope and the intercept on the pressure axis of the graph produced by this test give the membrane correction information for each arm.

Knowing that the membrane does not necessarily possess isotropic properties, it has been customary to derive a different set of figures for each arm position. However recent work indicates that an unconfined inflation in air exaggerates any variation in membrane properties; an average correction factor is more appropriate.

The membrane correction data is quoted as a pressure in kPa to move the membrane from its rest position together with a second pressure in units of kPa/mm representing the pressure increase necessary to maintain the inflation. Typical correction figures might be 20 kPa and 7.0 kPa/mm.

4 Instrument compliance

The instrument will deform as a consequence of the pressure being internally applied. Put simply, the instrument stretches. Because the displacement measuring system uses the body of the instrument as a reference, movements of the body are seen as apparent displacements of the membrane; some ingenuity is needed to immunise the displacement measuring system from this problem. This system compliance has implications for the measurement of shear modulus, and it can become a significant source of error when measuring very high modulus values.

There are a number of effects to consider but they are collectively determined using a single procedure. The correction figure which results is known somewhat inappropriately as 'membrane compression'.

The procedure which is normally suggested to obtain correction data for 'membrane compression' is to inflate the pressuremeter inside a number of cylinders of different bores; by comparing these known bores with the displacements actually obtained from the pressuremeter then a correction curve can be obtained. Because the correction has been assumed to be a function of membrane thickness, then it is expected that the effect reduces as the membrane thins. In other words, it is treated as a strain dependent variable, and a change in membrane means a new correction curve must be derived.

For the Cambridge family of pressuremeters real membrane compression, that is the membrane changing in thickness as a direct result of the pressure differential across it, is almost too small to be measurable. There are a number of other factors to consider of significantly greater magnitude than membrane compression.

Inflating the instrument inside a steel cylinder will in theory provide data on the magnitude of these effects. However a separate source of error, which is a function of the calibration procedure itself, then becomes apparent. The membrane is able to expand axially by a small amount, and as a result experiences a change in thickness which may not occur in the ground. Although steps can be taken to keep this axial movement to a minimum, it cannot be easily eliminated.

As a consequence of the poor fit of a calibration cylinder, and also of the relatively low coefficient of friction between the membrane and the steel by comparison with the membrane and the ground, the instrument will move about in the cylinder - its centre will not be the same as the centre of the cylinder. Only average radial movement can be derived from this calibration process, and it is not possible to obtain good data for each arm.

There is evidence that much of the correction is due to the Chinese lantern strips taking up the form of the cylinder, a process that would only occur in the ground if the material was good rock. This is the explanation for much of the initial curvature that occurs when an assembled probe is inflated inside a metal sleeve - it is a serious error to attempt to derive a correction factor from this part of the loading.

One approach is to take the membrane out of the correction loop by removing it altogether. A special cylinder is then fitted which seals to the body of the instrument, which is then pressurised. The displacement data which this test produces is used to determine the purely instrument related factors. Typically the data is reduced to a slope correction, on the order of
1 - 2 millimetres per GPa, and is a constant, being a function of the physical properties of the instrument.

The membrane is then fitted, and the instrument is expanded in the cylinder. The slope of the unloading path of the average radial displacement in this cylinder is used to obtain a value - it has been noted that the unloading path is much less unaffected by instrument movements.

The slopes obtained from the two methods are then compared. Typically they are the same within 1mm/GPa. This is to be expected. The bulk modulus of rubber is about 1GPa, and hence a membrane that is about 2mm in thickness will have a slope of 1mm/GPa. Further expansions inside other cylinders will not improve the quality of the correction so obtained.

To put the correction in context, a slope of 5mm/GPa (a relatively large correction) is equivalent to a modulus greater than 4GPa. Note that before the correction data is quoted the expansion of

the metal cylinders themselves must be removed from the data. One indication of the magnitude of the correction is that the instrument compliance correction is usually smaller than the calculated deflections of the calibration cylinder.

The correction data can be used in two ways. Applied as 'mm per GPa' it can be used to correct individual data points before analysis; this is our practice. It can also be quoted as a system modulus, and hence be applied subsequently to modulus parameters determined from analysing uncorrected data.

5 Membrane thinning

During a test the pressuremeter membrane changes in thickness as a consequence of being stretched. This change in thickness can be calculated by assuming to a first approximation that the cross-section area of the membrane remains constant. The calculation is incorporated into the program that converts raw data into engineering units.

Note that the term 'membrane' includes the stainless steel protective sheath, and that the measurement made by the arms is the radial distance to the inside of the membrane.

Definition of Terms

2a	is the I.D. of the membrane at rest
2b	is the O.D. over the membrane at rest
2c	is the I.D. of the membrane expanded
2r	is the O.D. over the membrane expanded
t	is the thickness of the stainless steel sheath strips
d	is the measured movement of the strain arm
E	is the actual expansion of the membrane

Calculation

At rest the cross-section area of rubber $= \pi(b-t)^2 - \pi a^2$

The expanded cross-section area of rubber $= \pi(r-t)^2 - \pi c^2$

Because the rubber is incompressible, these must be equal:-

therefore $(b-t)^2 - a^2 = (r-t)^2 - c^2$

Now:- $c = a + d$

and:- $r = b + E$

therefore $(b-t)^2 - a^2 = [(b+E)-t]^2 - (a+d)^2$

$$\therefore [(b-t)+E]^2 = (b-t)^2 - a^2 + (a+d)^2$$

$$= (b-t)^2 + d(2a+d)$$

$$\sqrt{(b-t)+E} = \sqrt{[(b-t)^2 + d(2a+d)]}$$

$$E = \sqrt{[(b-t)^2 + d(2a+d)]} - (b-t)$$

This is the form in which the calculation is commonly applied to the data, with **2a**, **2b** and **t** being known from the manufacturer's data, and **d** being the measurement made by the displacement sensors during the test. For a standard self boring pressuremeter fitted with a polyurethane membrane and Chinese lantern:-

2a	=	79.1 mm
2b	=	83.1 mm
t	=	0.18 mm

To apply the correction at a given expansion the *average* radius of the expanding membrane is calculated. This average is then entered into the equation and the ratio between the corrected average and the raw average is expressed as a scale factor (it turns out to be about 0.96 for an SBP at all expansions). The scale factor is then applied to the individual arm displacement outputs.

6 Displacement compliance

This is not so much a correction or calibration as a check on the mechanical performance of the self boring instrument.. Using the external pressurising cylinder gives information about small movements of the strain arms under load.

This mimics the situation in the ground where the instrument has the insitu lateral stress pressing against it prior to commencing the test. The presence of this stress can create small deflections of the strain arms. These deflections can create doubt about the precise point at which lift off is occurring.

Plotting the output of the strain arms as the pressure is removed during an external pressurisation test produces plots which can be compared with real test data. It will be observed that each arm has its own 'signature'. Steps should be taken to keep these small strain movements to a minimum by attending to the seating of the displacement follower.

It is possible that recognising these signatures can help with assessing the precise moment when membrane lift-off occurs. However in this calibration procedure there are no penalties for small instrument deflections - in the ground these movements will change the external pressure because soil has stiffness.

7 Instrument straightness

The self boring instrument can become bent during operations due to the large forces applied when it is being jacked down. Before bringing the instrument on site it is good practice to check that the instrument is straight (within a small tolerance). The method for doing this is to support the instrument at the points where the membrane is clamped, and then to rotate the instrument whilst the run out is observed at a number of points.

The instrument is never perfect, and it happens that frequently a consistent bias in the displacement system (especially in the vicinity of initial movement of the membrane) can be linked to a lack of straightness.

8 Repeatability (or how much effort should be devoted to calibrations)

Although it is important regularly to check the sensitivities of the strain gauge circuits, it is unusual for them to change markedly. Indeed it is common for the hysteresis to improve with use. 80% of the performance of a strain gauge bridge application can be predicted from its design; the calibration removes the uncertainty due to manufacturing tolerances, and can give early warning of impending problems in a particular circuit.

The pressuremeter test is concerned with making relative measurements, not absolute measurements. For example the SBP displacement measuring system will resolve movements of less than 0.5 microns over a range of 7 millimetres; the pressure measuring system will resolve changes of 0.5 kPa over a range of 5MPa. The HPD resolution is equally good. This resolution is considerably higher than can be seen with a standard micrometer or test gauge. To put it into context, 0.5 microns is approximately the wavelength of visible light. Obviously there is no practical possibility of checking by measurement a movement so small.

Hence the term 'calibrating' is inappropriate. What is done in practice is to check that the various sensors are linear over a number of relatively coarse steps or intervals. We assume that this linear behaviour will be true for very much smaller changes.

For this reason alone, without considering additional sources of error such as the skill of the operator carrying out the calibration, the accuracy of the standard used to derive this linearity is of secondary importance. We would expect successive calibrations on the same sensor to be within 2% and would question a difference greater than 5%.

We also ignore secondary sources of error in this assumption of linearity, such as temperature change. When critical measurements are being made during a test, for example when taking a reload loop, it is reasonable to assume that the temperature remains constant.

Using spreadsheet software to present the results of the calibrations for sensitivity has become common practice. One benefit of this is that slopes can be calculated by linear regression routines; this ensures that different operators given the same set of data will derive identical calibration factors. The calibrations are presented as a tabulation of transducer output against a known reference, with the linearity and hysteresis quoted for each calibration step.

If the ground is soft then membrane stiffness is important. If it is extremely stiff then correcting for instrument compliance is important. In between these two extremes the contribution of the imperfections of the machine to the derived parameters is negligible.

9 Table of derived scalar values

SBPM3 'Dougal'

DATE	ARM 1 mV/mm	ARM 2 mV/mm	ARM 3 mV/mm	TPC mV/MPa	PPC A mV/MPa	PPC B mV/MPa	Maximum pressure
23/12/05	264.7	293.9	299.6	493.2	232.5	237.3	400psi
03/02/06	265.1	294.3	298.2	488.5	-	240.3	600psi
07/03/06	264.0	295.4	297.2	493.9	231.4	237.6	"
07/06/06	262.1	293.2	295.9	492.0	231.3	237.2	"

HPD95 'Scotty'

Date	**Arm 1**	**Arm 2**	**Arm 3**	**Arm 4**	**Arm 5**	**Arm 6**	**TPC A**	**TPC B**
	mV/mm	mV/mm	mV/mm	mV/mm	mV/mm	mV/mm	mV/MPa	mV/MPa
07/02/06	120.9	119.9	120.3	120.3	118.7	120.3	79.1	80.6
11/04/06	121.9	122.3	122.8	120.5	120.5	122.5	80.1	82.3

Usually enough calibrations are given to demonstrate that they are stable and repeatable. An 'after job' calibration is included whenever possible.

10 Table of membrane calibrations

DATE	TEST	Membrane calibration		Membrane compression	COMMENTS
		kPa	kPa/mm	mm/GPa	
15/03/06	C0306T1	-	-	0.5	Typical SBPM
16/03/06	C0306T2	21	8	-	" "
10/04/06	S1004T06	63	5	-	Typical HPD, large expansion
28/04/06	S2804T06	-	-	4.7	To maximum pressure

Note that the plots are not straight lines, and a compromise must be made in choosing the values. Sometimes different values are used for tests with different expansions.

There is also a big gap between the loading and unloading paths of the membrane calibrations – again a compromise must be made.

Note that the accuracy of the membrane calibration is important for low pressure tests, whereas it is the membrane compression (otherwise known as 'system compliance') that is important for high pressure tests – they are the ones measuring high values of modulus.

The relevant tables and plots follow.

SBP Calibrations December 2005 S/n 920123 Dougal

Pressure cells - new PPCs STG: 10759918 (0-600 Psi)

psi	TPC (volts)	Linearity (%)	Hysteresis (%)	PPC A (volts)	Linearity (%)	Hysteresis (%)	PPC B (volts)	Linearity (%)	Hysteresis (%)
0	-2.4609	93.8	-0.10	-0.1902	93.2	2.79	-1.1789	93.1	0.00
50	-2.3015	97.1	-0.31	-0.1155	96.6	2.63	-1.1027	97.4	-0.08
100	-2.1364	99.2	-0.25	-0.0381	99.4	2.58	-1.023	100.1	0.00
150	-1.9677	100.7	-0.69	0.0416	98.9	2.33	-0.9411	100.2	-0.05
200	-1.7965	102.0	-0.25	0.1209	100.2	2.25	-0.8591	101.9	0.14
250	-1.623	100.3	0.01	0.2012	97.9	2.10	-0.7757	99.9	0.46
300	-1.4525	99.5	-0.10	0.2797	97.2	1.37	-0.694	98.9	0.25
350	-1.2833	102.0	-0.05	0.3576	99.4	0.69	-0.6131	101.9	0.11
400	-1.1098	-101.6		0.4373	-104.8		-0.5297	-102.8	
350	-1.2826	-99.1		0.3533	-102.5		-0.6138	-100.0	
300	-1.4511	-101.2		0.2711	-103.7		-0.6956	-101.6	
250	-1.6232	-99.9		0.188	-101.3		-0.7787	-99.4	
200	-1.7931	-97.2		0.1068	-99.5		-0.86	-98.8	
150	-1.9584	-102.7		0.027	-101.4		-0.9408	-100.5	
100	-2.133	-96.6		-0.0543	-96.9		-1.023	-96.8	
50	-2.2973	-95.4		-0.132	-94.4		-1.1022	-93.8	
0	-2.4595			-0.2077			-1.1789		
Zero	-2.4678	volts		-0.2031	volts		-1.1831	volts	
Slope	3.40	mV/psi		1.60	mV/psi		1.64	mV/psi	
Sensitivity	493.2	mV/MPa		232.5	mV/MPa		237.3	mV/MPa	

Strain arms

mm	Arm 1 (mV)	Linearity (%)	Hysteresis (%)	Arm 2 (mV)	Linearity (%)	Hysteresis (%)	Arm 3 (mV)	Linearity (%)	Hysteresis (%)
0	300.1	102.7	-0.01	439.0	104.6	0.02	-262.6	97.0	-0.04
1	572.0	102.1	0.10	746.4	104.5	0.19	27.9	102.0	0.17
2	842.2	100.5	0.24	1053.6	100.3	0.27	333.5	100.9	0.29
3	1108.2	99.8	0.21	1348.4	99.0	0.27	635.7	98.8	0.32
4	1372.4	98.1	0.24	1639.2	98.3	0.25	931.8	99.2	0.22
5	1631.9	99.6	0.11	1928.0	97.7	0.17	1229.1	98.5	0.14
6	1895.5	-100.2		2215.0	-98.7		1524.1	-99.3	
5	1630.2	-98.9		1925.0	-98.7		1226.6	-99.7	
4	1368.5	-99.6		1634.8	-99.1		927.9	-99.4	
3	1104.8	-100.7		1343.6	-100.3		630.0	-100.7	
2	838.4	-101.3		1048.8	-104.1		328.4	-101.3	
1	570.4	-102.1		743.0	-103.5		24.8	-95.7	
0	300.2			438.7			-261.8		
Zero	305.1	mV		449.1	mV		-266.0	mV	
Slope	264.7	mV/mm		293.9	mV/mm		299.6	mV/mm	
Max	2244.8	mV		2489.0	mV		1798.5	mV	
	7.33	mm		6.94	mm		6.89	mm	

SBP Calibrations 03rd February 2006 S/n 920123 Dougal by Leo

Pressure cells STG: 10759918 (0-600psi)

psi	TPC (mV)	Linearity (%)	Hysteresis (%)	PPC A (mV)	Linearity (%)	Hysteresis (%)	PPC B (mV)	Linearity (%)	Hysteresis (%)
0	-2466.5	91.4	1.00	3276.7	0.0	#DIV/0!	-1071.9	100.1	-1.87
100	-2158.8	99.4	0.08	3276.7	0.0	#DIV/0!	-906.0	107.0	-0.56
200	-1823.9	99.9	0.43	3276.7	0.0	#DIV/0!	-728.8	109.4	0.47
300	-1487.6	99.9	0.28	3276.7	0.0	#DIV/0!	-547.6	94.2	1.96
400	-1151.3	99.8	0.00	3276.7	0.0	#DIV/0!	-391.6	100.9	0.89
500	-815.3	100.4	-0.04	3276.7	0.0	#DIV/0!	-224.5	84.3	1.11
600	-477.3	100.2		3276.7	0.0		-84.9	90.9	
500	-814.6	100.0		3276.7	0.0		-235.5	99.5	
400	-1151.3	101.5		3276.7	0.0		-400.4	100.5	
300	-1493.2	100.7		3276.7	0.0		-566.9	100.5	
200	-1832.5	97.3		3276.7	0.0		-733.4	100.9	
100	-2160.3	96.8		3276.7	0.0		-900.5	92.3	
0	-2486.3			3276.7			-1053.4		
Zero	-2488.1	mV		3276.7	mV		-1062.4	mV	
Slope	3.37	mV/psi		0.00	mV/bar		1.66	mV/bar	
Sensitivity	488.5	mV/MPa		0.0	mV/MPa		240.3	mV/MPa	

Strain arms

mm	Arm 1 (mV)	Linearity (%)	Hysteresis (%)	Arm 2 (mV)	Linearity (%)	Hysteresis (%)	Arm 3 (mV)	Linearity (%)	Hysteresis (%)
0	360.0	101.4	0.01	566.7	105.5	0.22	-317.0	102.3	-34.90
1	628.9	101.4	0.12	877.1	104.4	0.32	-12.0	100.5	0.28
2	897.7	100.8	0.26	1184.4	99.9	0.47	287.8	100.5	0.26
3	1164.8	99.8	0.26	1478.6	98.4	0.42	587.5	99.9	0.18
4	1429.3	98.9	0.23	1768.3	99.2	0.19	885.3	99.3	0.28
5	1691.5	98.1	0.13	2060.2	97.1	0.23	1181.5	98.3	0.12
6	1951.5	-98.9		2346.0	-98.5		1474.5	-99.0	
5	1689.4	-99.5		2056.1	-98.9		1179.3	-100.3	
4	1425.7	-100.0		1764.9	-99.8		880.2	-99.2	
3	1160.6	-100.8		1471.1	-100.3		584.3	-101.0	
2	893.5	-100.5		1176.0	-103.5		283.1	-100.6	
1	627.0	-100.8		871.4	-104.9		-17.0	109.1	
0	359.8			562.7			308.2		
Zero	362.6	mV		576.2	mV		-162.2	mV	
Slope	265.1	mV/mm		294.3	mV/mm		298.2	mV/mm	
Max	2288.8	mV		2597.7	mV		1683.3	mV	
	7.27	mm		6.87	mm		6.19	mm	

SBP Calibrations 7th March 2006 S/n 920123 Dougal

Pressure cells STG: 10759918 (0-600psi)

psi	TPC (mV)	Linearity (%)	Hysteresis (%)	PPC A (mV)	Linearity (%)	Hysteresis (%)	PPC B (mV)	Linearity (%)	Hysteresis (%)
0	-2408.2	95.3	-0.23	-678.9	96.3	-0.16	-1180.8	95.7	-0.15
100	-2083.5	98.6	-0.25	-525.3	99.2	-0.15	-1024.0	98.9	-0.09
200	-1747.7	101.1	-0.25	-367.0	101.1	-0.12	-861.9	101.0	-0.06
300	-1403.4	100.6	-0.09	-205.6	100.5	0.02	-696.4	100.6	0.03
400	-1060.7	99.5	-0.13	-45.2	99.0	-0.03	-531.6	99.4	-0.07
500	-721.7	99.9	-0.16	112.7	99.7	-0.14	-368.7	99.1	-0.07
600	-381.4	99.0		271.8	98.9		-206.4	98.6	
500	-718.4	99.7		114.0	99.6		-368.0	99.4	
400	-1058.0	100.9		-44.9	100.8		-530.9	101.2	
300	-1401.5	100.2		-205.8	100.3		-696.7	100.5	
200	-1742.6	98.6		-365.9	99.0		-861.3	98.8	
100	-2078.5	95.4		-523.9	96.2		-1023.1	95.3	
0	-2403.5			-677.4			-1179.3		
Zero	-2414.9	mV		-681.4	mV		-1184.1	mV	
Slope	3.41	mV/psi		1.60	mV/psi		1.64	mV/psi	
Sensitivity	493.9	mV/MPa		231.4	mV/MPa		237.6	mV/MPa	

Strain arms

mm	Arm 1 (mV)	Linearity (%)	Hysteresis (%)	Arm 2 (mV)	Linearity (%)	Hysteresis (%)	Arm 3 (mV)	Linearity (%)	Hysteresis (%)
0	342.5	100.8	0.15	576.9	104.4	0.11	-208.9	101.8	0.08
1	608.6	102.2	0.27	885.3	105.6	0.19	93.7	101.9	0.23
2	878.4	100.5	0.44	1197.1	99.9	0.45	396.5	99.7	0.50
3	1143.8	99.7	0.37	1492.3	100.3	0.27	692.7	100.2	0.35
4	1407.0	98.7	0.32	1788.6	96.7	0.57	990.6	99.1	0.26
5	1667.5	97.2	0.18	2074.2	96.5	0.14	1285.2	97.2	0.16
6	1924.1	-98.3		2359.2	-97.3		1574.0	-98.2	
5	1664.6	-99.5		2071.7	-99.3		1282.3	-99.7	
4	1401.9	-100.0		1778.5	-98.5		986.0	-100.8	
3	1138.0	-101.0		1487.5	-101.1		686.5	-100.6	
2	871.5	-101.2		1189.0	-104.0		387.5	-100.2	
1	604.4	-100.1		881.9	-103.9		89.6	-100.9	
0	340.1			574.9			-210.3		
Zero	343.7	mV		587.0	mV		-206.2	mV	
Slope	264.0	mV/mm		295.4	mV/mm		297.2	mV/mm	
Max	2064.4	mV		2618.4	mV		1836.6	mV	
	6.52	mm		6.88	mm		6.87	mm	

SBP Calibrations 7th June 2006 S/n 920123 Dougal

Pressure cells STG: 10759918 (0-600psi)

psi	TPC (mV)	Linearity (%)	Hysteresis (%)	PPC A (mV)	Linearity (%)	Hysteresis (%)	PPC B (mV)	Linearity (%)	Hysteresis (%)
0	-2371.9	95.2	-0.14	-691.7	95.7	-0.12	-1193.1	96.0	-0.14
100	-2049.1	98.9	-0.13	-539.0	99.6	0.04	-1036.1	99.7	0.03
200	-1713.6	101.4	-0.28	-380.2	101.7	-0.09	-873.1	101.7	-0.08
300	-1369.6	99.0	-0.06	-218.0	98.8	0.18	-706.8	98.7	0.21
400	-1033.8	100.6	-0.32	-60.4	100.1	-0.12	-545.4	100.3	-0.12
500	-692.4	99.7	-0.21	99.3	98.9	-0.08	-381.4	98.6	-0.09
600	-354.1	98.5		257.0	98.4		-220.1	98.1	
500	-688.1	100.0		100.1	99.9		-380.5	100.1	
400	-1027.3	100.5		-59.3	100.6		-544.2	100.6	
300	-1368.3	100.1		-219.7	100.1		-708.8	100.0	
200	-1708.0	99.8		-379.3	100.4		-872.3	100.3	
100	-2046.4	95.1		-539.4	94.8		-1036.4	95.0	
0	-2369.0			-690.6			-1191.7		
Zero	-2387.6	mV		-698.3	mV		-1199.3	mV	
Slope	3.39	mV/psi		1.60	mV/bar		1.64	mV/bar	
Sensitivity	492.0	mV/MPa		231.3	mV/MPa		237.2	mV/MPa	

Strain arms

mm	Arm 1 (mV)	Linearity (%)	Hysteresis (%)	Arm 2 (mV)	Linearity (%)	Hysteresis (%)	Arm 3 (mV)	Linearity (%)	Hysteresis (%)
0	376.6	101.5	0.17	659.8	106.5	0.04	-364.4	101.1	0.11
1	642.6	102.1	0.22	972.0	103.5	0.26	-65.4	101.5	0.16
2	910.2	101.4	0.30	1275.4	99.7	0.35	234.9	99.7	0.20
3	1176.1	99.8	0.27	1567.8	99.5	0.38	529.8	99.6	0.19
4	1437.7	97.7	0.23	1859.5	98.5	0.34	824.5	99.9	0.22
5	1693.7	97.2	0.07	2148.4	98.5	0.24	1120.0	99.3	0.20
6	1948.4	-97.6		2437.2	-99.9		1413.9	-100.5	
5	1692.6	-98.6		2144.2	-99.2		1116.5	-100.0	
4	1434.1	-100.1		1853.5	-99.7		820.6	-99.4	
3	1171.8	-101.6		1561.1	-99.6		526.5	-99.7	
2	905.5	-101.6		1269.2	-103.0		231.4	-101.3	
1	639.1	-101.1		967.3	-105.1		-68.2	-100.8	
0	374.0			659.1			-366.3		
Zero	383.2	mV		681.9	mV		-360.6	mV	
Slope	262.1	mV/mm		293.2	mV/mm		295.9	mV/mm	
Max	2277.0	mV		2626.0	mV		1589.0	mV	
	7.22	mm		6.63	mm		6.59	mm	

95mm HPD Scotty Horizontal inclinometer can
Arm calibration 6th February 2006

mm	Arm 1 (mV)	Linearity (%)	Hysteresis (%)	Arm 2 (mV)	Linearity (%)	Hysteresis (%)	Arm 3 (mV)	Linearity (%)	Hysteresis (%)
0	-2259.7	103.4	-0.04	-1925.7	100.8	0.03	-1748.1	101.6	0.23
2	-2009.7	103.2	0.11	-1683.8	102.0	0.00	-1503.5	103.4	-0.05
4	-1760.2	101.8	0.12	-1439.0	102.4	-0.04	-1254.7	101.7	-0.08
6	-1514.0	101.6	0.09	-1193.4	101.0	0.02	-1009.8	100.5	-0.15
8	-1268.4	100.3	0.06	-951.0	99.9	-0.16	-768.0	99.9	-0.22
10	-1025.8	99.2	0.03	-711.4	99.4	-0.23	-527.6	99.4	-0.25
12	-785.9	98.2	-0.03	-473.0	99.8	-0.31	-288.3	98.1	-0.25
14	-548.4	98.5	-0.09	-233.6	99.0	-0.26	-52.1	99.5	-0.29
16	-310.3	98.5	-0.07	3.8	97.4	-0.20	187.4	99.5	-0.22
18	-72.2	97.8	-0.07	237.4	96.5	-0.15	427.0	99.8	-0.15
20	164.2	-97.1		468.8	-95.0		667.3	-98.4	
18	-70.6	-98.4		241.0	-96.9		430.5	-98.8	
16	-308.5	-98.3		8.5	-98.3		192.6	-98.7	
14	-546.2	-98.8		-227.3	-99.3		-45.0	-98.6	
12	-785.1	-99.9		-465.6	-100.2		-282.4	-99.3	
10	-1026.6	-100.6		-705.9	-100.5		-521.5	-100.3	
8	-1269.8	-101.9		-947.1	-102.9		-762.8	-101.1	
6	-1516.2	-102.2		-1193.9	-101.8		-1006.2	-102.5	
4	-1763.2	-103.0		-1438.0	-102.5		-1252.8	-103.6	
2	-2012.3	-102.0		-1683.8	-101.1		-1502.2	-104.4	
0	-2258.8			-1926.4			-1753.6		

Zero	-2242.5	mV		-1914.5	mV		-1733.8	mV
Slope	120.9	mV/mm		119.9	mV/mm		120.3	mV/mm
Maximum	897.9	mV		1194.3	mV		1426.3	mV
	26.0	mm		25.9	mm		26.3	mm

mm	Arm 4 (mV)	Linearity (%)	Hysteresis (%)	Arm 5 (mV)	Linearity (%)	Hysteresis (%)	Arm 6 (mV)	Linearity (%)	Hysteresis (%)
0	-1862.6	102.4	0.02	-1955.7	101.2	0.00	-1999.7	103.2	0.01
2	-1616.2	101.8	-0.02	-1715.5	102.1	-0.10	-1751.4	102.1	0.23
4	-1371.4	102.3	-0.09	-1473.0	102.5	-0.19	-1505.8	101.9	0.22
6	-1125.4	100.5	-0.17	-1229.7	101.5	-0.27	-1260.6	101.3	0.14
8	-883.6	99.7	-0.24	-988.6	100.5	-0.36	-1016.8	99.9	-0.06
10	-643.7	99.6	-0.27	-750.0	99.3	-0.40	-776.4	99.1	-0.07
12	-404.1	99.5	-0.26	-514.2	99.8	-0.46	-538.0	99.1	-0.04
14	-164.7	99.4	-0.21	-277.3	98.7	-0.43	-299.6	97.8	-0.05
16	74.4	98.3	-0.15	-43.0	96.6	-0.36	-64.2	98.8	-0.09
18	310.8	98.6	-0.17	186.3	96.9	-0.20	173.6	98.9	-0.07
20	548.0	-96.9		416.4	-94.9		411.5	-98.1	
18	314.8	-98.4		191.0	-95.0		175.4	-98.7	
16	78.1	-98.8		-34.5	-97.9		-62.0	-98.3	
14	-159.6	-99.0		-267.1	-99.5		-298.5	-99.1	
12	-397.8	-99.5		-503.3	-99.9		-537.0	-98.8	
10	-637.2	-100.0		-740.6	-100.8		-774.8	-100.0	
8	-877.8	-101.3		-980.0	-102.4		-1015.4	-103.3	
6	-1121.4	-103.0		-1223.2	-103.3		-1264.0	-102.7	
4	-1369.2	-102.5		-1468.4	-103.1		-1511.0	-102.3	
2	-1615.8	-102.8		-1713.2	-102.2		-1757.0	-101.0	
0	-1863.0			-1955.8			-2000.0		

Zero	-1848.3	mV		-1940.8	mV		-1985.8	mV
Slope	120.3	mV/mm		118.7	mV/mm		120.3	mV/mm
Maximum	1293.5	mV		1122.5	mV		1153.6	mV
	26.1	mm		25.8	mm		26.1	mm

Pressure cell calibration 7th February 2006 Star gauge s/n 38425 0 - 4000 psi

psi	TPC A (mV)	Linearity (%)	Hysteresis (%)	TPC B (mV)	Linearity (%)	Hysteresis (%)
0	720.8	98.3	-0.27	395.7	98.5	-0.28
200	828.0	102.7	-0.18	505.2	102.9	-0.25
400	940.0	98.1	0.05	619.6	98.4	-0.04
600	1047.0	101.7	-0.05	729.0	102.5	-0.09
800	1158.0	100.8	0.14	843.0	100.3	0.18
1000	1268.0	96.7	0.18	954.5	97.6	0.31
1200	1373.5	101.7	-0.82	1063.0	100.7	-0.45
1400	1484.5	98.5	-1.19	1175.0	100.7	-0.49
1600	1592.0	96.2	-1.19	1287.0	97.1	-1.08
1800	1697.0	99.0	-0.37	1395.0	96.3	0.27
2000	1805.0	-95.3		1502.0	-98.9	
1800	1701.0	-88.0		1392.0	-83.7	
1600	1605.0	-98.5		1299.0	-106.6	
1400	1497.5	-105.4		1180.5	-101.2	
1200	1382.5	-106.8		1068.0	-105.2	
1000	1266.0	-100.4		951.0	-98.9	
800	1156.5	-99.9		841.0	-99.8	
600	1047.5	-99.0		730.0	-98.9	
400	939.5	-100.4		620.0	-100.7	
200	830.0	-97.3		508.0	-98.2	
0	723.8			398.8		

Zero	721.5	mV	397.2	mV
Slope	0.55	mV/psi	0.56	mV/psi
Sensitivity	79.1	mV/Mpa	80.6	mV/Mpa

95mm HPD Scotty
Arm calibration 11th April 2006

mm	Arm 1 (mV)	Linearity (%)	Hysteresis (%)	Arm 2 (mV)	Linearity (%)	Hysteresis (%)	Arm 3 (mV)	Linearity (%)	Hysteresis (%)
0	-2225.9	107.0	0.05	-1871.5	104.3	-0.03	-1679.3	104.2	-0.06
2	-1965.0	104.0	0.06	-1616.2	101.9	0.02	-1423.4	102.9	-0.05
4	-1711.3	103.1	0.07	-1366.8	102.0	-0.01	-1170.7	101.9	-0.09
6	-1459.9	102.0	0.03	-1117.3	100.5	-0.09	-920.4	100.0	-0.18
8	-1211.1	102.2	-0.02	-871.5	101.0	-0.11	-674.7	99.5	-0.28
10	-961.8	100.0	0.00	-624.3	99.0	-0.15	-430.2	99.4	-0.33
12	-718.0	99.2	-0.05	-382.0	100.1	-0.25	-186.0	99.7	-0.32
14	-476.1	95.4	-0.05	-137.2	99.0	-0.22	58.9	98.7	-0.23
16	-243.5	95.3	-0.04	105.0	98.0	-0.18	301.3	99.7	-0.22
18	-11.2	95.7	-0.04	344.7	94.3	-0.14	546.2	99.4	-0.14
20	222.2	-95.3		575.4	-92.9		790.4	-98.0	
18	-10.3	-95.2		348.1	-97.6		549.7	-98.9	
16	-242.5	-95.3		109.4	-98.5		306.8	-98.6	
14	-474.8	-99.3		-131.7	-99.8		64.6	-98.9	
12	-716.9	-100.5		-375.9	-100.1		-178.2	-99.3	
10	-961.9	-102.0		-620.7	-101.4		-422.0	-100.1	
8	-1210.6	-102.5		-868.7	-100.7		-667.9	-101.0	
6	-1460.7	-103.4		-1115.2	-102.7		-915.9	-102.8	
4	-1712.9	-103.9		-1366.6	-102.2		-1168.4	-103.3	
2	-1966.4	-106.9		-1616.7	-103.9		-1422.2	-104.1	
0	-2227.2			-1870.8			-1677.9		
Zero	-2193.7	mV		-1852.4	mV		-1659.1	mV	
Slope	121.9	mV/mm		122.3	mV/mm		122.8	mV/mm	

mm	Arm 4 (mV)	Linearity (%)	Hysteresis (%)	Arm 5 (mV)	Linearity (%)	Hysteresis (%)	Arm 6 (mV)	Linearity (%)	Hysteresis (%)
0	-1796.4	120.6	-0.31	-1890.6	103.7	-0.19	-1921.3	103.4	-0.02
2	-1505.8	102.6	0.00	-1640.6	102.9	-0.05	-1667.9	102.2	0.02
4	-1258.7	102.2	-0.03	-1392.6	102.0	-0.16	-1417.5	102.0	-0.02
6	-1012.5	100.2	-0.08	-1146.7	102.8	-0.26	-1167.6	101.7	-0.06
8	-771.0	99.4	-0.18	-898.8	100.6	-0.33	-918.4	99.8	-0.05
10	-531.6	99.4	-0.23	-656.2	100.2	-0.38	-673.8	98.6	-0.05
12	-292.2	99.5	-0.30	-414.6	99.5	-0.39	-432.2	99.7	-0.10
14	-52.4	100.0	-0.27	-174.7	98.2	-0.37	-188.0	99.0	-0.05
16	188.5	99.2	-0.17	62.0	95.3	-0.27	54.7	98.7	-0.02
18	427.5	95.5	-0.09	291.7	92.4	-0.18	296.6	98.9	0.00
20	657.5	-94.6		514.4	-90.6		538.9	-98.9	
18	429.6	-98.3		296.1	-94.4		296.5	-98.5	
16	192.7	-99.0		68.6	-97.2		55.2	-98.8	
14	-45.8	-99.3		-165.8	-99.3		-186.8	-99.1	
12	-285.0	-100.1		-405.1	-100.4		-429.7	-99.1	
10	-526.1	-99.9		-647.0	-101.1		-672.5	-99.9	
8	-766.7	-101.2		-890.8	-103.6		-917.2	-101.6	
6	-1010.6	-102.7		-1140.5	-103.0		-1166.2	-102.3	
4	-1257.9	-102.9		-1388.7	-104.0		-1417.0	-102.5	
2	-1505.9	-117.5		-1639.4	-102.3		-1668.3	-103.1	
0	-1788.9			-1886.0			-1920.9		
Zero	-1737.8	mV		-1867.0	mV		-1904.6	mV	
Slope	120.5	mV/mm		120.5	mV/mm		122.5	mV/mm	

Pressure cell calibration Budenberg gauge s/n 10759918 0 - 600psi

psi	TPC (mV)	Linearity (%)	Hysteresis (%)	TPC B (mV)	Linearity (%)	Hysteresis (%)
0	-343.7	106.4	-1.70	-134.3	106.9	-2.37
100	-284.9	100.1	0.00	-73.6	101.1	-0.55
200	-229.6	98.5	0.57	-16.2	99.5	0.26
300	-175.2	99.9	-0.36	40.3	99.4	-0.58
400	-120.0	101.4	0.12	96.7	101.6	-0.29
500	-64.0	101.4	0.42	154.4	100.6	0.32
600	-8.0	-103.9		211.5	-102.5	
500	-65.4	-99.6		153.3	-97.9	
400	-120.4	-97.0		97.7	-97.6	
300	-174.0	-104.1		42.3	-104.6	
200	-231.5	-96.7		-17.1	-96.2	
100	-284.9	-96.1		-71.7	-95.8	
0	-338.0			-126.1		

Zero	-340.7	mV	Zero	-129.9	mV
Slope	0.55	mV/psi	Slope	0.57	mV/psi
Sensitivity	80.1	mV/MPa	Sensitivity	82.3	mV/MPa

Note this low pressure calibration was done as a check for the tests in glacial till.

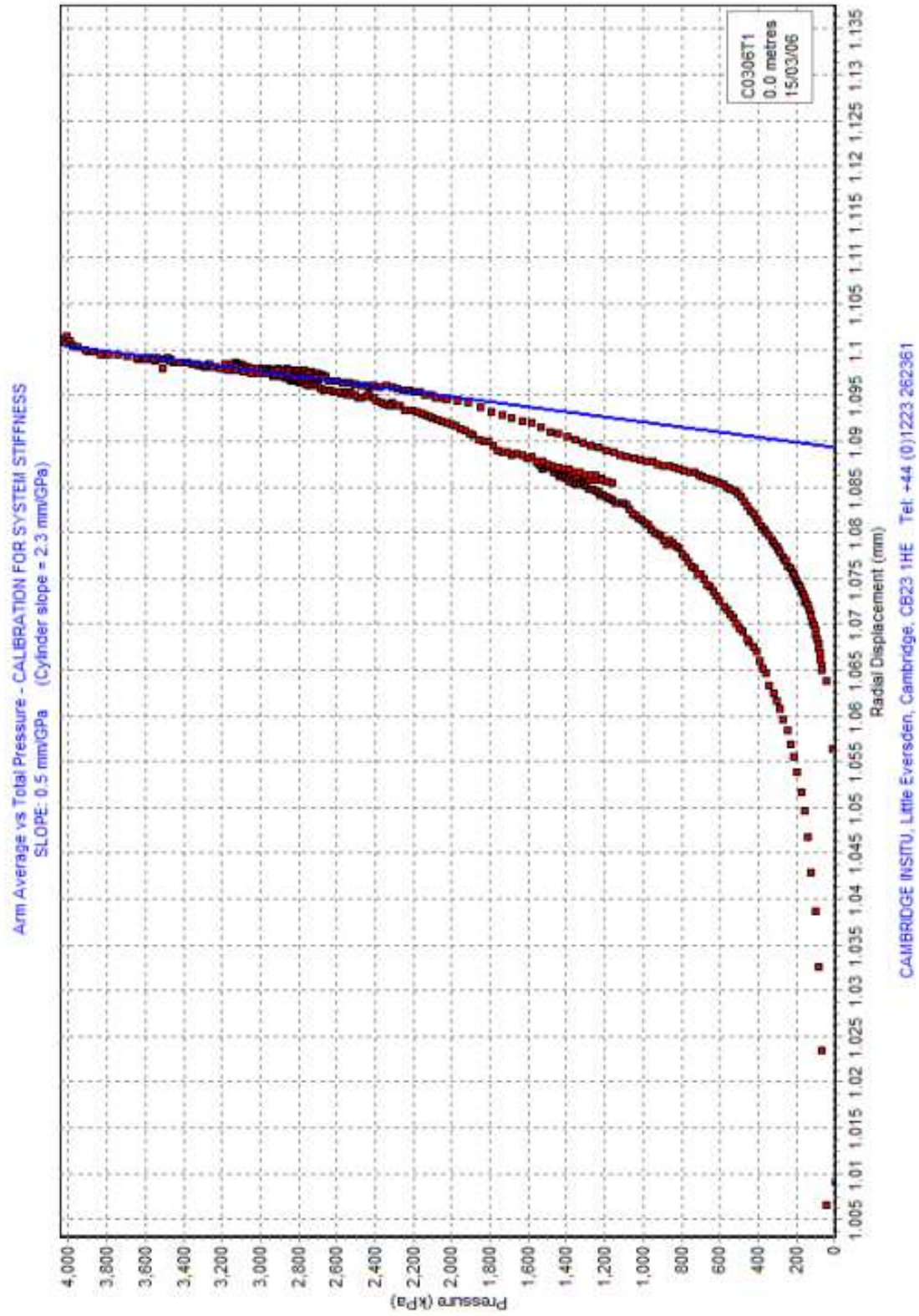
Arm Average vs Total Pressure - CALIBRATION FOR SYSTEM STIFFNESS
SLOPE: 0.5 mm/GPa (Cylinder slope = 2.3 mm/GPa)
C0306T1
0.0 metres
15/03/06
Radial Displacement (mm)
Pressure (kPa)
CAMBRIDGE INSITU, Little Eversden, Cambridge, CB23 1HE Tel: +44 (0)1223 262361

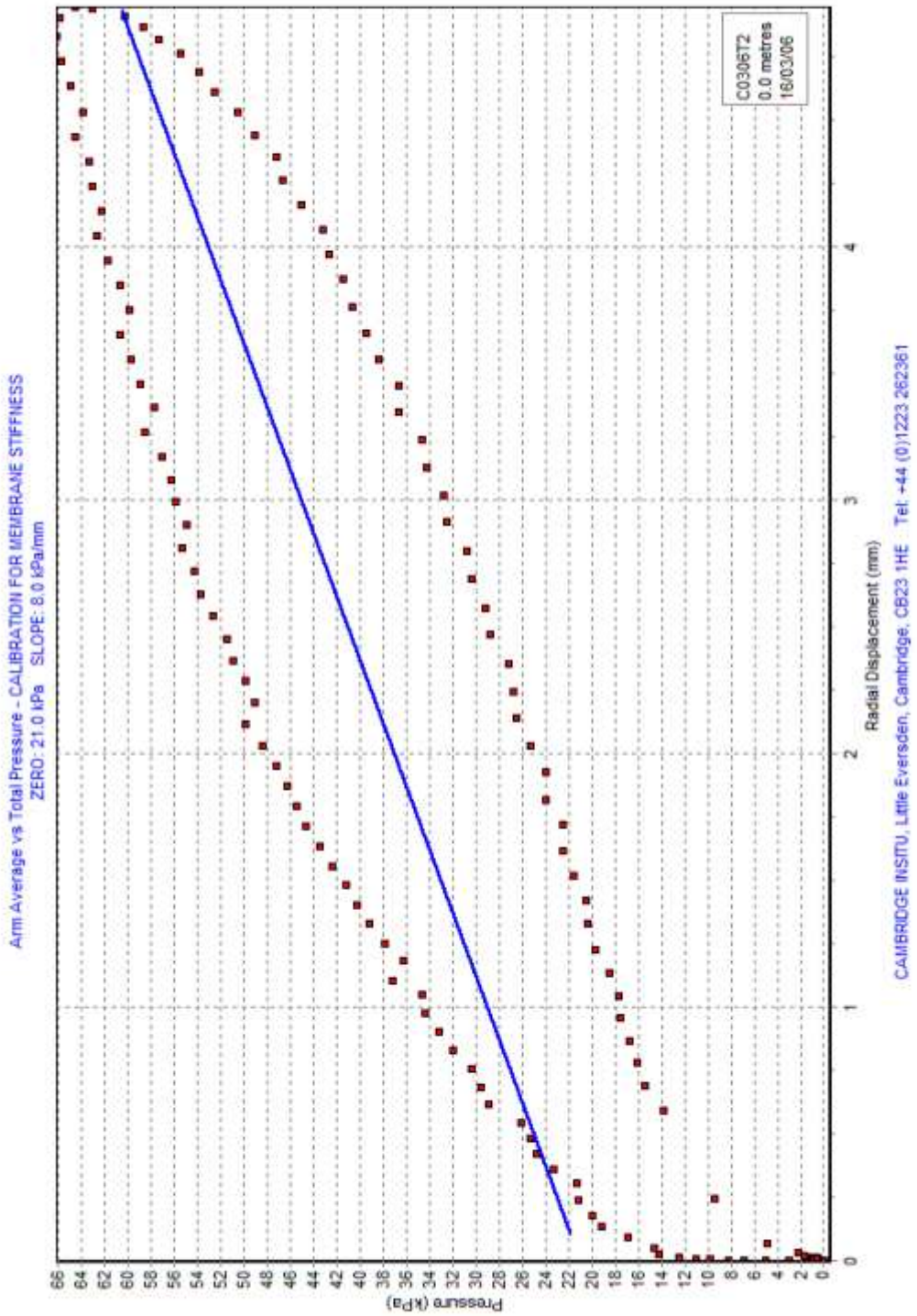
Arm Average vs Total Pressure - CALIBRATION FOR MEMBRANE STIFFNESS
ZERO: 21.0 kPa SLOPE: 8.0 kPa/mm
C0305T2
0.0 metres
16/03/06
Pressure (kPa)
Radial Displacement (mm)
CAMBRIDGE INSITU, Little Eversden, Cambridge, CB23 1HE Tel: +44 (0)1223 262361

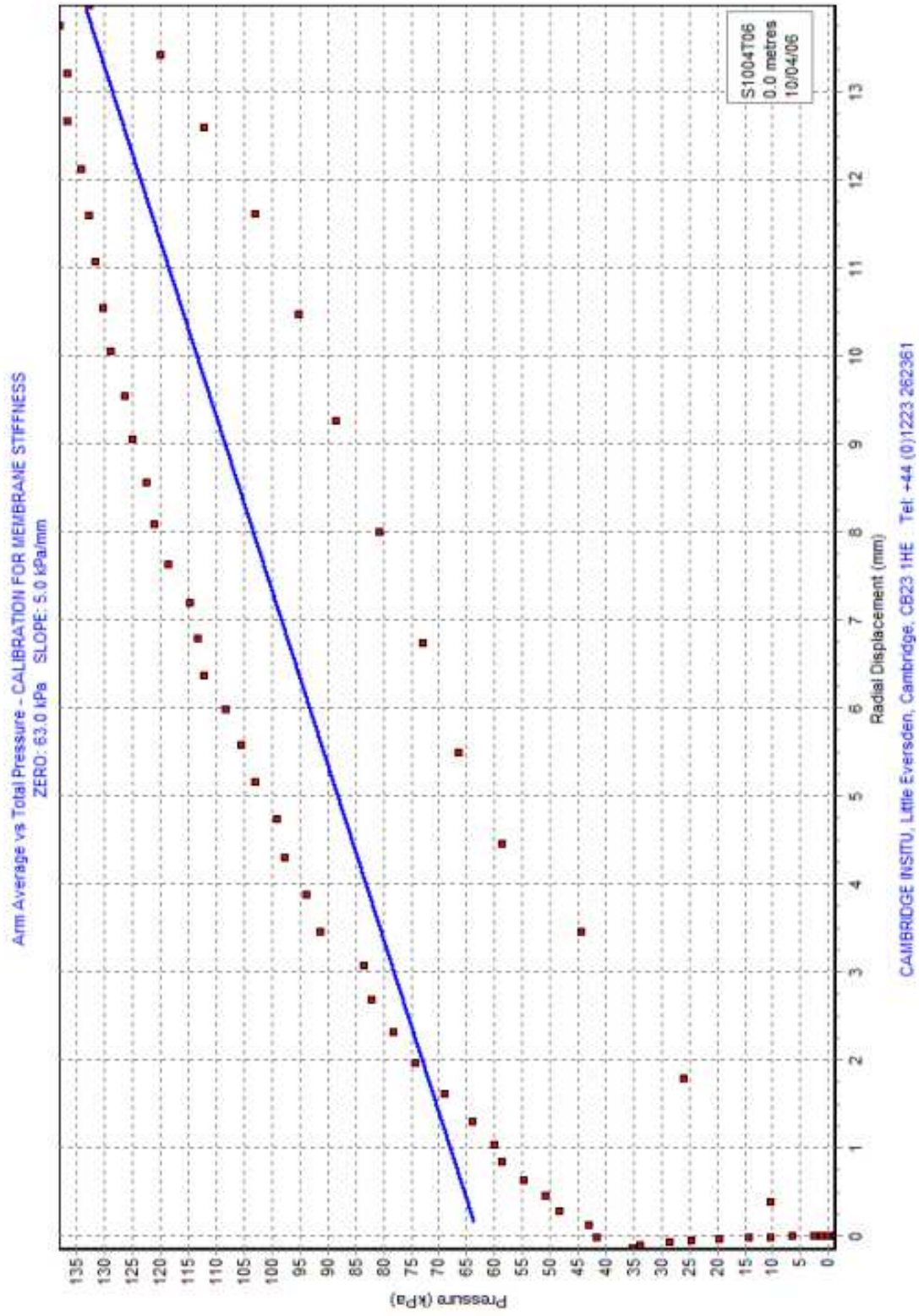
Arm Average vs Total Pressure - CALIBRATION FOR MEMBRANE STIFFNESS
ZERO: 63.0 kPa SLOPE: 5.0 kPa/mm
S1004T06
0.0 metres
10/04/06
Pressure (kPa)
Radial Displacement (mm)
CAMBRIDGE INSITU, Little Eversden, Cambridge, CB23 1HE Tel: +44 (0)1223 262361

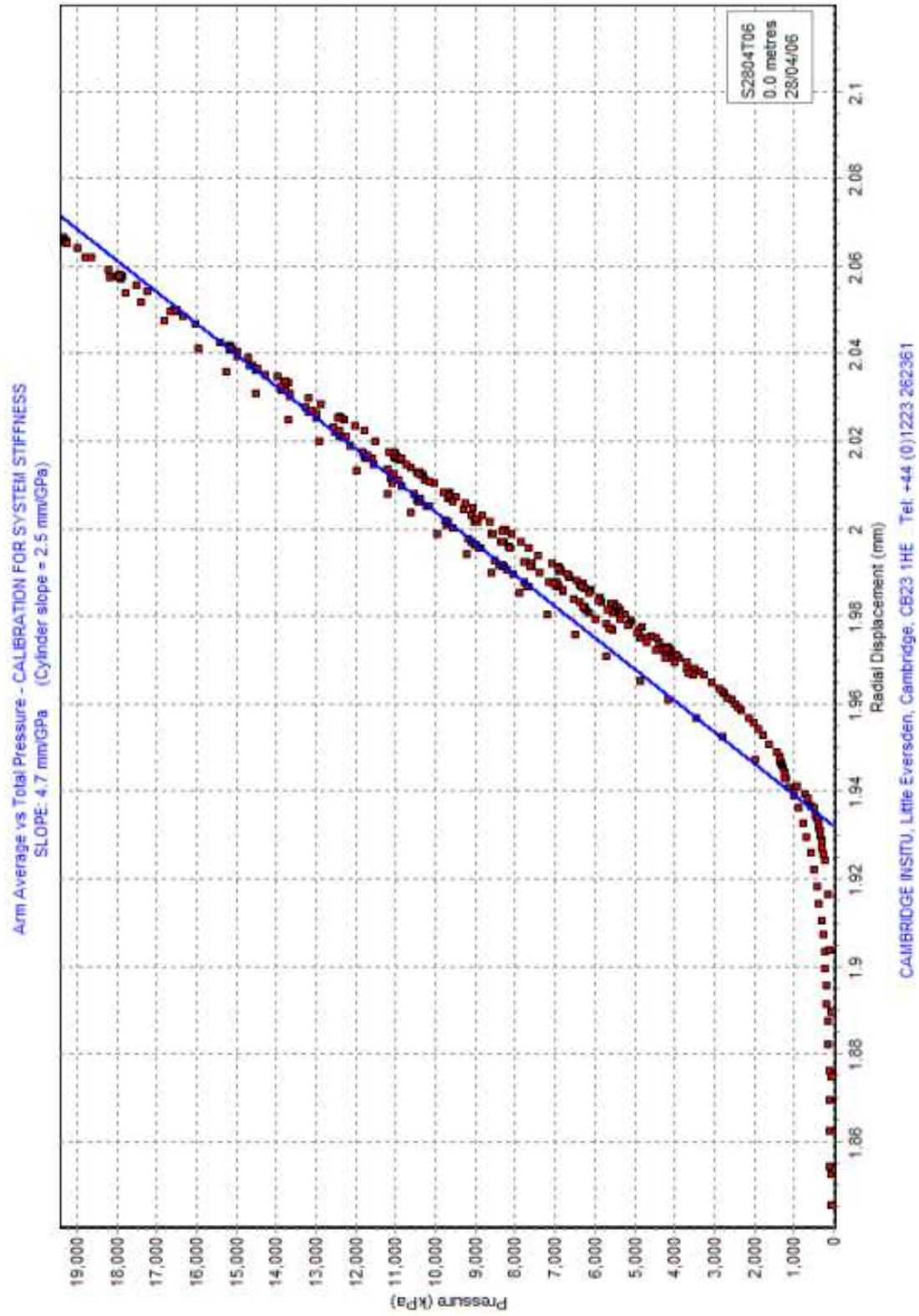
Arm Average vs Total Pressure - CALIBRATION FOR SYSTEM STIFFNESS
SLOPE: 4.7 mm/GPa (Cylinder slope = 2.5 mm/GPa)
S2804T06
0.0 metres
28/04/06
Pressure (kPa)
19,000
18,000
17,000
16,000
15,000
14,000
13,000
12,000
11,000
10,000
9,000
8,000
7,000
6,000
5,000
4,000
3,000
2,000
1,000
0
Radial Displacement (mm)
1.86
1.88
1.9
1.92
1.94
1.96
1.98
2
2.02
2.04
2.06
2.08
2.1
CAMBRIDGE INSITU, Little Eversden, Cambridge, CB23 1HE Tel: +44 (0)1223 262361

APPENDIX C THE TEST PROCEDURES

C.1 Installing the probe

The SBPM in both its Soft Ground and Weak Rock configurations is drilled to the test depth from the bottom of a borehole. The drilling may be done with a proprietary self-contained set of equipment or using the same drill rig used to produce the borehole. The latter method was used for this contract.

The bottom of the borehole was chosen to leave nominally 1m of self-boring. Note the following crucial measurements:

(a) From the foot of the instrument to the centre of the measuring section is 0. 5 metres.
(b) The expanding part of the instrument is about 0.5 metres in length.

From these dimensions it is apparent that the instrument must be at least 0.8 metres into the pocket, and for safety we would suggest 1.0 metres into the pocket as a minimum. The probe in Weak Rock configuration is more tolerant than the standard SBPM in this respect as the ends of the membrane are reinforced and resist over-expansion better.

What should be guarded against is having a softer layer in the test section, either above or below the centre of the membrane where the strain sensors are. This will result in the membrane bursting, or pulling out of the clamp ring, before the pocket has been properly loaded.

Details about the drilling are noted on the Test Record Sheet as they can be useful in interpreting the test results.

The HPD test is carried out in a 101mm pocket that has been formed by coring or more rarely by rock rollering. Coring is the conventional method because the recovered core can give some information about the pocket before the instrument is placed. Samples of the core are normally of sufficient quality to permit standard laboratory testing, which can then be compared with the pressuremeter results.

The pocket itself should be at least 2 metres long. This allows the user some choice about the exact point in the pocket in which to place the HPD. Note the following crucial measurements:

(a) From the foot of the instrument to the centre of the measuring section is 0.9 metres.
(b) The expanding part of the instrument is about 0.6 metres.
(c) The instrument is 2 metres long - if the BW extension rod is added to this then the effective length from the foot of the pressuremeter to the start of the rotary drill string is 3 metres. If the pocket is longer than 3 metres then the diameter of the drill rod used to place the pressuremeter must not exceed 75mm; this together with two thicknesses of hose, is the maximum that will fit into a 101mm pocket.

From these dimensions it is apparent that the instrument must be at least 1.3 metres into the pocket, and for safety we would suggest 1.5 metres into the pocket as a minimum. There is evidence that the very lowest part of the pocket should be avoided as this is often the area most spoiled by the coring, but as the test centre is some distance from the foot of the instrument this is not normally a problem.

Soft patches in the core suggest a point that ought to be in the test section. However soft patches at the ends of the expanding section may result in the membrane bursting before the pocket has been properly loaded.

Heavily fractured material around the test centre, although not likely to burst the membrane, will present problems of a different kind. The analyses that currently exist for the pressuremeter test assume that the material is intact - if this is not the case, then although the data may be good, deciding what they mean may prove complex.

It is a truism that the quality of the test is dependent on the quality of the initial coring. However many good tests have been made in pockets where no core at all was recovered. Standard coring practice is designed to preserve the core without regard for the borehole wall. This is the opposite of what the priorities need to be for the pressuremeter test.

Details about the core are noted on the Test Record Sheet as they can be useful in interpreting the test results.

C.2 The expansion test

Both probes conduct expansion tests on the ground, the main difference being that the HPD has to expand a little way before reaching the borehole wall, whereas the SBPM typically does not. Theoretically the SBPM, in its Weak Rock configuration, cuts a hole that is nominall about 0.5mm oversize, but in all but the stiffest materials this is lost as the material moves back in.

At the start of the test, gas is applied to the instrument at a constant steady rate. Once the test cavity starts to expand the flow rate may be adjusted to keep the rate of strain increase constant - 1% per minute is generally accepted as a sensible rate which is sufficiently fast to ensure undrained expansion and not too fast for a drained expansion. The strain control unit (SCU) will do this automatically for the SBPM, but HPD tests must be done manually.

Shortly after the cavity begins to expand an unload/reload loop is taken. The starting strain of the loop depends on the expansion being underway at all points around the membrane, and the pressure drop used depends on the current mobilised shear stress. This is not known exactly at this stage in a test, but it is possible to form a rough estimate. In general a pressure drop of about twice the estimate of the shear strength, relying on the fact that the material will respond elastically for more than this amount, will give the maximum possible loop. If the unloading continues too far, the material will begin to fail inwards.

Before initiating the unloading for a loop, the pressure in the membrane is held constant to allow time dependent deformations to slow to an acceptable level. Too long a pause will merely encourage drainage, so the pause is intended to minimise rate effects caused by the rapid rate at which the loading is conducted, and is usually no more than one minute. If the intention is to measure the creep, then the pressure should be held constant for at least three minutes.

A second loop is taken between 2%-3% cavity strain. Additional loops may be taken if thought to be necessary, as they are in sand.

The test ends when 10% expansion of the test cavity has been achieved at one or more measuring points. With the probe in Weak Rock configuration the expansion can be safely taken a little further. The HPD can take the expansion a lot further.

This is one advantage of the HPD – tests in sand can usually be taken past the peak friction angle.

The complete unloading curve is then monitored. Extra reload loops may be taken on the unloading, particularly if there has been a lot of creep.

C.3 Logging Rate

A line of data representing the output of all transducers was logged every 5 seconds for the SBPM (every 6 seconds for the 6 arm version) and every 10 seconds for the HPD.

C.4 A Typical Test Curve

From zero pressure to about 350kPa: this is the early part of the test where good definition of the loading curve is important for assessing the pressure at which the membrane first shows significant movement.

From 350kPa to about 600kPa: this is the elastic part of the initial loading curve, the slope of which gives a value for G_i, the initial shear modulus. The yield stress denotes the onset of plasticity and hence irrecoverable deformations. The estimate of the insitu lateral stress has been marked, which in this example does not coincide with the first movement of the membrane.

Following yield, at about 1% strain an unload/reload loop is taken.. The slope of the line which bisects the cycle provides an estimate of the shear modulus.

After the first unload reload loop, the strain interval between data points becomes regular, denoting that the expansion is now being controlled at a constant rate of strain.

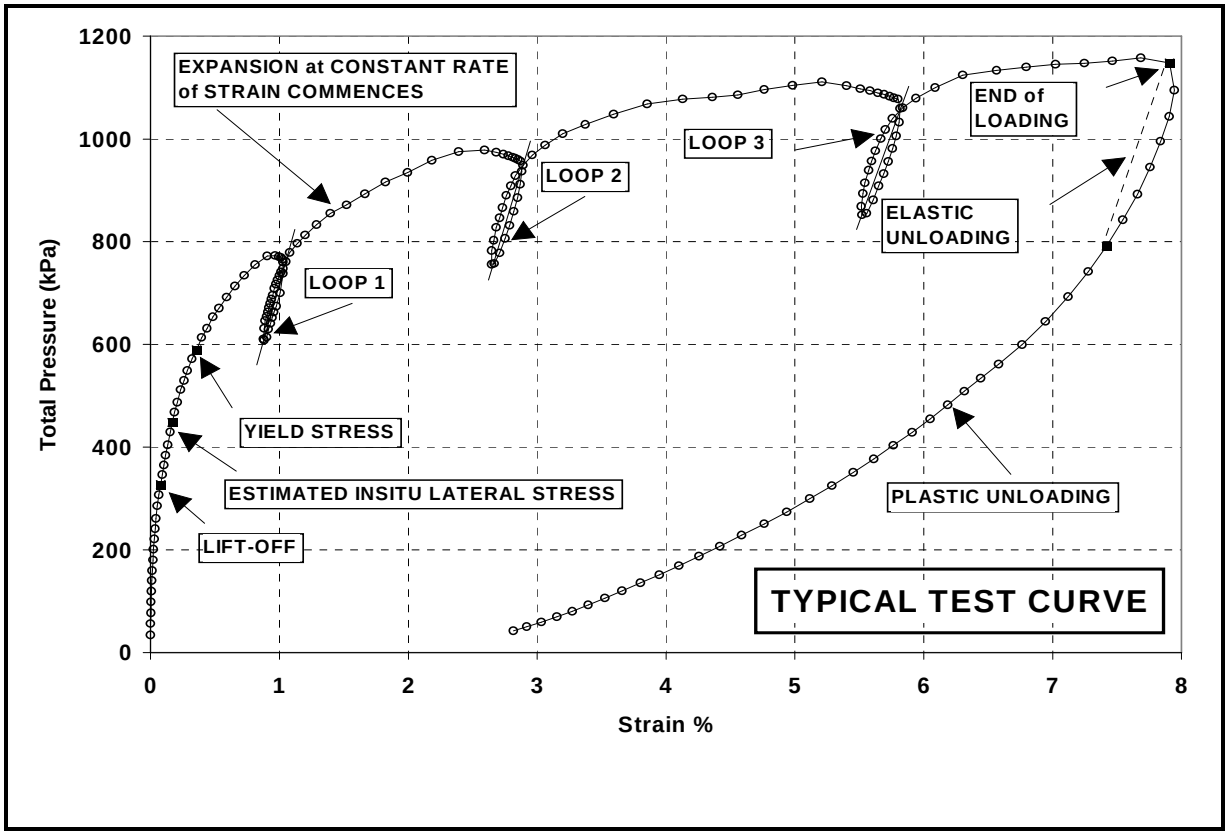

Figure C.1 A typical SBPM test

A second unload/reload loop is taken at about 2.5% strain. Note that the pause before unloading commences is not a true pressure hold; the cavity continues to expand a little and hence the pressure in the membrane falls slightly.

In this example a third unload/reload loop is taken between 5% and 6% strain. Note that the expansion of the cavity which takes place during the pause increases as the plastic zone around the probe enlarges. This is one reason why loops should be taken early in the loading.

In this example the end of loading occurs at about 1150kPa and 8% expansion. The example is showing the average of all arms, and one or more of the arms was beyond 10% expansion.

The initial part of the unloading is elastic, and the approximate extent of the elastic phase is indicated. Thereafter the curve indicates reverse plastic failure.

The test terminates once the pressure in the membrane is near zero.

Note that this is quite a low pressure SBPM test – an HPD test may look very different.

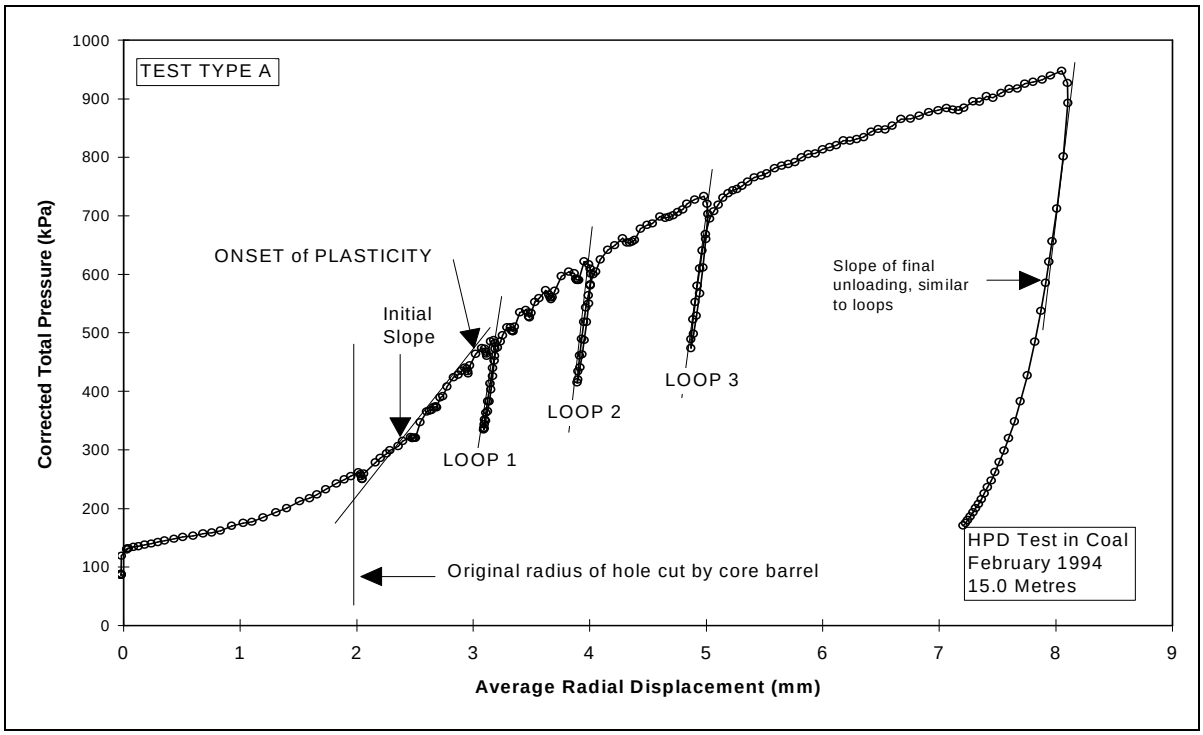

Figure C.2 A typical HPD test

The loading curve of the HPD test tends to take the 'S' shaped form. At the start of the test the membrane is lying on the body of the HPD. There are then several distinct parts to the test:

Pressure is applied, the membrane lifts off the body of the HPD and expands out to touch the sides of the borehole. Hence there are large displacements for very little pressure.

Further increments of pressure define the first curve of the 'S' shape; this curve is the instrument taking up the contour of the pocket and the cuttings left behind by the coring being squeezed out.

Following this is a linear part of the loading curve. The pressure being applied is remoulding the material adjacent to the HPD that has been failed by the coring process, but is not yet sufficient to extend the zone of failure into fresh material. In this part of the test the pressure is increasing but is having little effect on the strain.

Once the pressure is sufficient to extend the zone of failed material the upper curve of the 'S' starts to be defined, eventually reaching an almost linear condition once more where strain is increasing rapidly for very little increase in pressure.

At this stage the cavity can be unloaded and the full unloading curve be drawn. The first part of this will be nearly linear, curving away as the pressure and hence the strain reduce to zero.

There are several ways of using the data contained in the pressure/strain curve but the most common is to use it to derive fundamental parameters about the strength of the material being tested. Therefore the precise manner in which the test is carried out should be chosen to make it easier to assess these parameters.

The slope of the initial linear part can give a value for the initial shear modulus G_i but because this part of the curve is sensitive to the disturbance produced by the coring the derived value is of little significance in itself.

A better estimate of G can be made by taking unload/reload loops at intervals along the loading path. To do this a little of the pressure that has been applied is released and then reapplied in a controlled manner, taking readings of the changing strain. This produces a characteristic loop. The slope of the best fit straight line through the long axis of the loop can be used to derive G_r.

The value of G produced in this way is relatively insensitive to the initial drilling disturbance. The shear modulus is probably the single most useful parameter that the HPD test can produce, and it is used extensively in design calculations. Because of this significance it is usual to take at least two loops at suitable points on the test curve (even if the engineer supervising the test specifies only one). Suitable points would be on the linear part of the curve and as soon as there are indications of failure. Loops can also be taken on the unloading curve.

The ratio of G_i to G_r allows some assessment to be made about the extent of the disturbance created by the coring of the pocket.

Deductions about the undrained shear strength, Cu, are made from the part of the curve following yield until the end of loading.

From the linear part of the curve, can be deduced the insitu lateral stress, p_o. There are several methods. We use a modified version of the Marsland & Randolph argument (see references, Appendix D).

APPENDIX D. THE ANALYSIS PROCEDURE

Deriving parameters from pressuremeter tests in soil.

1. Introduction

There are two approaches to the interpretation of pressuremeter test data. The first, that developed by Menard, uses empirical correlations to allow measured co-ordinates of pressure and displacement to be inserted directly into design equations. This approach depends on a standardised test procedure and a large data bank of pressuremeter tests correlated with observations of the response of finished structures.

The second approach, which will be described briefly here and is the usual way of interpreting the pressuremeter test in the UK, relies on solving the boundary problem posed by the pressuremeter test.

The aim of the pressuremeter test is to expand a long cylindrical cavity within an undisturbed mass of soil. Fundamental strength properties of the material can be deduced from measurements made of cavity pressure and displacement.

In practice no instrument can be placed into the ground without affecting in some way the surrounding soil. In the case of a self-bored pressuremeter test the disturbance is usually elastic and can be allowed for in the analysis procedure.

1.1 The pressuremeter test in soil - initially elastic response followed by failure in shear.

Consider that the soil is homogeneous, and shows simple elastic behaviour before failing in shear. The stress path followed by an element of soil adjacent to the cavity is given in figure 1 and the corresponding pressure /strain curve is shown alongside.

The radial stress, ideally at the insitu horizontal stress for a perfectly self bored installation, increases at the same rate as the circumferential stress decreases, regardless of whether the material is deforming under plane strain or plane stress conditions. The line 0 - 0 represents stress equality, so that in the ideal case considered here the point P_0 is the insitu lateral stress.

Once the radial stress increases above the insitu stress then the shear stress in the soil at the cavity wall will increase. If the insitu lateral stress is low, then it is possible that the circumferential stress would go into tension. However in this example the insitu stress is high enough to ensure that the shear stress limit is reached before tensile stresses can be generated.

The pressure necessary to initiate shear failure is denoted P_f in figure 1. After this pressure the strain rate shows a substantial increase, and the form of this part of the pressure/strain curve

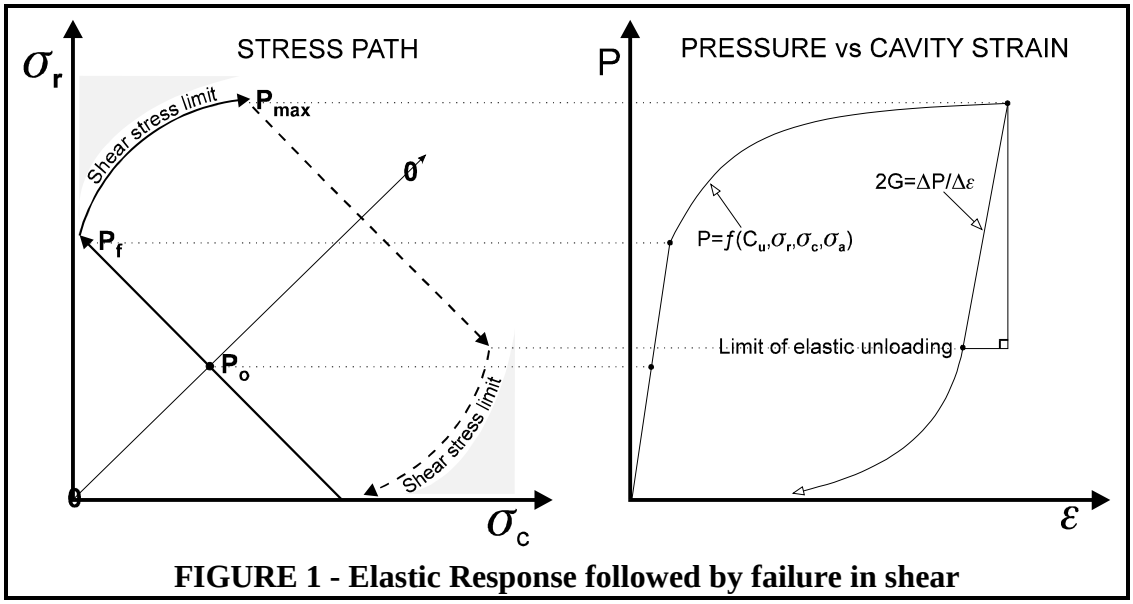

FIGURE 1 - Elastic Response followed by failure in shear

will be a function of the shear strength of the material. Radial stress and circumferential stress now increase together. If the shear stress limit is constant, and is not influenced by pressure, and if the material deforms at constant volume, then the failure shear strength can be determined by the analytical solution developed by Gibson & Anderson.

Before the shear stress limit is reached the pressuremeter response is elastic, both in loading and unloading. Assuming that the soil deformed at a constant modulus and the installation was perfect then the slope of the initial loading path would give the shear modulus of the material, using the classic procedure of Bishop, Hill & Mott. What is not shown on the diagram is that small cycles of unloading and reloading taken anywhere in a test after reaching the shear stress limit can be used to give plausible and repeatable estimates of the shear modulus (Hughes 1982).

As figure 1 implies, the complete unloading of the pressuremeter can also be analysed to give strength and stiffness parameters which are comparable with those obtained from the loading path.

1.2 Defining strain

For a pressuremeter which measures the radius of the expanding cavity the conversion from displacement to strain is $[R-R_0]/R_0$, where R is the current radius of the cavity and R_0 is the original radius of the cavity *in the insitu state*. This is simple strain and when displacements are measured at the borehole wall is termed cavity strain, ε_c.

R_0 can be approximated by the at rest radius of the instrument. The preferred approach is to identify when the applied pressure has reached the insitu lateral stress, and interpolate from this the corresponding radius which then becomes R_0.

Note that although the pressuremeter measures the radius of the cavity wall, ε_c is actually circumferential strain. It is usually expressed as a percentage.

Figure 2 shows how pressures and strains in the expanding borehole are defined.

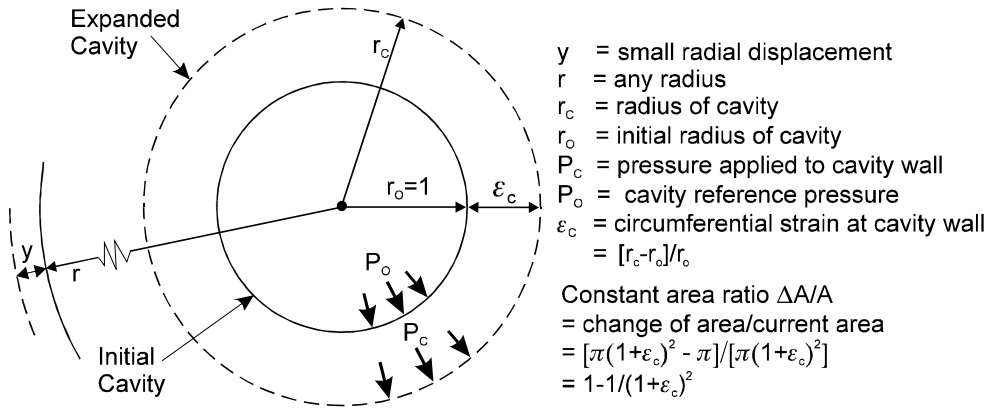

FIGURE 2. Pressures and strains around the expanding cavity

The other strain which is commonly used is the constant area ratio, which is shear strain. As figure 2 indicates it can be expressed in terms of simple strain.

1.3 Average displacements versus the output of the separate axes

Although there are a number of displacement sensors in the probe recommended practice is to quote parameters from the average displacement curve. This is for two reasons:

1. The reference for the measured displacements is the body of the instrument itself - trying to separate the individual axes means assuming that the body of the instrument remains fixed at all times, which is not realistic.

2. All available analyses assume isotropic properties in the surrounding soil, and only the average pressure/strain curve represents this condition.

These remarks assume that the instrument is in full working order throughout the test - failure of a displacement follower means that alternative strategies must be adopted.

The significance of the first point above has been demonstrated by an examination of cycles of unloading taken from separate arms (Whittle 1993) and by work with the six arm version of the SBP(Whittle et al 1995). The response of the separate arms yields clues to the initial stress state in the surrounding soil mass, allowing an assessment of the degree of insertion disturbance.

1.4 The analysis program

We use (and supply to others) software for analysing a pressuremeter test. The program is called **INSITU,** it has been in use for a number of years and is well proven.

To use the program the user must first read in a text file of test data in engineering units. The program needs to know the type of instrument being used, and the user may choose to enter additional background information about the test.

The next task is to identify for the program the nature of the individual data points. Broadly, speaking the options are these:

- a point can be part of the expansion curve
- or part of a reload loop
- or part of the contraction curve
- or none of the above. This might mean a 'rogue' data point, but it is more likely to be true of parts of the loading where the expansion was slowed prior to taking an unload/reload cycle. Data points recorded at this time are neither part of the expansion nor part of a cycle, and should be identified as such.

There is a quick on-screen routine for marking the points. Once marked, they appear in different colours and have different shapes (so that the distinction can be made clear on a black and white printout). Most of the analyses use a limited set of the available data - for example the Gibson & Anderson analysis for undrained shear strength uses only points on the expansion curve.

The program implements all the standard analyses mainly in a graphical form. As figure 1 implies, there are significant changes of gradient in the pressure/strain curve which denote critical soil parameters. The user of the program is provided with on-screen tools to mark these breakpoints or to obtain the slope of the loading curve. The tools can be visualised as rulers, and the chosen position of any ruler is stored by the program in the file of test data. The evidence for any derived parameter is a screen dump of the appropriate analysis which shows the position of any rulers set by the user and quotes the parameter obtained.

Even when the user declines to make a choice it is good practice to provide the screen dump as evidence of why a choice is difficult.

The results for a test appear as a summary sheet of derived parameters followed by a number of plots showing the application of the various procedures.

Sometimes analyses are required which are not included in the INSITU program. In such instances commonly available spreadsheet software is used to implement the new analysis. Inevitably in such circumstances there is some risk of human error affecting the conversion of data in engineering units to the form required for analysis. INSITU has comprehensive export facilities and wherever possible is used as the data source for the spreadsheet.

2. Analyses for expansion

2.1 Overview

The pressuremeter test is a sequence of measured co-ordinates of pressure and displacement of the cavity wall (once suitable corrections have been made to compensate for the response of the elastic membrane).

In order to solve the boundary problem, an origin for the expansion has to be determined. For insertion methods which imply stress *relief*, the origin is taken to be the point where insitu

conditions are restored to the cavity. This means that an estimate of the insitu lateral stress has to be made, and the measured radius of the cavity at the point where the insitu lateral stress is restored is used to convert subsequent displacements to strain.

For a self-bored pressuremeter test it is possible to recognise the insitu lateral stress by inspection, the so-called lift-off method. In addition it is possible to recognise by inspection the shear stress limit (the point marked P_f in figure 1) as this is signified by the onset of a markedly non-linear response. An iterative procedure first suggested by Marsland & Randolph (1977) allows the insitu lateral stress to be inferred.

Once the origin is known, the expansion phase of the test can be used to determine the material shear strength. For an undrained expansion the classic procedure is that developed by Gibson & Anderson (1961) where the slope of the pressure /strain curve plotted on semilog axes gives the shear strength directly and an estimate of the ultimate limit pressure. In most circumstances the assumption of failure at a constant shear strength is reasonable, but the complete shear stress:shear strain response of a material deforming under undrained conditions can be described by employing the analysis due to Palmer (1972).

For materials where the expansion is drained, so that there are volumetric as well as shear strains to take into account, the analysis due to Hughes et al (1977) is used to derive the peak angle of internal friction and dilation. Manassero (1989) is a more complex analysis that offers a complete description of the shear strain versus volumetric strain response of a material deforming under drained conditions.

Estimates of shear modulus are obtained either from the slope of the pressure/strain curve at places where elastic response can be assumed, or (preferably) from the slope of the chord which bisects small rebound cycles. The values for shear modulus obtained in this second manner are repeatable and seem to be largely independent of any disturbance caused to the material by the placing of the pressuremeter. It is important, however, to correlate the measured stiffness with the strain range covered by the rebound cycle.

2.2 Estimating the insitu horizontal stress

There are a number of strategies available for deriving an origin. Two are considered here:-

- **LIFT OFF** (Soft ground self boring pressuremeter only)
- **MARSLAND & RANDOLPH 1977** (Modified **Hawkins** et al 1990)

Both methods are outlined by Mair & Wood (1987). Note that these methods amount to obtaining a value for the cavity reference pressure, P_o. It is impossible to measure the insitu lateral stress σ_{ho} because the act of placing instrumentation must result in some disturbance, no matter how small. The methods above are indirect indicators for determining σ_{ho}. It is open to question whether the reference stress is equivalent to the insitu lateral stress, and it is usual to bring a range of evidence to bear in order to decide if a particular value for P_o is also a plausible value for σ_{ho} . External evidence might take the form of using the derived reference stress within a K_O calculation, or checking that the derived vertical/horizontal anisotropy can be supported by the material shear strength i.e.

$$\sigma_{ho} - \sigma_{vo} < 2C_u \; . \qquad \text{.....[1]}$$

The software is so arranged that the analyst must make an explicit choice of σ_{ho} the result being the 'best estimate' which is quoted on the results summary sheet. Having decided on the best estimate the displacement offset interpolated from this stress is treated as the origin for the expansion.

2.2.1 Lift-off:

This method is applicable only to the Cambridge Self Bored Pressuremeter. In principle it is a straightforward analysis; the instrument is assumed to be bored into the ground with insignificant disturbance to the surrounding material. As a consequence of this assumption the insitu conditions around the instrument remain unchanged by the insertion process; hence the pressure at which the membrane is first observed to move and the cavity to expand is P_o and the corresponding cavity diameter will be the same as the at rest diameter of the instrument.

Because the initial part of a SBP test is very stiff the choice is made from an enlarged view of the first 0.2mm (0.5% strain) of the expansion. Difficulties arise because the instrument has a finite stiffness and hence there is sometimes instrument compliance to be separated from the expansion of the cavity. In addition the instrument is being externally pressurised by the lateral stress when the test is started. This external load tends to deflect the arms of the instrument and reveals any imperfections in the seating of the arms. The imperfections, in effect small apparent movements, are revealed when the pressure differential across the membrane is equalised, i.e. exactly at the point where the likely cavity reference pressure is reached.

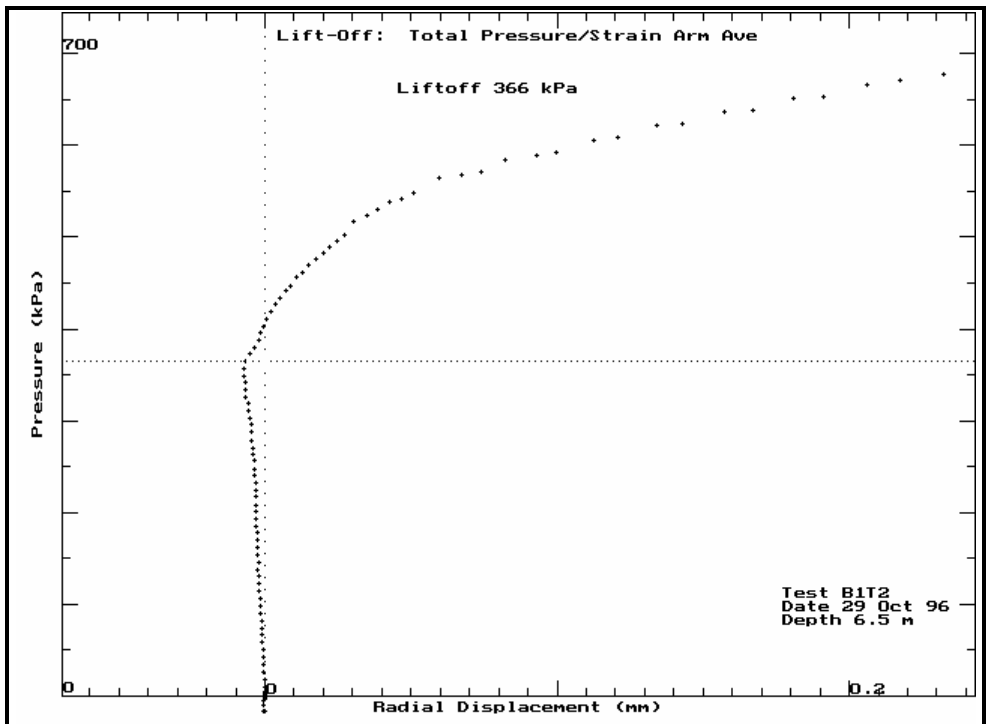

FIGURE 3. AN EXAMPLE OF LIFT-OFF

In a simplistic approach these arm 'signatures' could be considered as positive indications of the reference pressure. However it is not possible to have movement without some accompanying change in stress, which will add to or subtract from the reference pressure.

As a result of finite instrument stiffness and small movements from the displacement sensors applying the lift-off analysis means that there is sometimes uncertainty attached to identifying a plausible reference pressure.

Current practice for coping with this uncertainty is to relax the definition of 'lift-off' to mean something more like 'significant movement'. Mair & Wood (1987) show an illustration of 'lift-off' (page 38, fig.28) where the observed radial strain change from zero to lift-off point (at 265kPa) is 0.5%!. In their example the start of significant movement is indicated by an abrupt change of slope.

If the strict definition of 'lift-off' could be applied then no assumptions concerning soil response are required. Accepting that some movement takes place prior to ‘lift-off’ implies that assumptions be made about the mode of deformation. In the less rigorous application of 'lift-off' it is important that the analyst identifies the onset of plastic behaviour as a guide to deciding that some conspicuous change of form in the loading curve at a lesser stress is likely to be P_o. Our plots would still refer to such a break point as 'lift-off' but clearly it is something else, P_o by inspection perhaps.

The correct use of the Strain Control Unit can assist in this process. Initially the unit is set to input pressure into the probe at a rate that is too low to allow expansion at a constant rate of strain. Hence this part of the expansion is by default stress controlled and the initial elastic response from the soil is indicated by equally spaced data points along the displacement and pressure axes. As the soil response becomes plastic the SCU is gradually able to initiate constant strain rate expansion. There is a transition period where the pressure rate remains regular but each increment of pressure has an increasing effect on the displacement until eventually the displacement rate becomes constant. Thereafter the rate of pressure advance steadily reduces as the plastic zone around the pressuremeter increases. This changeover phase shows up clearly in a plot of total pressure versus time, and can be helpful for identifying yield.

The six arm SBP allows a fuller appreciation of the initial stress state around the instrument. The early part of the test, when the circumferential stress still exceeds the radial stress, is the only part of the test where the behaviour of the separate arms is more informative than the averaged output. The six arms allow average, pairs and individual arms to be inspected, and it is clear that in over-consolidated material the observed variations in behaviour of the separate arms invalidate the assumption of minimal disturbance. It is invariably the case that when one arm shows a very high lift-off stress, its opposite partner shows a very low level. This indicates insertion disturbance, due either to the drilling process itself or to imperfect vertical alignment of the probe. Axes which read similar on both sides are accorded greater significance in the analysis than axes which read very different. For further information see Whittle et al (1995).

2.2.2 Marsland & Randolph (1977) Analysis

Marsland & Randolph analysis relies on being able to identify the onset of plastic behaviour, the yield stress P_f. The argument is as follows:

- that in the vicinity of the insitu lateral stress the soil behaves elastically and therefore the pressure/strain plot will be linear
- that this elastic behaviour will cease when the undrained shear strength of the soil is reached in the wall of the cavity, and hence the pressure /strain plot will begin to curve

(see Figure 1).

This can be expressed as: $P_f = P_o + C_u$ .....[2]

From this it follows that P_o can be deduced by a process of iteration. Initially a guess is made of a value for P_o; using this guess to define a temporary strain origin a total pressure:log volumetric strain plot is then generated in order to derive a value for C_u. The sum of these two parameters is compared with the selected value of P_f. The choice of P_o is then suitably adjusted and the process repeated until a match is found. It is a straightforward matter to carry out this procedure on the computer.

The modified method in current use is a response to the difficulty that the Gibson & Anderson model is too simple for use in most materials and yield may occur at a shear stress that is different from the large strain shear strength. Hawkins et al (1990) suggested that the most appropriate choice was that value of shear stress pertaining at the apparent onset of plasticity, so that equation [2] above now becomes:

$$P_f = P_o + \Upsilon_f \quad .....[3]$$

Υ_f can be obtained from a total pressure:log volumetric strain plot by selecting the slope at the pressure and strain corresponding to the choice of P_f (in practice, using the Palmer (1972) argument to identify the mobilised shear stress at failure).

The analysis is implemented graphically, using a number of rulers to identify significant points on the curve. See Fig. 4 for an example.

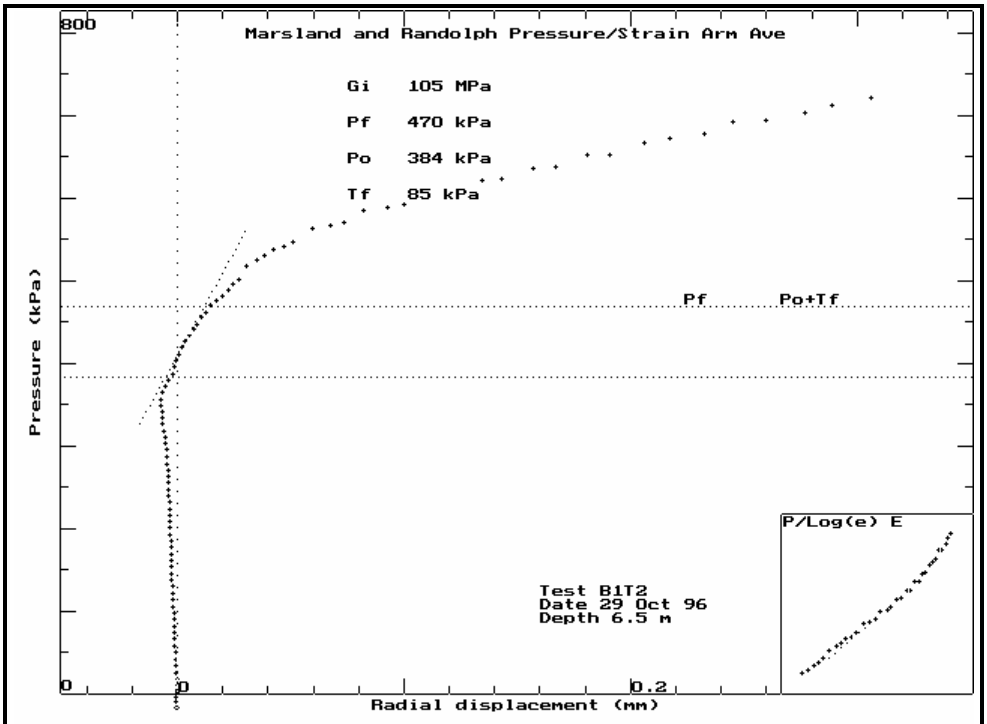

FIGURE 4. AN EXAMPLE OF THE MARSLAND & RANDOLPH ANALYSIS

There are a number of problems.

- There can a choice of slopes for G_i , giving two possibilities for P_f . In practice the first slope encountered is usually too stiff to make a credible choice for G_i and is probably an indication of insertion disturbance.

- The assumption of simple elastic response - in practice most soils exhibit marked non-linear elastic characteristics, so that the pressure at which the material appears to go fully plastic is more than one increment of shear strength above P_0 - this point is developed later.

- The original analysis was developed as an aid to the interpretation of pre-bored pressuremeter tests where the process of forming the pocket results in the complete unloading of the cavity prior to the test commencing. It is certain therefore that the soil has seen stress relief. It is arguable whether in these circumstances that the yield point remains unchanged, as more than elastic unloading has taken place. However the form of such tests does tend to give an unambiguous choice for the onset of plasticity.

- In a self bored pressuremeter test the situation is not so clear cut. The very factors that make the test desirable also results in more realistic behaviour being seen in the form of the early part of the test, with non-linear elasticity being a feature. Hence a choice of P_f is by no means easy. In general the better the test the harder such a choice becomes. However it is probable that in a good test the lift off pressure would be a credible choice so that in the wider context it is not a serious problem.

A disturbed SBP test does not necessarily imply stress relief. Typically disturbance arises out of damage to the shoe cutting edge; if the shoe is enlarged then stress relief will result. However if the shoe is damaged in such a way that it cuts undersize then stress increase will take place and plasticity will be masked by a rise in the pore water pressures around the instrument. In this event the analysis can contribute nothing.

2.3 Undrained shear strength (C_u)

There are two analyses for deriving estimates of undrained shear strength :

- **Gibson & Anderson (1961)**
- **Palmer (1972)**

Usually only parameters derived from the Gibson & Anderson analysis are quoted, although plots of the Palmer analysis may be supplied.

2.3.1 Gibson & Anderson (1961) - Prior to yield, the assumption of linear elastic behaviour means that pressures and strains measured at the borehole wall are related by

$$P - \sigma_{ho} = (\Delta\gamma)G \qquad \ldots.[4]$$

where P is the total pressure applied to the cavity wall. For pressuremeters which measure changes in volume such as the Ménard probe for which the Gibson & Anderson solution was developed, shear strain γ is the change in volume divided by the *current* volume, usually expressed $\Delta V/V$. For pressuremeters which measure the radius of the cavity wall, γ is the change in area divided by the *current* area, $\Delta A/A$. Because plane strain expansion is assumed both expressions are identical.

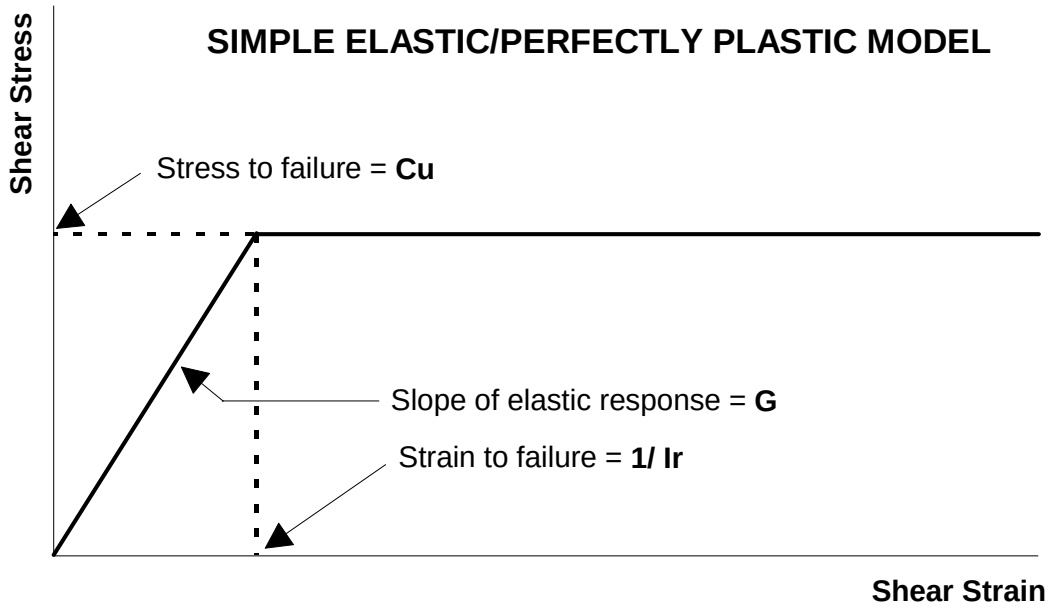

FIGURE 5.

For pressures which exceed the yield stress of the soil, the simple elastic/perfectly plastic solution is usually expressed in terms similar to the following:

$$P - \sigma_{ho} = C_U\{1+Ln[(G/C_U)(\Delta V/V)]\} \quad \ldots.[5]$$

Strictly, equation [5] is a simplified version of the Gibson & Anderson solution developed by Windle & Wroth (1977). The ratio G/C_U is the inverse of the elastic shear strain required to reach the fully plastic condition, and is often replaced with the term I_R meaning index of rigidity.

Equation [5] can also be written:

$$P - \sigma_{ho} = C_U[1-Ln(1/I_R)+Ln(\Delta V/V)] \quad \ldots.[6]$$

From this it is clear that the change from simple elastic to perfectly plastic response occurs at a shear strain $1/I_R$ at which point the log terms in equation [6] cancel and $P - \sigma_{HO}$ equals the undrained shear strength C_U.

The limiting pressure P_{Limit} at which indefinite expansion of the borehole occurs is given by

$$P_{Limit} - \sigma_{ho} = C_U[1+Ln(G/C_U)] \quad \ldots.[7]$$

Equations [5] and [7] can be combined to give the result

$$P = P_{Limit} + C_U Ln[\Delta V/V] \quad \ldots.[8]$$

This is a particularly convenient form of the solution with the undrained shear strength and limit pressure being the gradient and intercept respectively of a plot of total pressure against the natural log of the shear strain at the cavity wall.

The analysis assumes a constant shear strength, so the slope chosen should be that which best fits this assumption. There is no theoretical justification for selecting a slope at a specific strain and claiming this to be C_u. If the plot indicates that the gradient of the plastic phase is not more

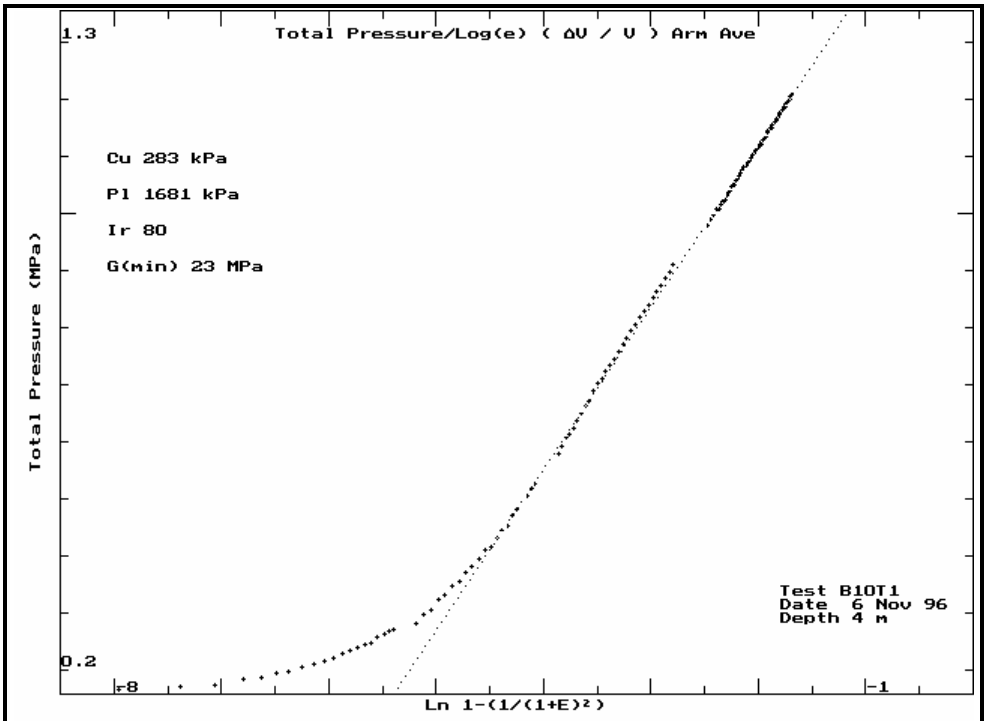

FIGURE 6 The Gibson & Anderson Analysis

or less constant then the assumptions underpinning the analysis have been violated, and other strategies must be adopted.

Equation [7] shows that if P_L , P_0 , and C_U are known then the rigidity index I_R and the shear modulus at yield strain G_{yield} can be determined without going outside the analysis for additional data. This has been done for the example plotted in Figure 6. The rigidity index and the modulus value derived in this fashion are plausible, suggesting that the origin for strain is not far from the truth. However caution should be applied before using these parameters as they stand. The slope of the semi-log plot is relatively insensitive to the choice of initial conditions so the value for shear strength is always better conditioned than other parameters. The analysis is also sensitive to the assumptions concerning the mode of deformation. A non-linear elastic response will increase the elastic contribution of the material and will affect the value for I_R and G_{yield} accordingly.

2.3.2 Palmer

The Palmer analysis (1972) is an example of more information being obtained from the pressuremeter test if fewer assumptions are made. The analysis shows that the pressure:strain graph is the integrated shear stress:shear strain curve. Taking the slope of the pressure:strain graph at any point gives the mobilised shear stress directly, and allows the complete shear stress:strain curve to be plotted. In terms of cavity strain the shear stress Υ is:

$$\Upsilon = \tfrac{1}{2}\varepsilon_c(1+\varepsilon_c)(2+\varepsilon_c)dP/d\varepsilon_c \quad \text{....[9]}$$

More conveniently, perhaps, equation [9] can also be written in terms of volumetric strain as:

$$\Upsilon = dP/d[\ln(\Delta A/A)] \quad \text{....[10]}$$

This implies that the gradient at any strain of the semilog plot used for the Gibson & Anderson analysis gives the mobilised shear stress directly. The example in Fig. 7 is the same test as Fig.6:

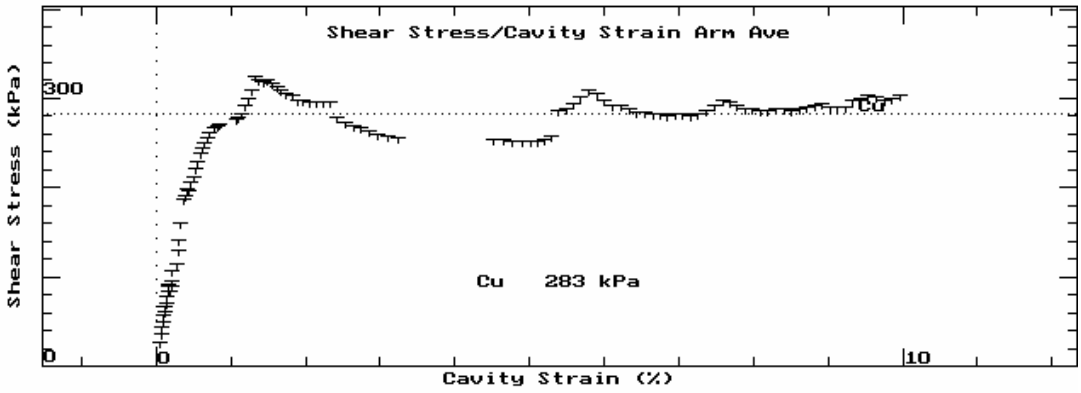

FIGURE 7. AN EXAMPLE OF THE PALMER (1972) ANALYSIS

The analysis is awkward to implement on the computer because the differentiation process highlights any irregularities in the data. This is especially irritating because the stress strain response must be a smooth curve. Possible strategies involve curve fitting the measured data prior to applying the solution, but this may be a mistake. Minor changes of gradient on the loading path are usually not random, but a response to some event such as the taking of an unload/reload cycle.

If the material does indeed deform in the manner required by Gibson & Anderson then the two analyses give identical answers. Included on the plot is a horizontal ruler marking the value of shear strength obtained from applying the previous Gibson & Anderson analysis. If there are clear indications of peak and residual shear strength then additional horizontal rulers are available to mark these values. However the true value of the plot is that it is a 'map' of the shear stress, and it is the form of the complete curve which is of interest.

The analysis is very sensitive to insertion disturbance - in particular insufficient allowance for stress relief will give an apparent peak in the stress/strain response.

2.4 Shear stress of sands

There are two significant analyses available for describing the shear stress/shear strain behaviour of sand:

- **Hughes et al (1977)**
- **Manassero (1989)**

2.4.1 Hughes et al (1977)

In addition to the usual conditions governing the expansion of a cylindrical cavity in plane strain this analysis assumes the following:

- A simple elastic/perfectly plastic model
- The expansion is fully drained, i.e. no pore water pressures are allowed to develop
- Following yield the sand deforms at a constant angle of internal friction
- Volumetric and shear strains are connected by Rowe’s dilatancy law (1962)

Rowe's dilatancy law can be expressed as:

$$[1 + \sin \phi'/1 - \sin \phi'] = [1 + \sin \phi'_{cv}/1 - \sin \phi'_{cv}][\ 1 + \sin \Psi/1 - \sin \Psi] \quad ....[11]$$

where ϕ' is the peak angle of internal friction
ϕ'_{cv} is the critical state angle of friction
Ψ is the angle of dilation.

At failure the effective pressure p' is :

$$p' = \sigma'_{ho}(1 + \sin \phi') \quad ....[12]$$

following failure:

$$\ln [p'] = S\ln[(\varepsilon_c /(1+\varepsilon_c) + c/2)] + A \quad ....[13]$$

where A is a constant
S is $[(1 + \sin \Psi) \sin \phi']/(1 + \sin \phi')$
c is a small elastic strain that has been shown (Hughes et al, appendix) to be negligible.

Equation [13] indicates that *s* is approximately the gradient of effective pressure plotted against cavity strain on log scales. Once obtained, both $\sin \phi'$ and $\sin \Psi$ can be derived:

$$\sin \phi' = S/[1 + (S -1) \sin \phi'_{cv}] \quad ....[14]$$
$$\sin \Psi = S + (S -1) \sin \phi'_{cv} \quad ....[15]$$

The factor c/2 is usually ignored - it has been shown to introduce an error of about 0.03% in the strain scale for a typical dense sand, a negligible amount.

Withers et al (1989) shows that the same argument leads to a complete expression for the loading path, as follows:

$$p' = [2\sigma'_{ho} /(1+N)][(G/\sigma'_{ho})(1+n)[(1+N)/(1-N)]\ \varepsilon_c + (1-n)/2]^{[1-N/1+n]} \quad ....[16]$$

where n is $(1- \sin \Psi)/(1 + \sin \Psi)$
N is $(1- \sin \phi')/(1 + \sin \phi')$ and is the ratio of the minor to major principal effective stresses at failure.

Note that the power term [1-N]/[1+n] is the gradient of the log-log plot.

An example of the Hughes analysis is shown in Fig. 8. Note that both the ambient pore water pressure u_o and ϕ'_{cv} are required to implement the analysis. Because the expansion is drained the membrane normally collapses at the head of water pressure, and an estimate of u_o can often be made from this behaviour. ϕ'_{cv} must either be given or estimated.

Deciding on the strain origin for a test in sand is a problem. It is rarely the case that membrane lift-off gives a plausible value for σ_{ho} so a value has to be inferred. Despite the theoretical inappropriateness , the modified Marsland & Randolph method is often used to give an

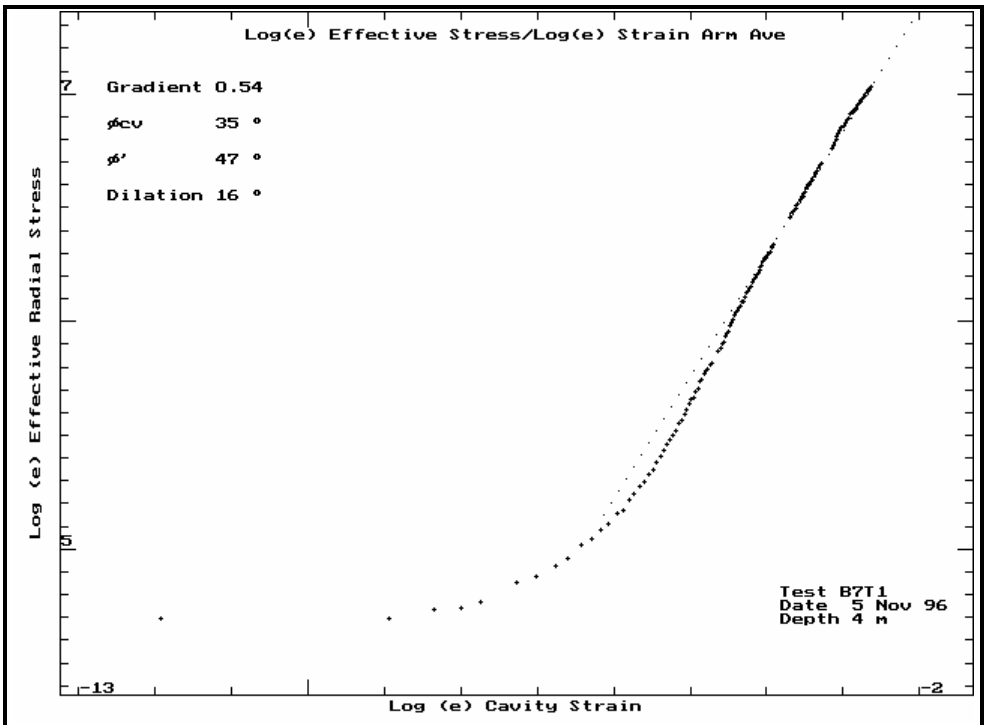

FIGURE 8. EXAMPLE of HUGHES et al (1977) SANDS ANALYSIS

estimate. Because the material is only just plastic at the point where the failure shear stress is derived, the error is likely to be small.

Hughes et al assume a single value for the peak angle of internal friction throughout a typical SBP test, but this is often not the case. We have found that in dense sands the pressuremeter test often expands sufficiently to indicate a plateau in the shear stress, suggesting that the sand is approaching critical state.

2.4.2 Manassero (1989)

This analysis is a numerical procedure that essentially makes the same assumptions as that of Hughes et al (1977). The difference is that Rowe's dilatancy relationship is employed as a flow rule, so that the requirement for deformation at a single value of friction angle is not necessary.

The great advantage of this analysis is that it can produce a comprehensive stress/strain curve analogous to that of the Palmer (1972) analysis for an undrained expansion. The disadvantage is that the numerical method is very sensitive to minor fluctuations in the measured data. Manassero suggests that the measured data be fitted with a polynomial function prior to implementing the numerical calculations. However a polynomial curve is wrong in concept and better results can be obtained by employing a hyperbolic function.

The pressuremeter test provides data for the radial pressure and circumferential strain at the wall of the cavity. The radial strain ε_R at a point (i) corresponding to a measured data point of circumferential strain ε_C and effective pressure P is as follows:

$$\varepsilon_R(i) = \frac{p(i)[\varepsilon_C(i-1) + k_a^{cv}\varepsilon_R(i-1)] - p(i-1)\varepsilon_C(i)}{2[p(i)(1+k_a^{cv}) - p(i-1)]} + \frac{p(i)[\varepsilon_C(i-1) - \varepsilon_R(i-1)] + p(i-1)[\varepsilon_R(i-1)(1+k_a^{cv}) - \varepsilon_C(i)]}{2k_a^{cv}\,p(i-1)} \quad \text{....[17]}$$

where k_a^{cv} is $1/k_p^{cv}$ and k_p^{cv} is $\frac{1+\sin\phi_{cv}}{1-\sin\phi_{cv}}$, the constant volume stress ratio coefficient .

Equation [16] is solved for each data point in turn, knowing that the expansion starts from zero strain.

Once the radial strain is known, volumetric strain ε_V and shear strain ε_γ can be obtained as follows:

$$\varepsilon_\gamma = \varepsilon_R - \varepsilon_C \quad \text{....[18]}$$
$$\varepsilon_v = \varepsilon_R + \varepsilon_C \quad \text{....[19]}$$

Further more the principal stresses are connected by:

$$\frac{\sigma_R}{\sigma_C} = -k_p^{cv}\frac{d\varepsilon_c}{d\varepsilon_R} \quad \text{....[20]}$$

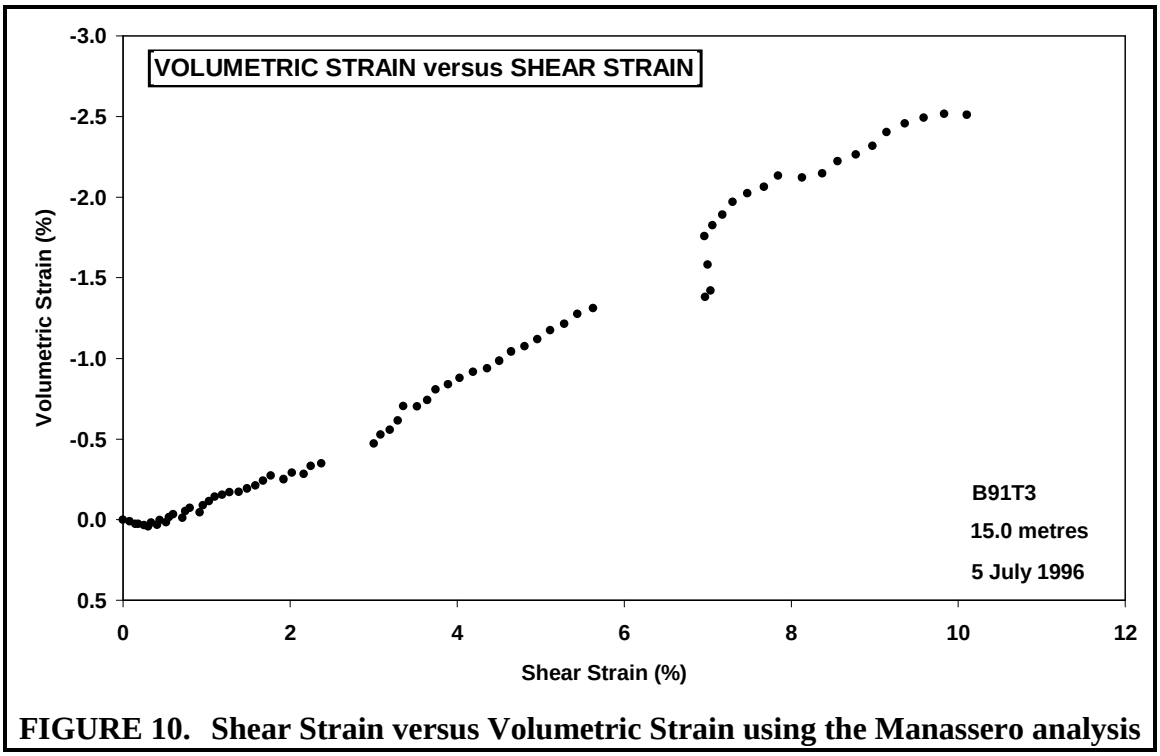

FIGURE 10. Shear Strain versus Volumetric Strain using the Manassero analysis

The following figures show shear strain plotted against shear stress, stress ratio and angles of friction and dilation:

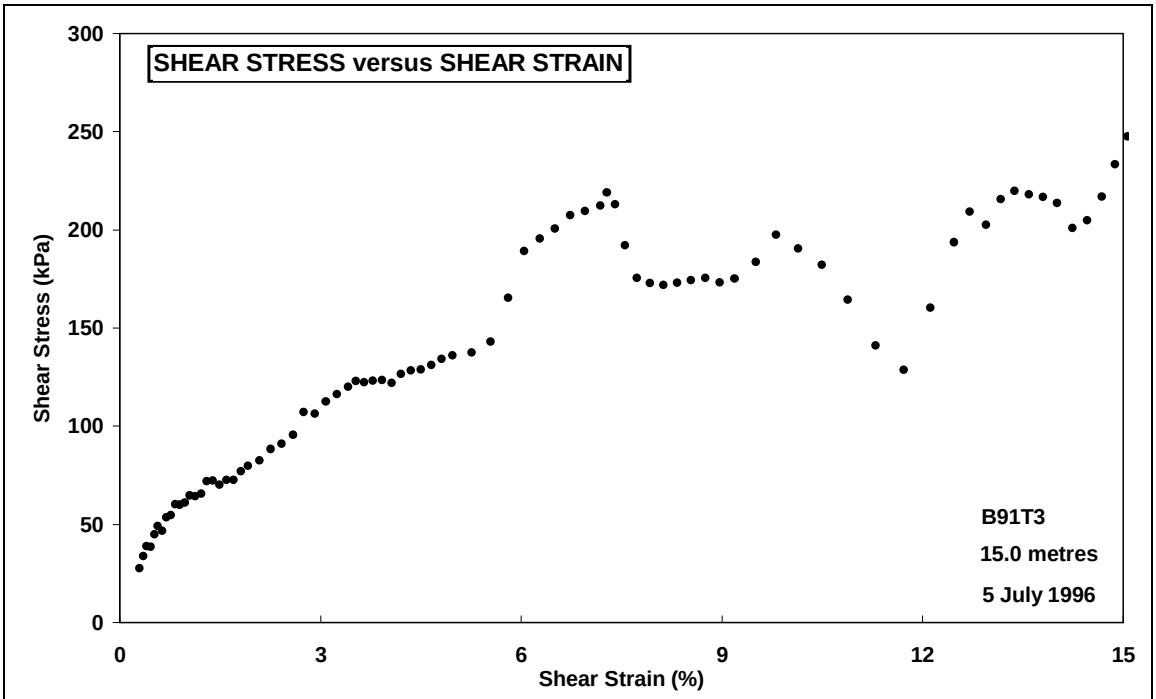

FIGURE 11. Shear stress versus shear strain using the Manassero analysis

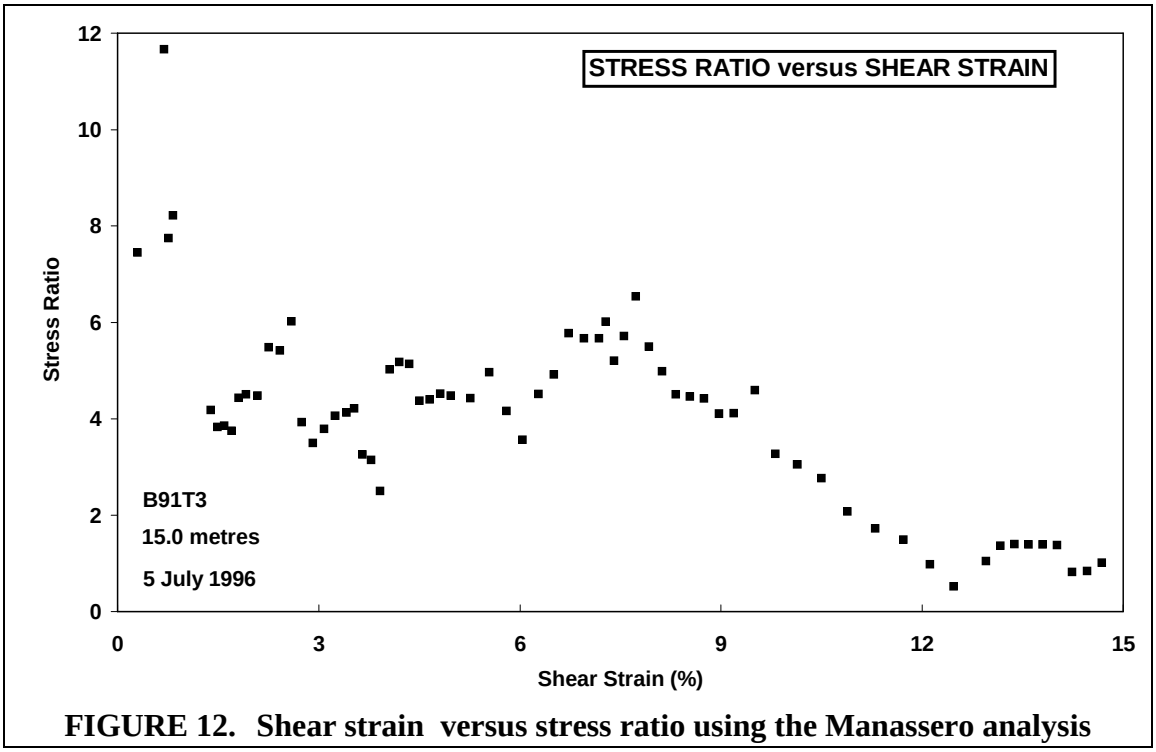

FIGURE 12. Shear strain versus stress ratio using the Manassero analysis

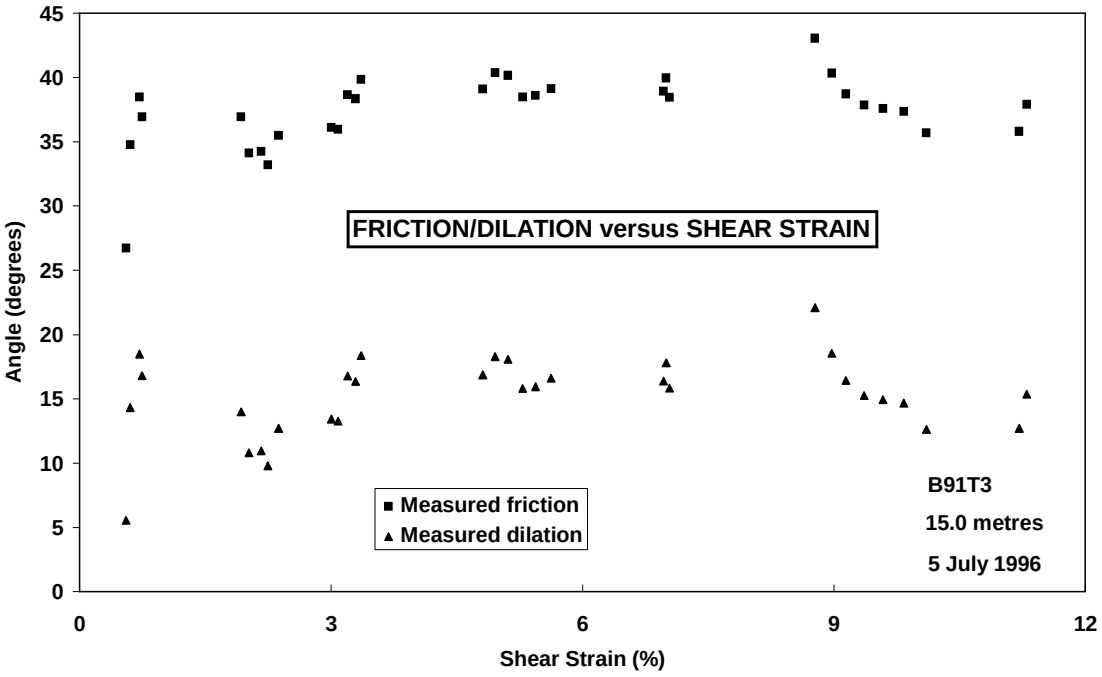

FIGURE 13 Shear strain versus angles of friction & dilation, Manassero analysis

For both the Hughes and the Manassero, values for critical state friction angle and ambient pore water pressure must be given before either analysis can be implemented. If the expansion is taken far enough, it appears to approachn a state of constant volume expansion. Using a technique suggested by De Sousa Coutinho (1990) in a similar way to Manassero, it is possible to adjust the value of $\varnothing_{cv}$ until consistent parameters are achieved.

3. Shear Modulus

There are four parts of the pressuremeter curve capable of providing information concerning shear modulus:

- From the slope of the initial elastic loading phase
- From the slope of the chord bisecting small rebound cycles
- From the analysis for shear strength
- From the slope of the first part of the contraction curve

Whatever method is used to determine shear modulus, the value obtained is strain dependent.

3.1 The Initial Shear Modulus

Shear modulus derived from the slope of the initial part of the loading curve is quoted as part of the Marsland & Randolph analysis (see figure 4). In a self-bored pressuremeter test this can give a reasonable result for shear modulus, but one difficult to identify in terms of the appropriate shear strain.

As figure 1 shows, the calculation for shear modulus G is:

$$G = dP/2d\varepsilon_c \qquad .....[21]$$

Strictly, because the cavity strain ε_c is *simple* strain it is only the initial modulus for which this calculation is true. Once the expansion is underway modified calculations should be used which take account of the change in the reference condition.

3.2 Cycles of elastic unloading and reloading

Graphical plots of the reload loops are the preferred method of obtaining a value for shear modulus. The plots provided show the position of a cursor which has been placed by eye to bisect the loop. The slope of the cursor is the gradient of the reload loop and the program uses this slope to derive a value for shear modulus. This value is quoted in the top left hand corner of the plot together with an indication of the size of the loop expressed as the change of pressure and strain, and the co-ordinate of the centre of the loop. The equation used is:

$$G = [1+\varepsilon_c][dP/2d\varepsilon_c] \qquad .....[22]$$

In addition, the program carries out a regression analysis of the data points which are part of the reload loop. If the loop is good, that is symmetrical and without indications of scatter, then the two values of modulus obtained will be the same. However the regression analysis is sensitive to erroneous data points, which the visual technique can ignore. The value obtained by regression is quoted in the bottom right hand corner of the plot.

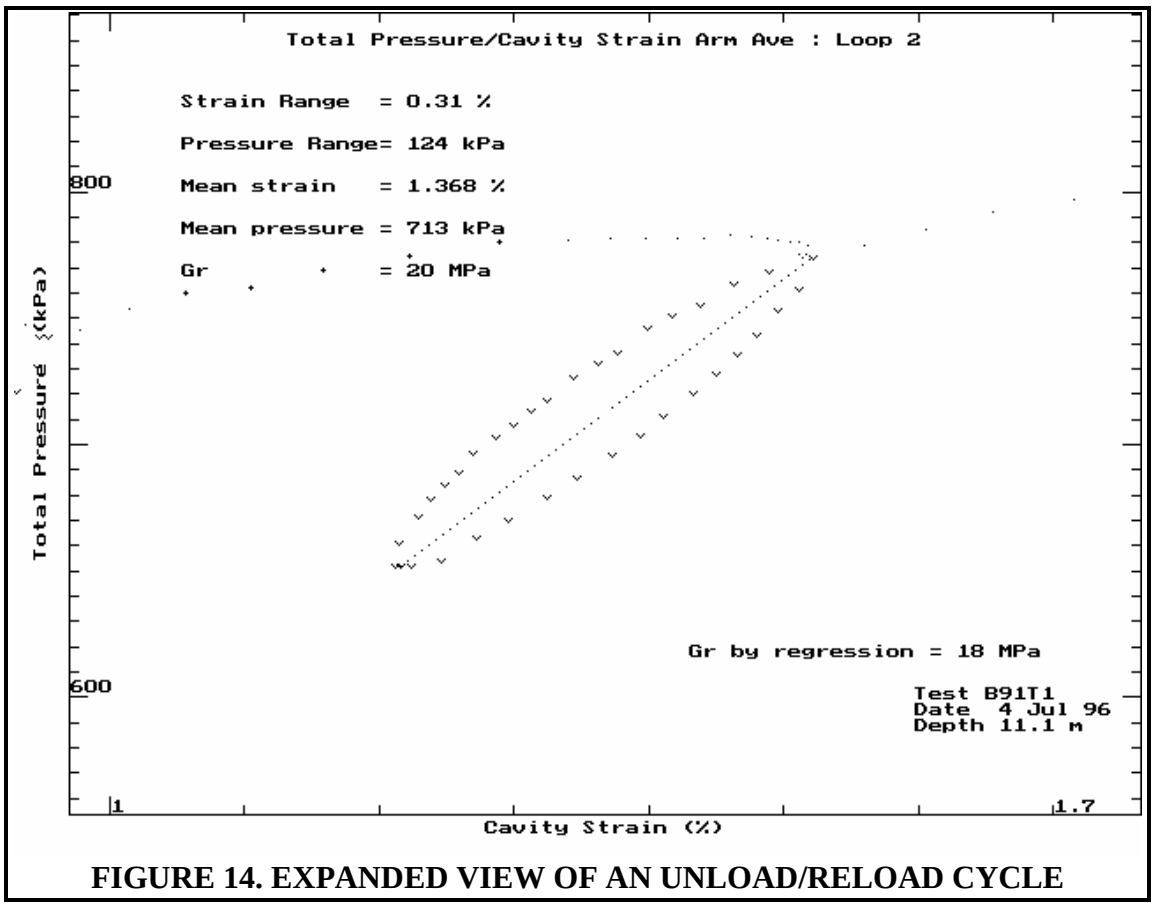

FIGURE 14. EXPANDED VIEW OF AN UNLOAD/RELOAD CYCLE

It is important that the effects of creep (for whatever cause) be minimised before starting the cycle, and in Fig. 14 'deleted' points before the start of the unloading show where the pressure in the probe was held for a period of time.

3.3 Non-linear stiffness/strain response

In recent times it has become widely acknowledged that the stiffness/strain relationship is not linear. The unload/reload cycle can be made to give a comprehensive description of this non-linear relationship by looking at smaller steps of pressure/strain other than the points at the extreme ends of the cycle.

For reasons which are explained in Whittle et al (1992) it is preferable to examine one half of the rebound cycle only, that which follows the reversal of stress in a loop. The lowest recorded value of stress and strain then becomes the origin for subsequent data points until the original loading path is rejoined.

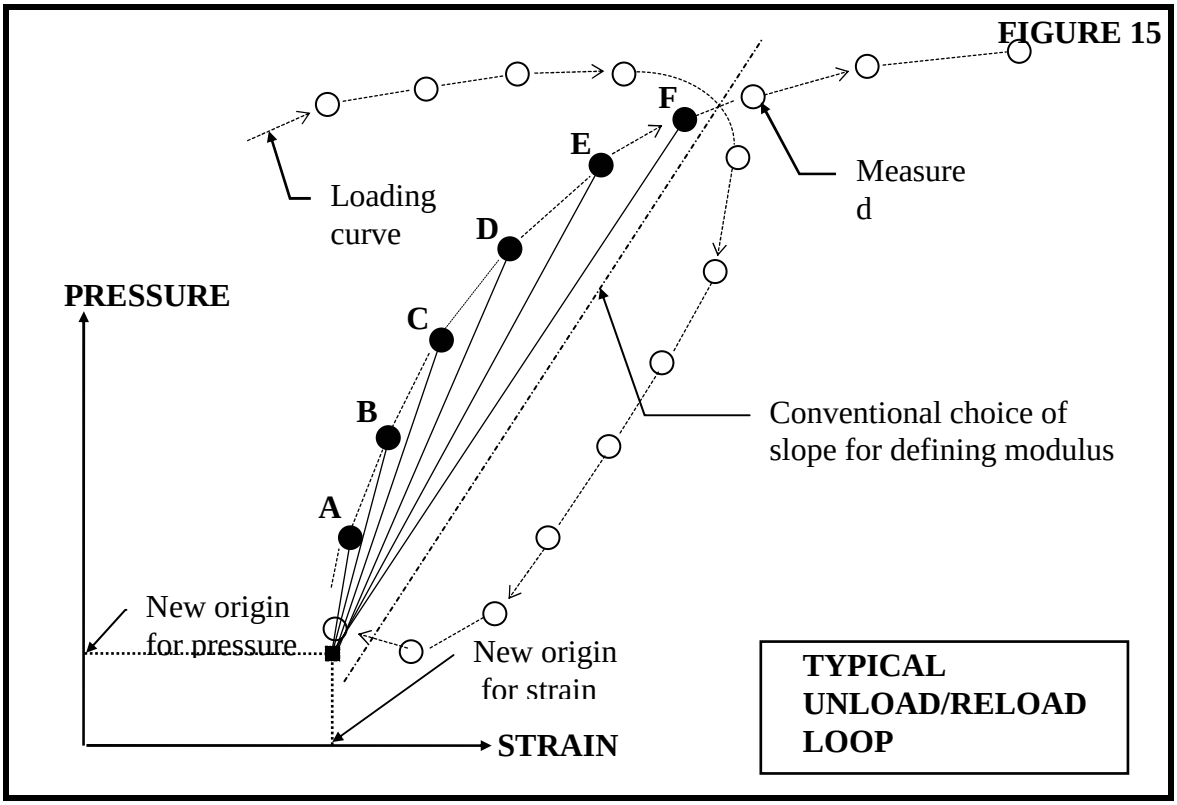

In Fig. 15, once a new origin is defined then every data point on the reloading part of the loop (A, B, C etc.) can be used to give a value for shear modulus. This value can then be plotted against the associated strain increment as measured from the new strain origin.

In Fig. 16 the reloading data from three unload/reload cycles are plotted using the technique described above.

The procedure for deciding the origin is not ideal - even better results for very small strains could be obtained if the origin were decided by inspection. The procedure suggested here is readily implemented on a spreadsheet, however, and means that any person handling the data will obtain identical results.

It follows that it is not necessary to take loops of small strain amplitude in order to obtain small strain stiffness parameters. Indeed it is better to make the cycles as large as possible in order to obtain parameters for as wide a strain range as possible.

It is often stated as a caution that unload/reload loops should have a pressure amplitude no greater than twice the mobilised shear stress (Fig. 1 shows why). Strictly speaking this is true, if one wants to use the whole loop to derive a single modulus parameter as in Fig. 14. However the response is still elastic immediately following the turnover point in the loop, so

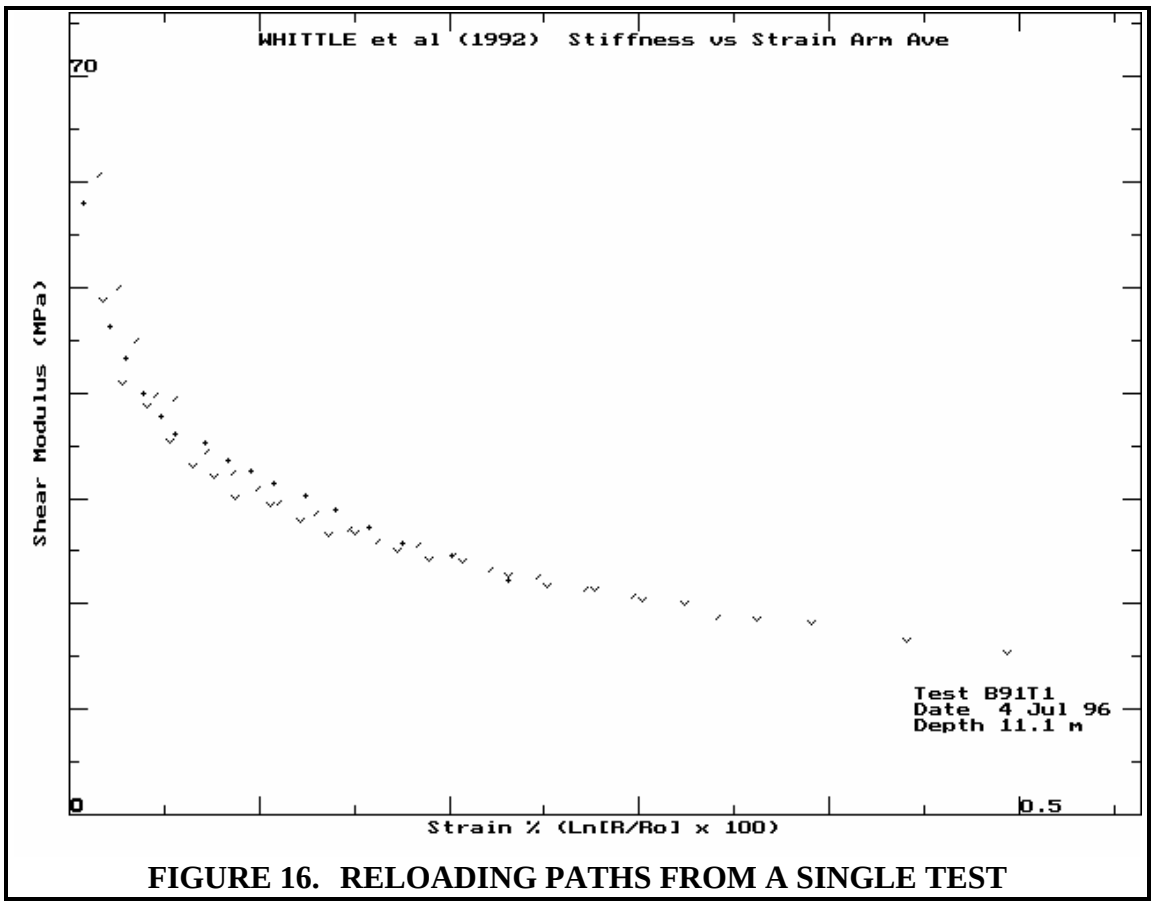

FIGURE 16. RELOADING PATHS FROM A SINGLE TEST

the data is by no means useless if an incremental approach is used. The real penalty for a loop that exceeds the elastic range of the material is a permanent and irrecoverable shift in the strain origin; the loading curve following such a loop is **not** a continuation of the loading path prior to the loop.

Provided the loops were taken at the same effective stress then the data from all will plot the same trend. Conversely, if the loops plot one above the other then this indicates different effective stress conditions which in a clay test would prove that the expansion was not undrained.

The reloading data can also be plotted on axes of log ΔP versus log $\Delta V/V$. Fig. 17 is an example, using the same data as that in Fig. 16. The gradient of the best fit straight line to the data points is used elsewhere as the non-linear elastic exponent. As is evident from the correlation coefficients quoted in Fig. 17 the correspondence to a straight line is excellent.

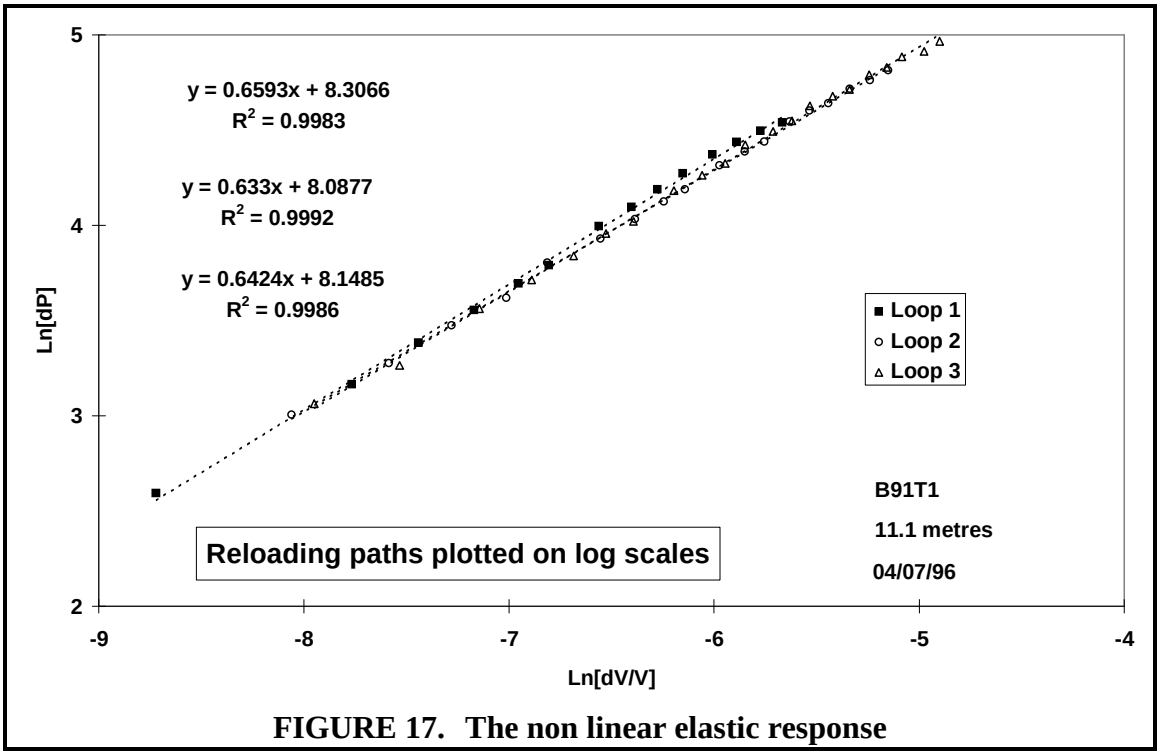

FIGURE 17. The non linear elastic response

The linear relationship between pressure and shear strain on log scales expands to a power law with the general form $\tau = \alpha\gamma^{\beta}$ where τ is the change in shear stress, γ is the corresponding shear strain and α and β are the intercept and gradient of the log log relationship.

One advantage of expressing modulus in this manner is that it gives a means of quoting secant and tangential shear modulus directly from any elastic shear strain. Given that at the borehole wall
$P = \tau/\beta$ and pressuremeter modulus G_p is P/γ (equation 21) then the variation of reload modulus with strain is given by

$$G_p = \alpha/\beta\ \gamma^{\beta-1} \quad \ldots.[23]$$

The secant shear modulus, G_s is given by

$$G_s=\alpha\gamma^{\beta-1} \quad \ldots.[24]$$

Tangential shear modulus G_τ can also be quoted directly from the power law:

$$G_\tau=\alpha\beta\gamma^{\beta-1} \quad \ldots.[25]$$

Note:
When comparing triaxial results with pressuremeter results, invariant shear strain γ_T is given by: $\gamma_T = \gamma_c /\sqrt{3}$ ….[26]

For the purpose of finding the single value of secant shear stiffness governing the pressuremeter response seen in the measured loading curve, G_{100} is required. This is the secant modulus at the

maximum elastic shear strain, sometimes termed G_{min} or G_{yield}. It is probably too conservative a value for design purposes.

There is an alternative way of deriving G_s and G_t from pressuremeter unload/reload cycles, what might be described as the transformed strain approach. If the data points of an unload/reload cycle are used to derive a *pressuremeter* modulus G_P (in effect $\Delta p_c/\Delta\gamma_c$) curve then Jardine (1991) gives two empirically derived expressions for G_s and G_t. The expressions are

$$\gamma_c/\gamma_s = 1.2 + 0.8 \log_{10}(\gamma_c/10^{-5}) \quad \text{for converting } G_P \text{ to } G_s \quad \ldots.[27]$$

and

$$\gamma_c/\gamma_s = 4.5 + 2.65 \log_{10}(\gamma_c/10^{-5}) \quad \text{for converting } G_P \text{ to } G_t \quad \ldots.[28]$$

The effect of applying equations [27] and [28] is to re-calculate the strain at which a given value of pressuremeter modulus applies.

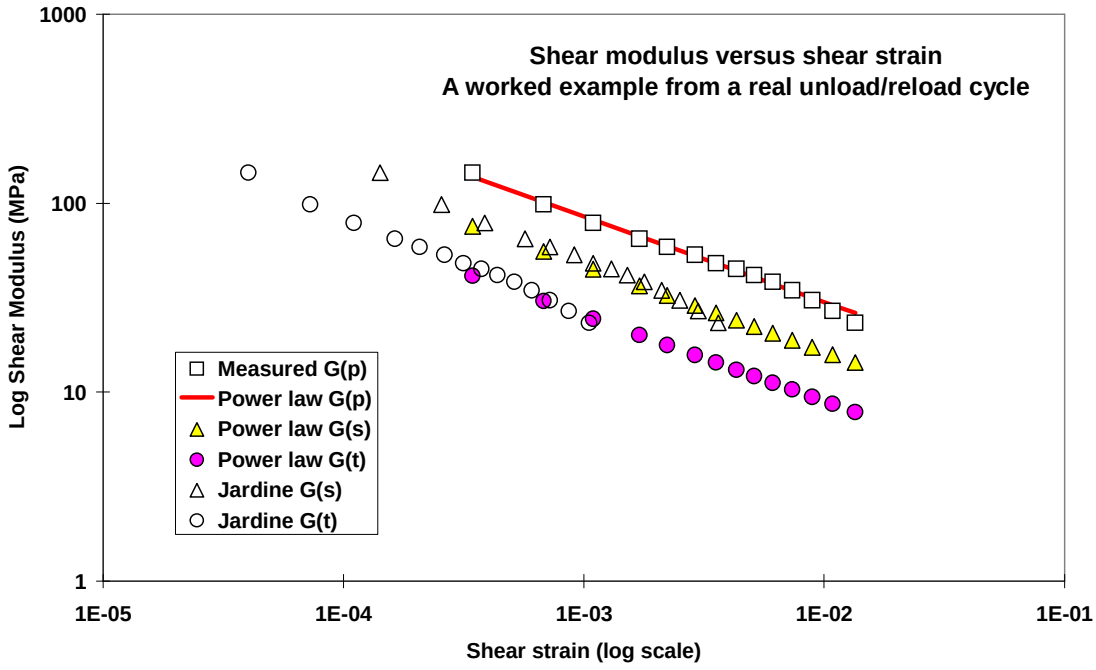

Figure 18 Alternative ways of plotting stiffness strain curves

Fig. 18 shows all these possible ways of quoting modulus applied to a single unload/reload cycle from a pressuremeter test in clay. There is good agreement between the empirically derived Jardine transformations and the rigorous derivatives from the power law expression.

3.4 Stress level

For modulus parameters derived from undrained expansion tests the mean effective stress remains unchanged throughout the expansion and all stiffness:strain data will plot the same trend. Conversely, failure to plot the same trend implies changes in the mean effective stress. This is true of tests affected by consolidation, but is also true of a heavily disturbed loading where the effects of the pressuremeter installation method have yet to be overcome. For such data it is reasonable to take modulus parameters from as late in the loading as possible. Division of the modulus values by a normalising stress such as the effective insitu lateral stress or yield stress gives a dimensionless parameter for modelling purposes.

3.5 Cross hole anisotropy

The pressuremeter test gives values for G_{HH}, the shearing stiffness in the horizontal plane. This is directly applicable to the analysis of radial consolidation or cylindrical cavity expansion due to pile insertion. G_{VH} is applicable all shearing which has an element of deformation in the vertical plane, such as under a footing or round an axially loaded pile.

To convert from G_{HH} to G_{VH} some relationship between the two must be assumed. Wroth et al (1979) suggest that anisotropy arises from two causes:
Structural anisotropy due to the deposition of soil on well defined planes
Stress induced anisotropy, due to the differences in normal stress acting in different directions.

The second cause implies the stiffness in any direction will be a function of the effective insitu stress in that direction, ie a function of K_O.

It can be shown	$G_{HH} = E_H/[2(1+\nu_{HH})]$	....[29]
For undrained expansion	$\nu_{HH} = 1-n/2$	….[30]
and	$n = E_H/E_V = K_O$	….[31]
From this it follows	$E_H = (4-n)G_{HH}$	….[32]
and	$E_V = (4-n)G_{HH}/n$	….[33]

This is as far as argument from first principles can go, because of the additional contribution of the manner in which the material is deposited. K_O is likely to lie between 0.5 and 2, so from equation [32] E_H/G_{HH} lies between 2 and 3.5. From equation [33] E_V/G_{HH} lies between 1 and 1.75.

It is likely that G_{VH} will be linked to E_V by Poisson's ratio in a relationship of the form of equation [29]. Plausible values of E_V/G_{VH} would seem to be 2.4 to 3. Hence in a material with K_O of 2, G_{VH} could be as low as $G_{HH}/3$. Simpson et al (1996) come to the same conclusion, but find in practice heavily over-consolidated London clay gives relationships of the order of $G_{VH} \cong 0.65G_{HH}$. The influence of the strain range is not separately considered in these studies, and it is quite possible that the G_{100} values would be similar in all planes.

Lee & Rowe (1989) give details of the anisotropy characteristics of many clays varying from lightly overconsolidated to heavily overconsolidated. The general conclusion is E_V/G_{VH} lies between 4 and 5, rather more than the isotropic relationship of 3. However their paper was concerned with the impact of anisotropic stiffness properties on surface settlement. Deriving G_{VH} from E_V is therefore unsatisfactory, because although G_{VH} is insensitive to the direction of loading, E_V is not.

In material with a K_O of 1 it is likely that G_{VH} will be the same as G_{HH}. For values of K_O smaller than 1 then the vertical shear modulus G_{VH} may even be greater than the horizontal value.

3.6 Recommendations for manipulating pressuremeter unload/reload data

- Convert all the unload/reload cycle data to a power law expression.
- Derive the parameters for the secant and tangential modulus expressions.
- Decide the shear strain of interest, and derive the appropriate secant and tangential stiffness.

- Determine K_O .
- Given K_O, derive E_H, E_V and G_{VH}.

3.7 Shear modulus from other parts of the pressuremeter curve.

The initial part of the loading will give a value for secant shear modulus, usually referred to as G_i. Provided the insertion disturbance is low this will be a plausible value but affected by the same considerations of stress level and strain range as other parts of the curve.

The first part of the unloading can in principle give a similar parameter but by the time the pressuremeter unloads the creep strains due to consolidation and rate effects will be large, so there will be a tendency for the initial unloading to be too stiff. However provided some allowance is made for this then reasonable estimates of the shear modulus will be obtained.

Analyses such as Bolton & Whittle also imply a value for the secant shear modulus at yield – it will be c_u/γ_{ye}, called G_{ye} in fig.6. Although this is not likely to be the best way of deriving shear modulus data it is important justification for using the analysis that it can predict this independently measurable stiffness.

4. Creep

If, during the loading, the pressure is held constant, the probe continues to expand. This phenomenon is called creep.

The rate of creep decreases with time, and a plot of the creep against the log of the time since the start of the creep becomes a straight line after about one minute. Thus the pressure need only be held constant for 2 – 3 minutes to accurately determine the creep rate.

The two plots that follow, show one such hold and the resulting plot of creep rate.

Figure 19

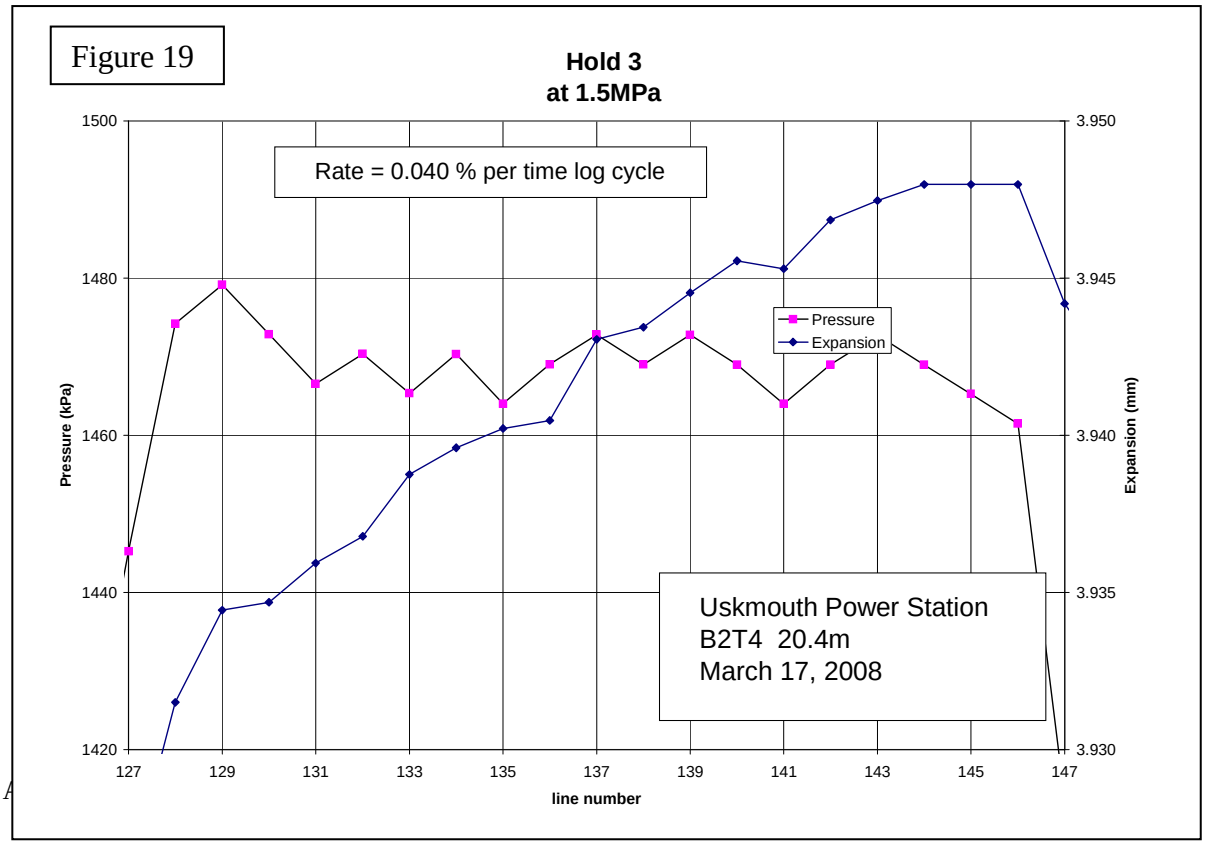

Figure 20

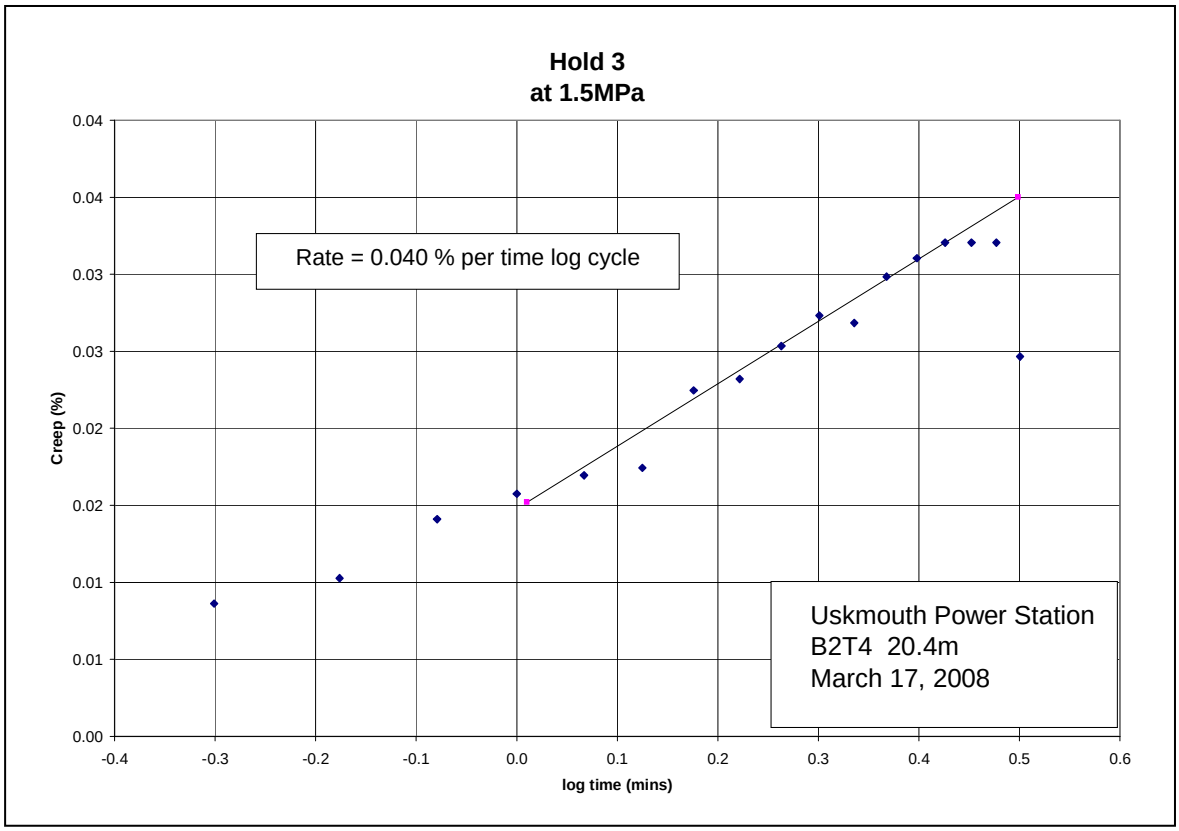

5. Analyses for contraction

5.1 Overview

The contraction method assumes only that the preceding expansion has been taken far enough to overcome the effects of installation disturbance. The end of loading pressure and displacement can then be treated as an origin for the subsequent contraction.

The simple elastic/perfectly plastic response which leads to the Gibson & Anderson solution for undrained expansion has been solved for the contraction by Jefferies (1988) and for the special case where the end of the loading is at limit pressure by Houlsby and Withers (1988).

The procedure described here uses a combination of the Gibson & Anderson solution, the Jefferies solution and a new non-linear elastic analysis not yet published to provide parameters for the pressuremeter contraction. The steps are these:

- Use the Jefferies solution to derive an estimate of the undrained shear strength.
- Given this value, take the end of loading pressure and displacement and derive the limit pressure for the material using a relationship suggested by Gibson & Anderson.
- Plot the unload/reload loops from the expansion part of the test on new axes of log changing pressure vs log changing shear strain, and derive an exponent for the non-linear elastic response.

- Introduce this exponent and other results into a solution for non-linear elastic/perfectly plastic undrained expansion and contraction.
- Hence draw the pressure/strain curve for the complete expansion and contraction - this requires an estimate of the insitu lateral stress, which at first is guessed and then refined until the calculated contraction curve matches the measured contraction curve.
- Finally derive a value for the minimum shear modulus which can be compared directly for qualitative purposes with the values obtained from cycles of elastic unloading and reloading.

The procedure seems complex but in reality is straightforward and will be described in detail because so much is novel. The essence of the procedure is the dependence on the coupled nature of soil strength and stiffness parameters obtained from undisturbed parts of the test to reconstruct those parts of the test curve where disturbance is a factor. For a very badly disturbed pressuremeter test in soil, as will be shown, this can mean ignoring all but the last point of the expansion data.

5.2 Jefferies (1988) analysis

This analysis extends the Gibson & Anderson equations to account for pressures and strains recorded during pressuremeter contraction. The purpose of the analysis was to obtain the set of parameters that gave a calculated pressure:strain curve that matched the measured curve. Aspects of this approach to the pressuremeter test problem are contentious, but the equations used are useful in their own right.

From figure 1 it is apparent that the first part of the contraction starts from the maximum pressure and displacement recorded during the test, and is elastic until reverse plastic failure is initiated after a shear stress change of $2C_U$. The equation for this is similar to equation 3:

$$P_{max} - P = \gamma G \quad \ldots.[34]$$

and ceases at a limiting elastic shear strain of

$$2C_U/G \quad \ldots.[35]$$

Shear strain γ is obtained from cavity strain ε_c by:

$$[(1+\varepsilon_{cmax})/(1+\varepsilon_c)] - [(1+\varepsilon_c)/(1+\varepsilon_{cmax})] \quad \ldots.[36]$$

The measured pressures and displacements once reverse plastic failure is initiated are related by:

$$P = P_{max} - 2C_U[1+Ln(\gamma)-Ln(2/I_R)] \quad \ldots.[37]$$

In a similar manner as the Gibson & Anderson analysis, plotting pressure P against the log of the current shear strain gives a curve whose ultimate gradient is $-2C_U$

An example is given in Fig. 21.

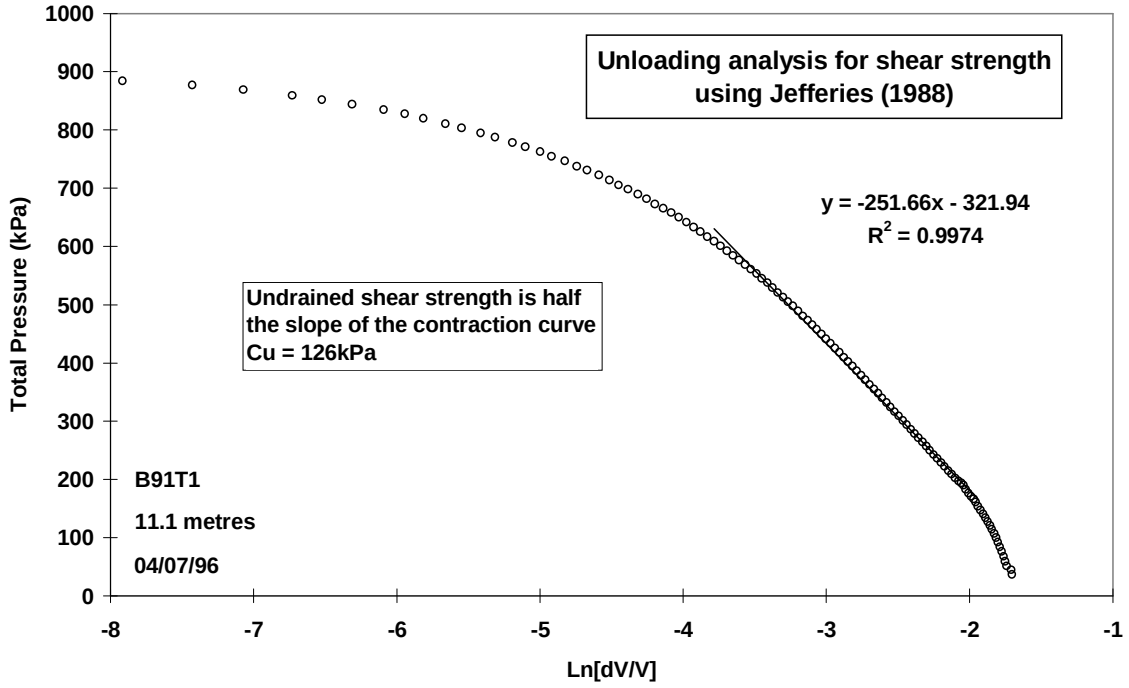

FIGURE 21. Using the contraction curve to derive C_U

It is not usually possible to use the last few data points of the contraction as this part of the test is dominated by other considerations than the venting of pressure inside the membrane of the probe.

5.3 Non-linear elastic analysis (Bolton & Whittle 1996)

It has already been demonstrated that the non-linear elastic response of soils can be fitted with a power law of the form

$$\tau = \alpha\gamma^{\beta} \quad \ldots.[38]$$

Around the pressuremeter, assume that the soil is deformed under conditions of axial symmetry and the expansion is undrained. The following relationships apply (see figure 2 for an explanation of the symbols used):

Axial strain $\varepsilon_a = 0$
Circumferential strain $\varepsilon_\theta = -\rho/r$.
The expansion is undrained so radial strain $\varepsilon_r = -\varepsilon_\theta = \rho/r$
Shear strain $\gamma = \varepsilon_\theta + \varepsilon_r = 2\rho/r = \delta A/A$
The equation of radial equilibrium applies throughout the expansion:

$$r\frac{d\sigma_r}{dr} + (\sigma_r - \sigma_\theta) = 0 \quad \ldots.[39]$$

where σ_r is radial stress and σ_θ is circumferential stress.

Using τ to represent shear stress at 45°, equation [29] becomes:

$$r\frac{d\sigma_r}{dr}+2\tau=0 \qquad \ldots.[40]$$

Now using the constitutive relationship $\tau = \alpha\gamma^{\beta}$ derived from inspection of unload/reload data and writing the current area in terms of radius:

$$\frac{d\sigma_r}{dr}+\frac{2a}{r}\left(\frac{\delta A}{\pi r^2}\right)^{\beta}=0 \qquad \ldots.[41]$$

Noting that $(1/r)(1/r^2)^{\beta} = r^{-(2\beta+1)}$:

$$\frac{d\sigma_r}{dr}+2a\left(\frac{\delta A}{\pi}\right)^{\beta} r^{-(2\beta+1)}=0 \qquad \ldots.[42]$$

and integrating between the reference state, and the pressure and radius at the cavity wall:

$$\int_{Po}^{P}\sigma_r = -2a\left(\frac{\delta A}{\pi}\right)^{\beta}\int_{\infty}^{r_C} r^{-(2\beta+1)}dr \qquad \ldots.[43]$$

so

$$P - P_O = 2a\left(\frac{\delta A}{\pi}\right)^{\beta}\left(\frac{1}{r^2}\right)^{\beta}\left(\frac{1}{2\beta}\right)=\frac{a}{\beta}\left(\frac{\delta A}{A}\right)^{\beta} \qquad \ldots.[44]$$

The right hand side of this result is the shear stress mobilised at the cavity wall and can be written as τ_C/β. Note that if $\beta = 1$, the condition for linear elastic response, the right hand side of equation [44] reverts to the form of equation [3], and α is the shear modulus G.

The end of the elastic phase is reached when $\tau_C = C_U$ for the expansion, hence

$$P - P_O = C_U/\beta \qquad \ldots.[45]$$

Thereafter, there is a plastic zone confined by the limiting elastic radial stress of C_U/β. The factor β is the only new feature of this analysis, so equation [6] becomes:

$$P - P_O = C_U[(1/\beta)-Ln(1/I_R)+Ln(\delta A/A)] \qquad \ldots.[46]$$

For the contraction, the end of the elastic phase is reached when $\tau_C = -2C_U$, hence

$$P_{max} - P = 2C_U/\beta \qquad \ldots.[47]$$

The effect of this is to change equation [37] to

$$P_{max} - P = 2C_U[(1/\beta) +Ln(\gamma)-Ln(2/\beta I_R)] \qquad \ldots.[48]$$

If $\beta = 1$, the condition for simple elastic response, equations [44] and [48] revert to the earlier solutions of equations [6] and [37]. Fig. 22 shows the shear stress:shear strain curve for the non-linear elastic/perfectly plastic material.

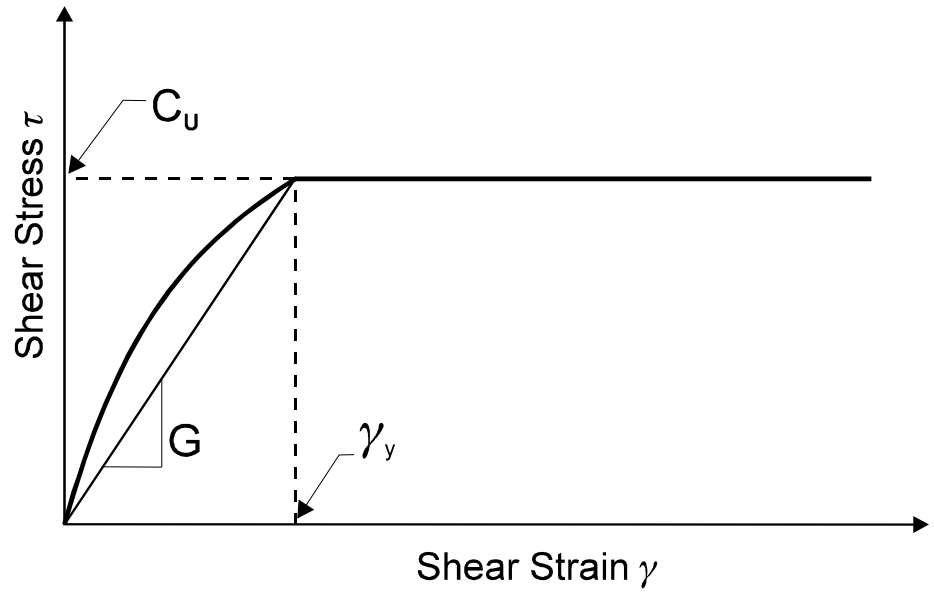

Figure 22 Shear stress:shear strain curve for non-linear elastic/perfectly plastic material

5.4 Reconstructing the pressuremeter curve:

Equations [44], [46] and [48] are sufficient to draw the theoretical pressure:strain curve, using the following input parameters:

- $\mathbf{P_{max}}$, the maximum pressure reached during the test
- $\boldsymbol{\varepsilon_{cmax}}$, the maximum cavity strain reached during the test.
- $\boldsymbol{\alpha}$, the shear stress coefficient derived from the log-log plot of reloading data.
- $\boldsymbol{\beta}$, the non-linear elastic exponent derived from the log-log plot of reloading data.

Step 1: Estimate the creep, and hence the amount by which the true maximum strain exceeds the measured maximum strain.

Step 2: Determine the shear strength from the unloading, by the method of Jefferies, from the plot of pressure versus the log of the contraction shear strain.

Step 3: Adjust the zero offset to give the same shear strength for the loading, by the method of Gibson & Anderson, from the plot of pressure versus the log of the shear strain.

Step 4. *Draw the pressure:strain curve*:
For every displacement recorded during the test calculate the theoretical pressure that ought to have been recorded from the deduced parameter set. Equations [44], [46] and [48] are used. This can be done on a spreadsheet using conditional statements to decide in which of the four possible states a data point lies - the choices are elastic loading, plastic loading, elastic contraction, plastic contraction. Both the measured and calculated curves should be drawn on the same scales.

Step 5: Adjust the insitu stress to get the best match of both the loading and unloading curves.

Step 6: Repeat from step 1 again until the best fit is achieved.

An example of the final state for one test is given below:

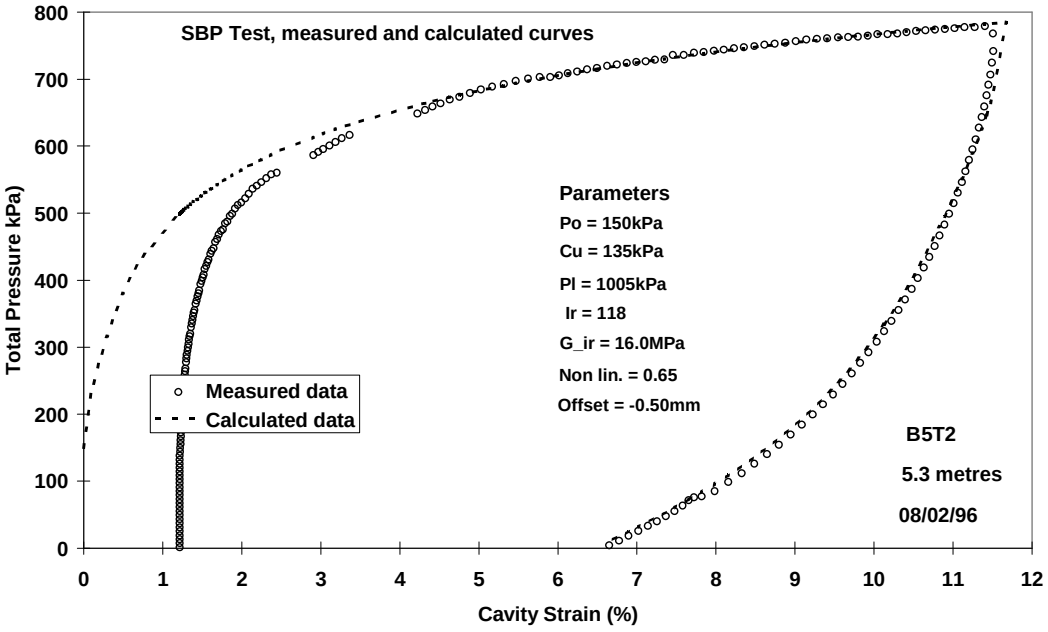

FIGURE 23. Reconstructing an SBPM curve

It happened that the instrument was left in the ground for some time after carrying out test B5T2, and before removal the material was reloaded. The result of this experiment is shown in Fig. 24, with the same analysis technique is applied once more.

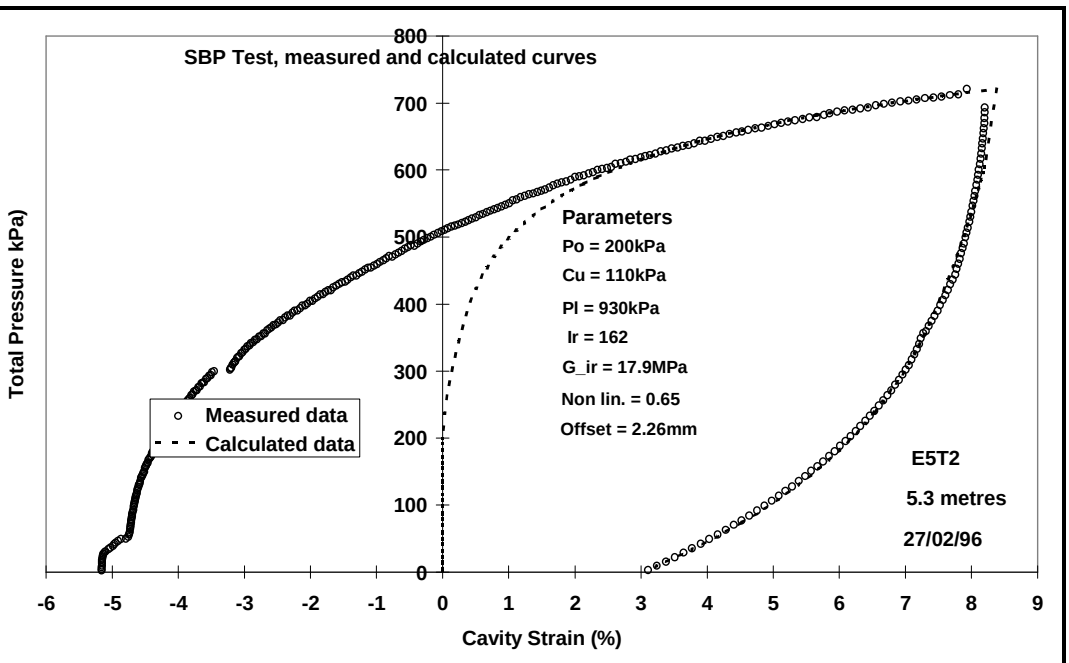

FIGURE 24. An SBPM test in remoulded material analysed for best fit

There are differences between the two results but the extent to which the original set of parameters has been recovered is encouraging.

It has now become possible to extend the concept of curve matching to sands, at least for all except the final plastic unloading. The loading curve uses the equations derived by Carter et al, and the unloading modulus is found from the reload loops, using the Janbu correlation between modulus and mean effective stress.

An example follows :-

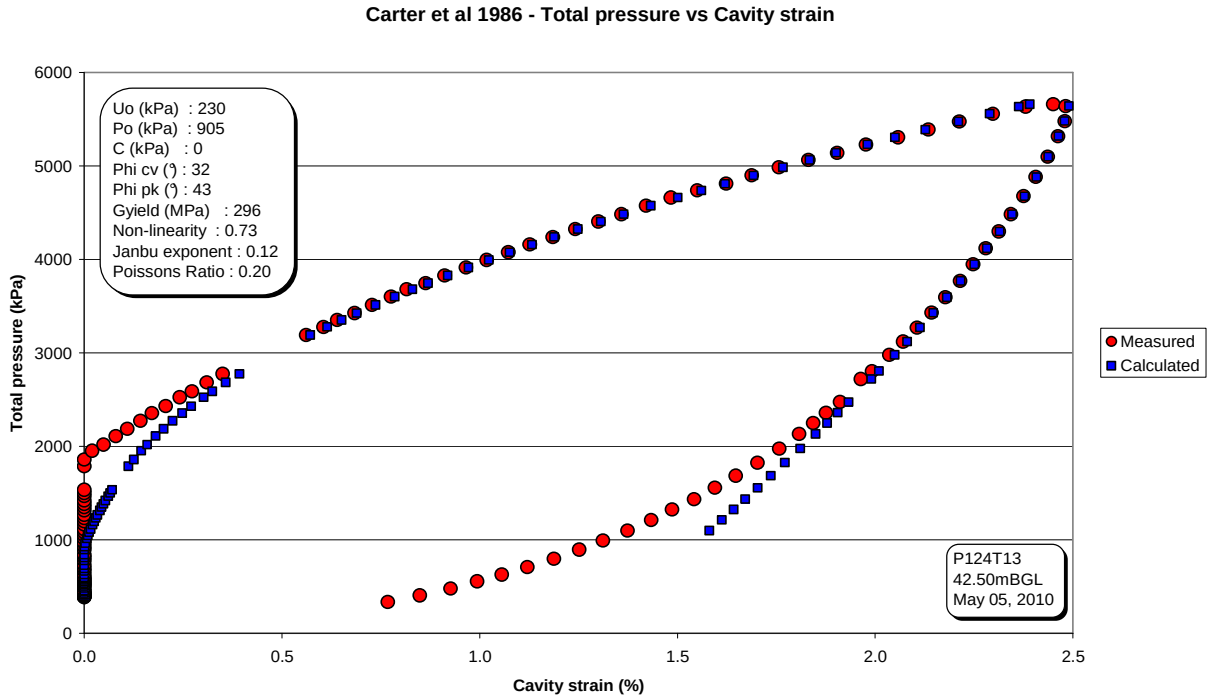

FIGURE 25 An SBPM test in Thanet Sand

Note that, although the match to the start of the unloading is good, the model over-predicts the depth of the elastic unloading.

A problem with this procedure is that there are usually too many variables, and it is possible to get similar matches with different sets of values. Data from other sources may be used to reduce the number of unknowns.

APPENDIX E THE HOLDING TEST & ITS ANALYSIS

1. The generation of excess pore pressures

The theory describing the generation of excess pore pressures around an expanding pressuremeter is based on the analysis procedure introduced by Gibson & Anderson (see Appendix D).
The pore pressures at any distance from the pressuremeter can be defined in terms of G, C_u and the volumetric expansion as follows :-

$$U_r = C_u \{Ln(G/C_u) + Ln(\Delta V/V) - 2Ln(r/r_o)\}$$

where r_o = expanded radius of the pressuremeter
and r = the radius of measurement

At the pressuremeter, $r = r_o$:-

$$\text{so } U_o = C_u \{Ln(G/C_u) + Ln(\Delta V/V)\}$$

$$\text{or } U_o/C_u = Ln\{(G/C_u).(\Delta V/V)\} \quad . \quad . \quad . \quad . \quad . \quad . \quad 1$$

Expressing U_r in terms of U_o :-

$$U_r = U_o - 2C_u . Ln (r/r_o) \quad . \quad . \quad . \quad . \quad . \quad . \quad 2$$

At the boundary of the failed zone, where $r = R$, the excess pore water pressure is zero :-

$$0 = C_u \left[Ln\{(G/C_u).(\Delta V/V)\} - 2Ln(R/r_o)\right]$$

$$\text{hence } R/r_o = \sqrt{\{(G/C_u).(\Delta V/V)\}} \quad . \quad . \quad . \quad . \quad . \quad . \quad 3$$

Equations 1 and 3 define the magnitude and extent of the excess pore water pressures in terms of the expression $\{(G/C_u).(\Delta V/V)\}$

2 The decay of excess pore pressures

Once the expansion has stopped, the excess pore water pressures begin to decay. (In practice this may occur during the expansion, if the material is sufficiently permeable.)
The exact manner in which they decay depends on the initial radial distribution, which depends on the size of the failed zone. (see eqn. 3)

For the case of a driven pile, $\Delta V/V = 1$ and therefore

$$U_o/C_u = Ln (G/C_u)$$

$$\text{and} \quad R/r_o = \sqrt{(G/C_u)}$$

The decay may be characterised in terms of G/C_U , and typical plots are shown in Fig. 1. The time is expressed in units of 'Ct/r_0^2', where C is the Coefficient of Consolidation. This expression is referred to as the 'Time factor' and is denoted by T. Its function will become apparent later.

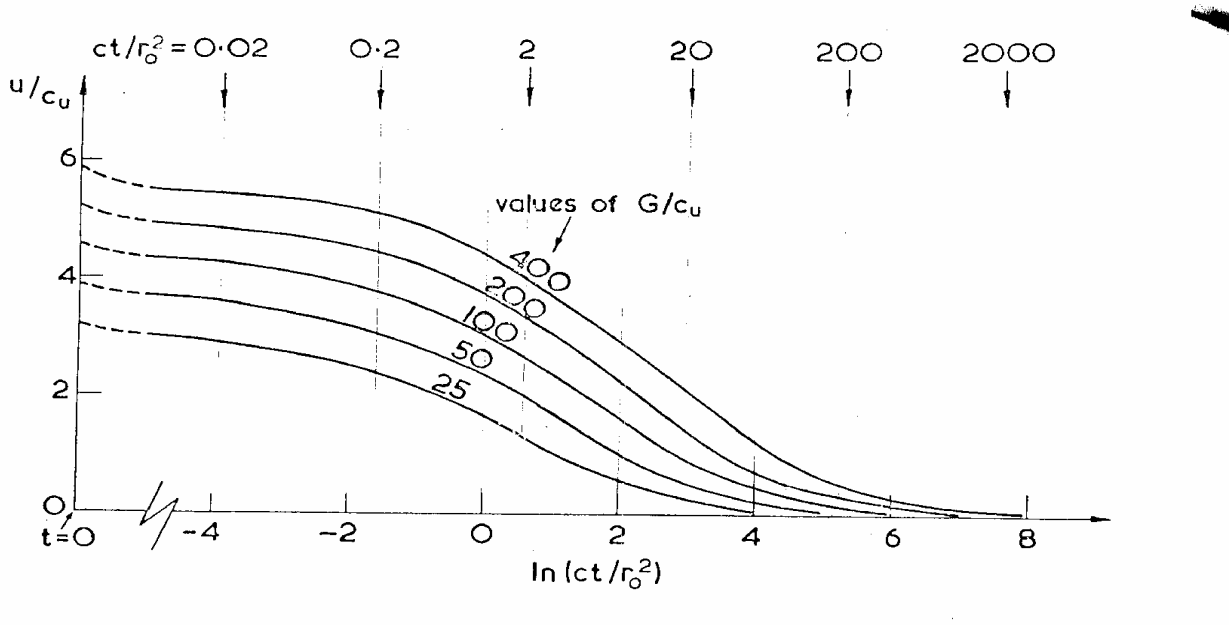

Figure 1 Variation of excess pore pressure at the pile face with time.

Fig. 2 gives a pictorial representation of the decay for one value of G/C_u. More use will be made of this plot later.

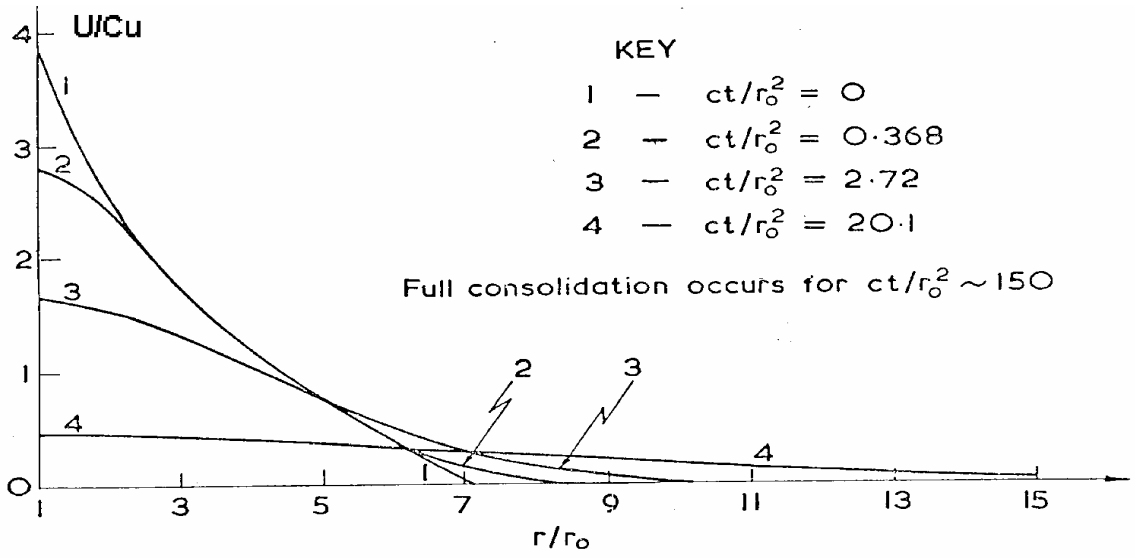

Figure 2 Variation of radial distribution of excess pore pressure with time after driving, for soil with G/Cu = 50.

These two plots are copied from a paper by Randolph & Wroth (1979) - "An Analytical Solution for the Consolidation round a Driven Pile".

3 Consolidation and Permeability

The theory of vertical consolidation is described by Terzaghi and introduces the Coefficient of Consolidation - C, defined by the equation :-

$$C = k/(m_v . \gamma_w) \quad . \quad . \quad . \quad . \quad . \quad . \quad . \quad 4$$

where k = permeability
(strictly "coefficient of permeability" or "hydraulic conductivity")
m_v = volume compressibility

γ_w = unit weight of water

Now volume compressibility is normally the inverse of bulk modulus, but here the compression is one-dimensional and it would appear that the true modulus E_o is that appropriate to this mode of deformation :-

$$m_v = 1/E_o \quad . \quad . \quad . \quad . \quad . \quad . \quad . \quad . \quad 5$$

now $$E_o = E (1 - \nu)/\{(1 + \nu)(1 - 2\nu)\} . \quad . \quad . \quad . \quad . \quad 6$$

and $$G = E/\{2(1 + \nu)\} . \quad . \quad . \quad . \quad . \quad . \quad . \quad 7$$

where ν = Poisson's ratio.

Combining equations 6 & 7 gives :-

$$E_o = 2G (1 - \nu)/(1 - 2\nu) \quad . \quad . \quad . \quad . \quad . \quad . \quad 8$$

which gives $$C = 2G k (1 - \nu)/ \gamma_w (1 - 2\nu) \quad . \quad . \quad . \quad . \quad . \quad 9$$

so defining C in terms of k and G.

4. Practical considerations

When the permeability is high, it is not possible to decide accurately when the dissipation starts, or what the peak pore pressures are. This makes the measurement of the time for the pressures to reach half the peak value doubly difficult. The slope of the log plot can be used to determine the half-life of the decay but this is a subjective process, and different operators can get different results.

It is possible to get a better idea of the peak pore pressures from a plot of pressure against 'root time'. The initial part of this plot should be a straight line, so it can be projected back to give the pressure at the start.

The uncertainty over the ambient pore pressure is less of a problem than originally expected. The effect of the change in U/Cu is almost exactly counteracted by the change in $t_{50.}$ This might be expected from Fig. 2 – during the first half of the decay the pressure stays constant at intermediate radii, so differences at larger radii have little effect. The same argument applies to pore pressures generated during the elastic phase.

The theory is based on the decay of excess pore water pressures, but the total pressure response follows that of the pore pressure. Thus it is possible to obtain a figure for the half life of the decay of the total pressure - as long as a suitable zero is chosen. The best guess for this would appear to be the 'Failure Pressure' predicted by the parameters derived from the curve matching procedure.

5. Analysis procedure

The five parameters needed are :-

U the maximum excess pore pressure
G the Shear modulus.
C_u the Shear strength.
t_{50} the half life of the decay.
d the probe diameter at hold.

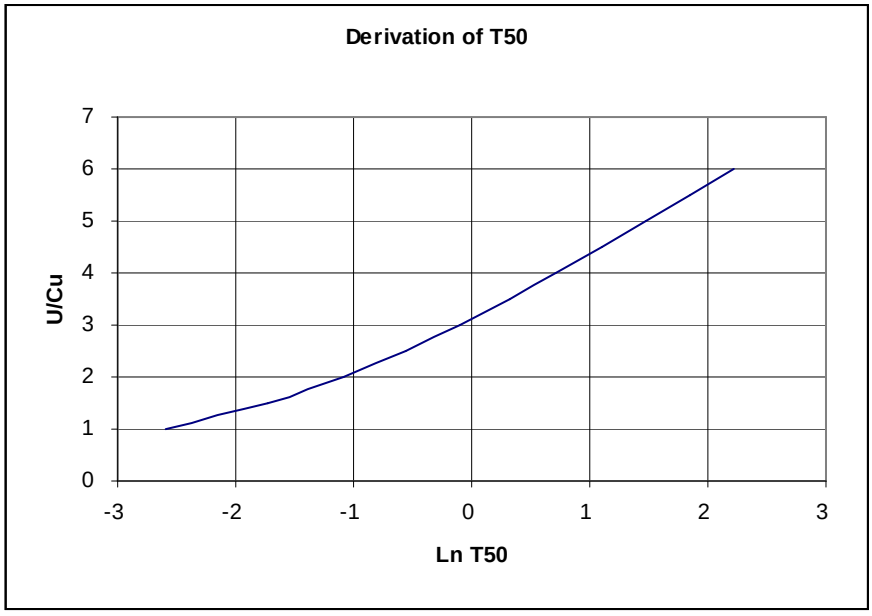

Figure 3. The relationship between Ln T50 and U/Cu.

Reference to the curve in Fig. 6 (taken from the paper by Randolph & Wroth) leads to a value for Ln T_{50}, and hence T_{50} itself.

Substituting in the equation :-

$$C = r_o^2 (T/t)$$

where now $T = T_{50}$ and $t = t_{50}$, yields a value for C_H.

Equation 9 can be re-arranged :-

$$k = C \gamma_w (1 - 2\nu)/2G(1 - \nu)$$

if C is in m^2/yr
G is in MPa
γ_w is 9.81 kPa/m or 0.00981 MPa/m
ν is assumed to be 0.2 for drained material

then $k = C/G \times 1.166 \times 10^{-10}$ m/s

6. The 'New method'

The concept of 'half-life' used earlier applies to an exponential decay, where it is a constant. The decay of excess pore water pressure around a cylindrical probe is not exponential, although it can be made to appear so (after an initial steeper portion) by suitable selection of the 'aiming pressure'. This was utilised in the original analysis method used by Cambridge Insitu.

In an attempt to understand the problem better a spreadsheet program was developed to simulate the pressures and flows around an expanded pressuremeter. This produces curves like those in Figs. 2 & 3, but with the possibility of varying input parameters at will.

Some interesting relationships are evident :-

1. The rate of decay is inversely proportional to 'k/m_v' (and hence C_h – see equation 4.)
2. It is uniquely related to 'U/Cu', being almost proportional to $(U/Cu)^2$.
3. On a plot of 'Pressure' against 'Log time' the maximum slope depends only on U.
4. This maximum slope occurs at a value close to the 'half maximum pressure', which is exploited in the analysis of both the piezo-cone and DMT dissipation tests.
5. On a plot of 'Pressure' against 'Square root of time' the initial slope is proportional to Cu and the square root of 'k/m_v' – it appears to be independent of U.
6. For the first half of the decay, the way the pressures and flows interact in the zone around the probe is not affected by the pressures further away. Thus pore pressures produced by drilling or non-linear elastic effects do not interfere, within reason.
7. The derivation of permeability depends on a knowledge of the drained bulk modulus, and hence the true volume compressibility.

It is possible to measure the maximum slope, if the hold is of long enough duration, and hence derive the consolidation. An alternative approach is to use the spreadsheet to match the field curve by setting a few basic parameters, one of which is the permeability.

An added advantage is that both the decay of pore pressure and total pressure can be matched at the same time. They are related by 'β' the non-linearity, but the same permeability applies to both.

Note that the shear strength used is that from the unloading. The modulus used is G_{MIN}, the modulus at yield.
A pair of typical plots is shown :-

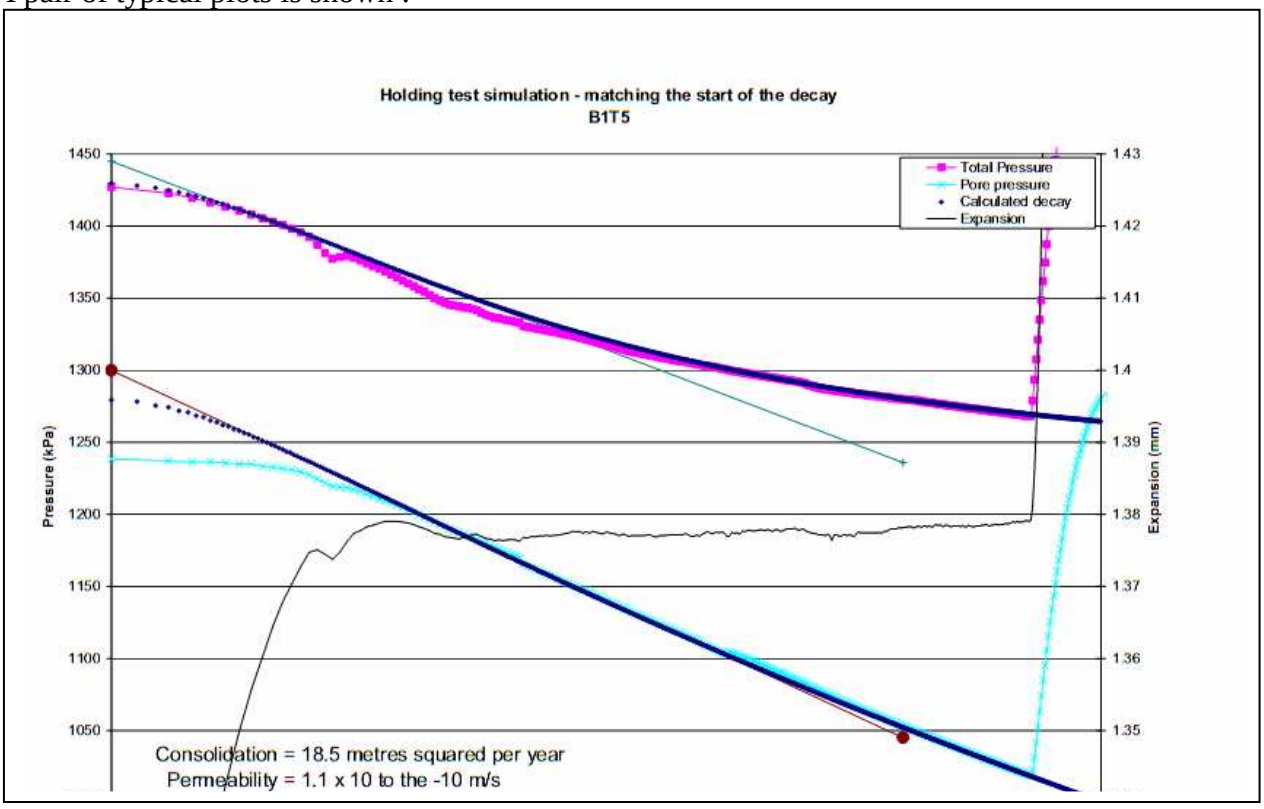

Figure 4. The 'square root of time' plot

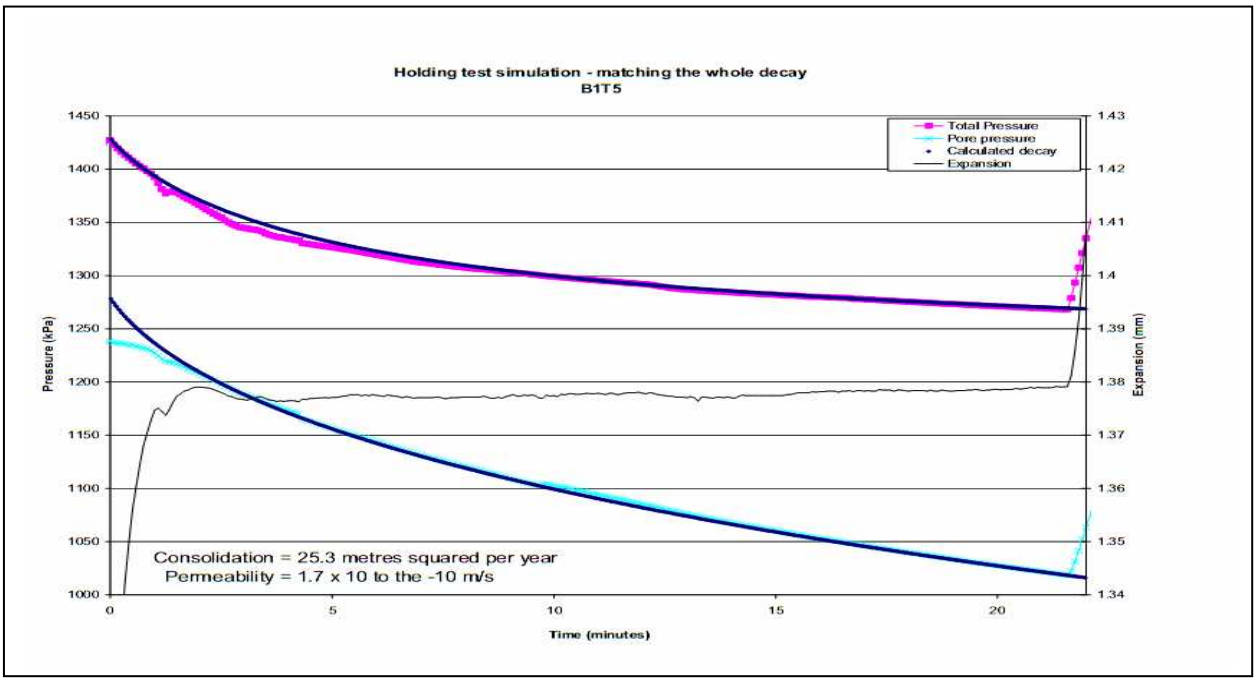

Figure 5 Matching the whole curve

APPENDIX F THE SELF BORING PERMEAMETER

1. Background

The tests for establishing the insitu horizontal permeability were carried out with a self boring pressuremeter used in permeameter mode. This is known as MK2 permeameter testing .

Fig. F1 Well point-filter in uniform soil

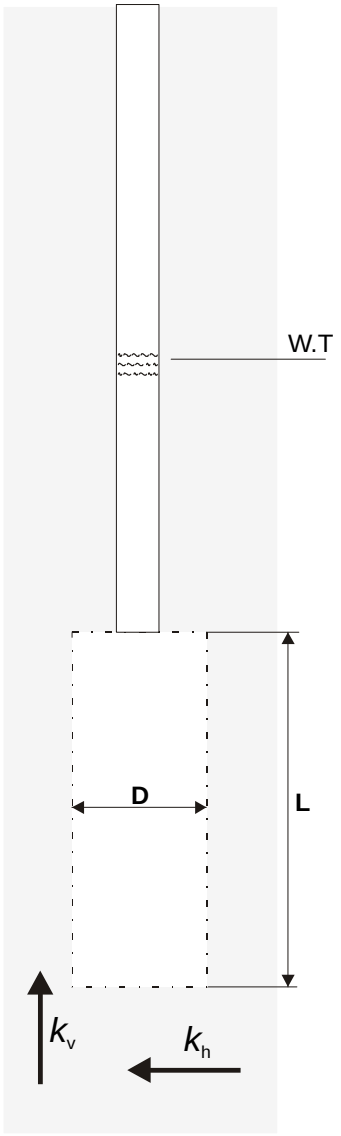

The 'permeameter' consists of a self boring pocket, the SBP itself just being the water delivery pipe. The height of the permeameter cavity is set by lifting the pressuremeter up after drilling. If no pull back is used then the permeameter cavity can have zero height. This is convenient because the geometry of the cylindrical cavity is different from that of the flat surface and allows the user to discover the relationship between the vertical and horizontal permeability.

Once in position in the ground, water is pumped down the instrument casing out of the bottom cutting shoe and into the pocket cut by the pressuremeter. The water is delivered at a constant rate of flow, and an equilibrium driving pressure is discovered for maintaining a constant flow throughout the soil. The pressure for a given flow is a function of the permeability and the geometry of the arrangement of parts.

The conventional solution for a permeameter test uses an equation of the following form derived from Darcy's flow rule:

$$k = Q_\infty/FH \qquad \text{...[Equ.1]}$$

where k is permeability
Q_∞ is flow under steady state conditions
H is the applied head of water
F is a shape factor depending on the geometry of the permeameter setup and variations in the horizontal to vertical permeability.

A practical version of Equation [1] is given by Hvorslev (quoted in Lambe & Whitman 1969) who offers a solution for the horizontal permeability from a well point-filter in a uniform soil, the model for the self boring permeameter test with height:

$$k_h = [Q/2\pi LH_c].\mathrm{Ln}[(mL/D)+\sqrt{(1+(mL/d)^2)}] \qquad \text{... [Equ.2]}$$

where k_h is permeability in the horizontal direction in cm/second
Q is flow in mLitres/second
L is length of sample in cm.
D is the diameter of the source
H_c is constant piezo head (cm)
m is a transformation ratio dependent on the ratio of the horizontal to vertical permeability $= \sqrt{[k_h/ k_v]}$

Figure F1 shows the physical arrangement on which this solution is based. The shape factor F in equation [2] combines L, D and *m*. In practice these three parameters are only a starting point for deriving F and a finite element study reported by Ratnam et al (2000) gives the following expression for the dimensionless shape factor F/d:

$$F/d = 1.1872\ (L*m/d) + 2.4135\ (L*m/d)^{0.5} + 3.1146 \quad \text{... [Equ.3]}$$

Table F1 Geometries tested and associated shape factors (for isotropic conductivity):

L/d	F/d (Hvorslev)	F/d (Ratnam)
0.178	6.32	4.34
0.289	6.37	4.75
0.400	6.44	5.12
1.178	7.39	7.13
2.178	9.00	9.26

Table F1 shows the effect of applying equations [2] and [3] to some typical geometries encountered during testing. For L/d ratios > 1 the differences are small but below 1 the differences are substantial.

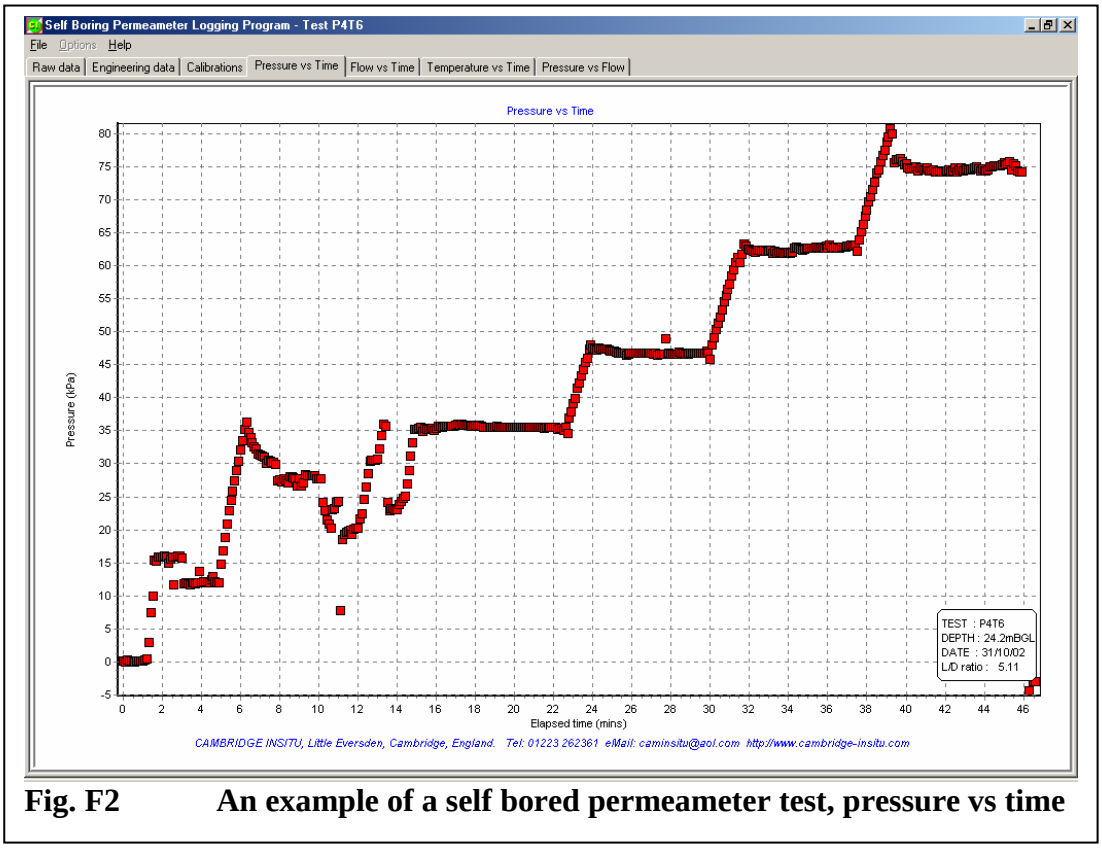

Fig. F2 An example of a self bored permeameter test, pressure vs time

By setting different constant flow rates a range of pressures is discovered. Plotting flow rate against head gives a graph whose gradient can be used to give the permeability directly. Figure F2 is an example of raw test data, where pressure is plotted against time and a number of equilibrium pressures are recorded. Figure F3 shows the reduced data taken from this plot, where the equilibrium pressures are plotted against flow rate.

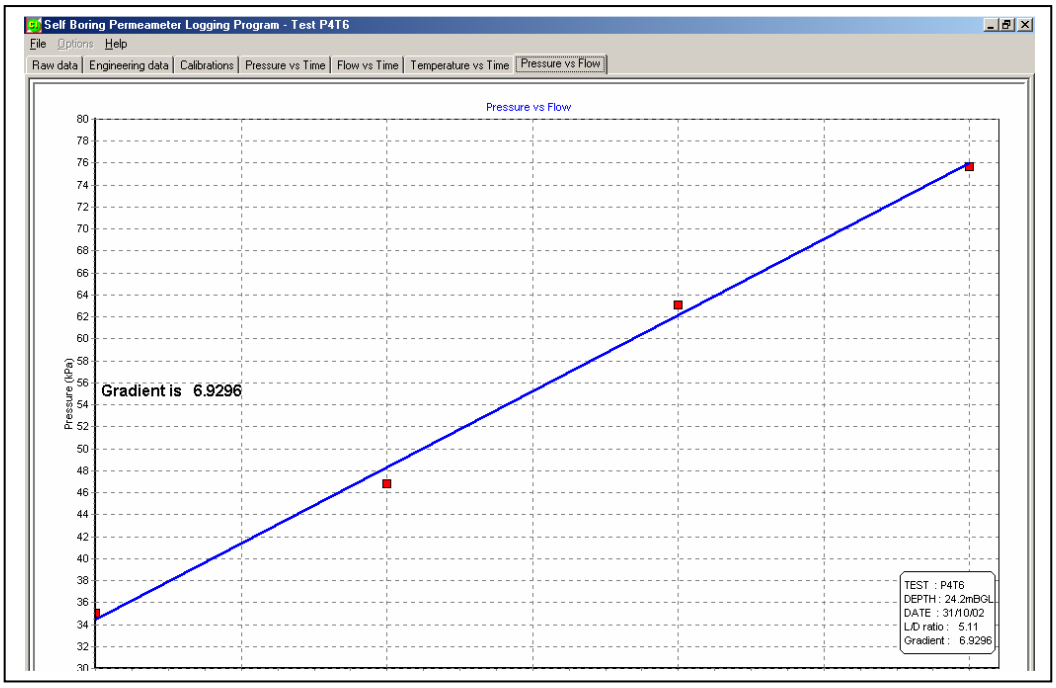

If the slope of the plot in fig.F3 is *S* then the permeability is given by:

$$K_m = 9.81 /(F*3.6 * 10^9 * S) \quad \text{...[Equ.4]}$$

where F is the relevant shape factor multiplied by the diameter of the probe, 0.09 metres. K_m is in units of metres/second.

2. Comments

The solution assumes, among other things, directional isotropy, so k_h is constant. No disturbance, swelling, segregation or consolidation of the material is allowed. In practice the application of water pressure greater than the insitu ambient level has an unknown but assumed to be small affect on the ground and other users of permeameters have reported some consolidation taking place.

The plots of pressure against time do not always look as plausible as figure F3. The best results seem to be achieved when the driving pressure changes rapidly to bring the test close to the steady state condition in the shortest possible time – once one pressure has been established, the value for others can be predicted so it is possible to accelerate the test.

Acceleration is achieved by setting the desired flow rate, then pressing the turbo key of the Flow Control Unit for a few seconds. On release of the key the pressure will continue to climb if not yet at the equilibrium pressure, or will fall if the steady state pressure level has been overshot. If the assumptions governing the use of equ.[3] are correct then this accelerated procedure should make no difference to the time taken to reach steady state but the results indicate it does. There is no explanation yet for this effect.

The other big problem is temperature and the effect of direct sunlight on the supply hose from the pump to the permeameter casing. This is reduced if this supply hose can be kept short, but that was not possible in this case. This temperature effect causes less disturbance at high pressures and flow rates.

APPENDIX G SAMPLE CALCULATION OF A LINE OF DATA

What are described in some detail in this appendix are the steps necessary to convert the raw data output from the pressuremeter into engineering units. The data line used is from a test called P9T1 and is line no. 224.

In order to convert self boring pressuremeter signals into calibrated data the following steps are taken:

A. The raw data is in units of volts, and needs to be corrected for zero offsets and scaled using the sensitivities quoted in the calibration data.

The calibrations for this particular test are presented as follows:-

INSTRUMENT CALIBRATIONS: P9T1 DEPTH: 18.50m DATE: 14 Mar 96

	ZERO		SLOPE	CORRECTION & COMPRESSION			
ARM 1	-122.4 mV	&	321.1mV/mm	21.2kPa	&	8.2 kPa/mm	2.0mm/GPa
ARM 2	277.6 mV	&	334.7mV/mm	21.2kPa	&	8.2 kPa/mm	2.0mm/GPa
ARM 3	-96.6 mV	&	310.2mV/mm	21.2kPa	&	8.2 kPa/mm	2.0mm/GPa
TPC	-1155.5 mV	&	396.3mV/MPa				
PPC A	-1079.8 mV	&	227.0mV/MPa				
PPC B	-428.9 mV	&	232.0mV/MPa				

The line of raw data reads from left to right as follows. Note that the units are volts:-

LINE	ARM 1	ARM 2	ARM 3	TPC	PPC A	PPC B
224	0.2448	1.7477	1.1993	-0.6390	-0.8283	-0.1944

The first operation is to deduct the zero offsets. These are the figures found in the first column of the calibration information. They are quoted here in volts:-

	ARM 1	ARM 2	ARM 3	TPC	PPC A	PPC B	
Outputs	0.2448	1.7477	1.1993	-0.6390	-0.8283	-0.1944	
Zero	-0.1224	0.2776	-0.0966	-1.1555	-1.0798	-0.4289	
Result	0.3672	1.4701	1.2959	0.5165	0.2515	0.2345	.....[1]

This result can now be scaled. The information for this is found in the second column of calibration data, and is expressed as millivolts per millimetre to calculate displacement, and as millivolts per megaPascal to calculate pressure.

They are written below as volts:-

	ARM 1	ARM 2	ARM 3	TPC	PPC A	PPC B	
From [1]	0.3672	1.4701	1.2959	0.5165	0.2515	0.2345	
Slope	0.3211	0.3347	0.3102	0.3963	0.2270	0.2320	
Result	1.1436	4.3923	4.1776	1.3033	1.1079	1.0108	.....[2]
	(mm)	(mm)	(mm)	(MPa)	(MPa)	(MPa)	

B. The data is now in engineering units which reflect what is taking place inside the membrane. The remaining corrections are introduced to give a better representation of what is taking place at the point where the membrane bears on the borehole wall.

The pressure information is in units of MPa and must be adjusted for membrane stiffness. This is calculated separately for each strain arm, but note that the average strain is used to apply the slope correction:-

The displacement data is adjusted for the instrument displacements due to the pressure being applied to it. This is expressed as a linear movement in millimetres per gigaPascal of pressure being applied, and is found in the 5th column of the calibration details:

	ARM 1	ARM 2	ARM 3	
Correction Factor (mm/GPa)	2.0	2.0	2.0	.....[8]
Internal Pressure (MPa)	1.3033	1.3033	1.3033	....(from result [2])
Adjustment ([8]*[2])/1000	0.0026	0.0026	0.0026	.....[9]
Internal Displacement (mm)	1.1436	4.3923	4.1776	....(from result [2])
Corrected Displacement (mm)	1.1410	4.3897	4.1750	.....[10]

C. The next step is to calculate the total membrane correction that needs to be made for each arm position. This is the sum of the zero figure plus the increased stiffness with strain. This second component uses the fourth column of calibration data and is quoted as kPa per millimetre movement:-

	ARM 1	ARM 2	ARM 3	
From Result [10]	1.1410	4.3897	4.1750	
Ave. Displacement	******	3.2352	******	..... [3]
Slope per mm (kPa)	8.2	8.2	8.2	..... [4]
Result [3]*[4] (kPa)	26.5	26.5	26.5	..... [5]
Correction zero (kPa)	21.2	21.2	21.2	
Add zeroes to result [5]	47.7	47.7	47.7	..... [6]

This is the total membrane correction at each arm position and is now deducted from the total pressure cell readings to give three files of corrected pressure:

	TPC 1	TPC 2	TPC 3	
Uncorrected pressure in kPa	1303.3	1303.3	1303.3	(from result [2])
Membrane correction in kPa	47.7	47.7	47.7	(from result [6])
RESULT	1255.6	1255.6	1255.6	..... [7]

The pressure data is now in its final form. The data from the two pore pressure cells need only to be quoted in kPa rather than MPa and that too are complete.

D. The strain data calculated so far is the movement measured by the strain arms to the inside of the membrane. The figures quoted in the calibrated data listings are the movement of the outside of the protective sheath. This is derived from the internal strain movement by assuming that the cross-section area of the memebrane is a constant. A full explanation of this and the derivation of the equation used is discussed in the appendix on calibration technique.

The equation is $E = \sqrt{[(R-t)^2 + D(2r+D)]} - (R-t)$ [11]

where E is the actual expansion of the pressuremeter
2R is the O.D of the pressuremeter at rest
2r is the I.D of the membrane at rest
D is the movement measured by the strain arm
t is the thickness of the chinese lantern steel

For the pressuremeter used to produce this example:-

2R = 83.1 mm
2r = 79.1 mm
t = 0.18 mm

Alternatively, in weak rock configuration:-

2R = 88.0 mm
2r = 79.1 mm
t = 0.5 mm

Because the membrane can be assumed to have the same thickness at all points on the cross-section the technique employed is to calculate a scale factor from the average strain.

	ARM 1	ARM 2	ARM 3	
Corrected Displacements	1.1410	4.3897	4.1750	...(from result [10])
Average Displacement	******	3.2352	******	.....[12]
Result of equation [11] using D = 12	****	3.1030	****	.....[13]
Scale Factor [13]/[12]	****	0.9591	****	.....[14]
Apply [14] to [10]	1.0944	4.2103	4.0044	.....[15]

E. The result, using displacements from [15], Total Pressure from [6] and Pore Pressures from [2];

NO	ARM 1	ARM 2	ARM 3	TPC (1)	TPC (2)	TPC (3)	PPC A	PPC B
224	1.0943	4.2103	4.0044	1255.6	1255.6	1255.6	1107.9	1010.8

In practice the errors introduced by rounding-off calculations may result in small differences in the final figure.

Other Pressuremeters:
The format of the PRN file for other pressuremeter types vary with the number of transducers but in general the calculation procedure for other pressuremeters is similar to the above:

- Deduct the zero readings from all transducers
- Scale the transducer readings
- Deduct the effect of membrane compression from the readings of displacement
- Deduct the effect of membrane thinning from the readings of displacement

Six arm pressuremeters (which includes the HPD) do not implement the membrane correction at the time the PRN file is formed, but later as part of the analysis procedure. Uncorrected total pressure is input to the analysis program which then deducts the membrane effect using the data in the calibrations header.

APPENDIX H REFERENCES

ARNOLD, M. (1981)
An Empirical Evaluation of Pressuremeter Test Data, Civil Engineering Department, University of Adelaide, South Australia.

BAGUELIN, F., JEZEQUEL, J.F. and SHIELDS, D.H. (1978)
The Pressuremeter and Foundation Engineering, Transtech Publications, Clausthal, Germany ISBN O-87849-0l9-l

BELLOTTI, R., GHIONNA, V., JAMIOLKOWSKI, M., ROBERTSON, P. and PETERSON, R. (1989).
"Interpretation of moduli from self-boring pressuremeter tests in sand". *Géotechnique* Vol.XXXIX, no.2, pp.269-292.

BENOIT, J.(l983).
"Analysis of Self-Boring Pressuremeter Tests in Soft Clay", A dissertation submitted to the Department of Civil Engineering and the Committee on Graduate Studies of Stanford University in Partial Fulfilment of the Requirements of the Degree of Doctor of Philosophy.

BENOIT, J. and CLOUGH, G.W. (l985).
"Principal Stresses Derived from the Self-Boring Pressuremeter Tests in Soft Clays", The Pressuremeter and its Marine Applications, 2nd International Symposium.

BOLTON M.D. and WHITTLE R.W. (1999)
“A non-linear elastic/perfectly plastic analysis for plane strain undrained expansion tests.” Géotechnique Vol. **49**, No.1, pp 133-141.

BRUZZI, D., GHIONNA, V., JAMIOLKOWSKI, M., LANCELLOTTA, R., & MANFREDINI G (l986).
"Self-Boring Pressuremeter in Po River Sand", 2nd International Symposium on The Pressuremeter and its Marine Applications.

CARTER, J.P., BROOKER, J.R. and YEUNG, S.K. (1986).
“Cavity Expansion in Cohesive Frictional Soils”. *Géotechnique* Vol. **36**, No. 3, pp 349-358.

CLARKE, B.G., CARTER, J.P. and WROTH, C.P. (l979).
"In Situ Determination of Consolidation Characteristics of Saturated Clays". Design Parameters in Geotechnical Engineering, VII ECSMFE, Brighton, Vol. 2, , pp 207- 211

CLARKE, B.G. (l98l).
"In Situ Testing of Clay Using Cambridge Self-Boring Pressuremeter"
PhD Thesis, Cambridge University.

CLARKE, B.G and WROTH, C.P. (l984)
Analysis of Dunton Green retaining wall based on results of pressuremeter tests. *Géotechnique* **34**, No. 4, pp 549-561.

CLOUGH, G.W., and DENBY, G.M. (1980)
Self-boring Pressuremeter study of the San Francisco Bay Mud, J. Geotech Eng. Divn. ASCE V l06, No. GTl pp 45-63

DALTON, J.C.P., HAWKINS, P.G.(1982)
Fields of Stress, some measurements of the in-situ stress in a meadow in the Cambridgeshire countryside. *Ground Engineering* Vol. 15, No. 4 pp 12 -23.

DENBY, G.M. and CLOUGH, G.W. (l980)
Self-boring Pressuremeter Tests in Clay. J. Geotech Eng. Divn. ASCE V l06 No. GTl2 pp l369-l387.

DENBY, G.M. (l978)
Self Boring Pressuremeter Study of the San Francisco Bay Mud. PhD Thesis, Department of Civil Engineering, Stanford University Technical Report, CE232

DENBY,G.M., COSTA,C.A., CLOUGH,G.W. and DAVIDSON,R.R. (l98l)
"Laboratory and Pressuremeter Tests in Stiff Clay". Proceedings of the Tenth International Conference on Soil Mechanics and Foundation Engineering, Stockholm, Sweden.

DENBY, G.M. and HUGHES, J.M.O. (l982)
Horizontal stress interpretation of pressuremeter tests. Proc. ASCE Conf. on Updating Subsurface Sampling of Soils and Rocks and their In-Situ Testing, Santa Barbara, California.

ERVIN, M.C., BURMAN, B.C. and HUGHES, J.M.O.(1980).
The use of a high capacity pressuremeter for design of foundations in medium strength rock. International Conference on Structural Foundations on Rock, Sydney.

FAHEY, M. (1980)
A Study of the Pressuremeter Test in Dense Sand. PhD Thesis University of Cambridge.

FAHEY, M. and JEWELL, R.J. (1990)
Effect of Pressuremeter Compliance on Measurement of Shear Modulus. Paper submitted to The Third International Symposium on Pressuremeters, Oxford University 2 - 6 April 1990

FAHEY, M., and RANDOLPH, M.F. (1984)
Effect of disturbance on parameters derived from Self- boring Pressuremeter tests in sand. *Géotechnique* **34**, No. 1, pp 81-97

GHIONNA, V., JAMIOLKOWSKI, M., LACASSE, S., LADD, C.C., LANCELLOTTA, R. and LUNNE, T (1983).
Evaluation of Self-Boring Pressuremeter. Symposium International Vol. 2 Paris.

GHIONNA, V., JAMIOLKOWSKI, M., and LANCELLOTTA, R.(1982)
Characteristics of Saturated Clays as Obtained from SBP Tests. Proc. Int. Symp. Pressuremeter and its Marine Appls., Paris, pp 165-186.

GHIONNA, V., JAMIOLKOWSKI, M., LANCELLOTTA, R., TORDELLA, M.L. and LADD, C.C. (1981)
Performance of Self-Boring Pressuremeter tests in cohesive deposits. Dept of Civil Engineering, MIT, Report FHWA/RD- 8l/l73.

GHIONNA, V., JAMIOLKOWSKI, M., LANCELLOTTA, R. & MANASSERO, M (1989).
Limit Pressure of Pressuremeter Tests. Proc. of 12th ICSMFE, Rio De Janeiro.

GIBSON, R.E. and ANDERSON, W.F. (1961)
In situ measurement of soil properties with the pressuremeter, Civil Engineering and Public Works Review, Vol. 56, No. 658 May pp 6l5-6l8 .

HAWKINS, P.G., MAIR, R.J., MATHIESON, W.G. and MUIR WOOD, D. (1990)
Pressuremeter measurement of total horizontal stress in stiff clay, Proc. ISP.3 Oxford.

HOULSBY, G., CLARKE, B. and WROTH, C.P. (1986).
"Analysis of the unloading of a pressuremeter in sand". Proc. of the 2nd International Symposium on The Pressuremeter and its Marine Applications pp 245-262.

HUGHES, J.M.O. (l973).
An instrument for in situ measurement in soft clays, PhD Thesis, University of Cambridge

HUGHES,J.M.O., ERVIN, M.C. (1980)
Development of a High Pressure Pressuremeter for determining the engineering properties of soft to medium strength rocks.Proc. 3rd Aus.-NZ Conf. Geomechanics, Brisbane, pp.292-296.

HUGHES, J.M.O., WROTH, C.P. and PENDER, M.J. (l975).
A comparison of the results of special pressuremeter tests with conventional tests on a deposit of soft clay at Canvey Island, Internal Report No. CUED/C - SOILS TR 20, Cambridge University Engineering Department.

HUGHES, J.M.O., WROTH, C.P. and WINDLE, D. (l977)
Pressuremeter tests in sands, *Géotechnique* **4**, pp 455-477

JARDINE, R.J. (1991)
Discussing ‘Strain-dependent moduli and pressuremeter tests’ . *Géotechnique* **41**, No. 4., pp 621-624

JARDINE, R.J. (1992)
Nonlinear stiffness parameters from undrained pressuremeter tests. *Can. Geotech*. **29**, pp 436-447

JARDINE, R.J., POTTS, D.M., FOURIE, A.B. and BURLAND, J.B. (1986)
Studies of the influence of non-linear stress strain characteristics in soil structure interaction. *Géotechnique* **36**, No. 3, pp 377-396.

JEFFERIES, M.G. (1988)
Determination of horizontal geostatic stress in clay with self-bored pressuremeter. *Can. Geotech*. **25** (3), pp 559-573

JEWELL, R.J., FAHEY, M. and WROTH, C.P. (1980)
Laboratory Studies of the Pressuremeter Test in Sand. *Géotechnique* **30**, No. 4 pp 507-531

LACASSE, S. and LUNNE, T. (l982)
In Situ Horizontal Stress from Pressuremeter Tests". Proc. of the Symp. on the Pressuremeter and its Marine Applications, Paris.

LADANYI, B. (1973)
"Expansion of a Cavity in a Saturated Clay Medium". Journal of the Soil Mechanics and Foundation Engineering Division, ASCE, Vol. 89, No. SM4, Proc. Paper 3577, July l973, pp l27-l6l.

MARSLAND, A. and RANDOLPH, M.F. (l977).
Comparison of the Results from Pressuremeter Tests and Large Insitu Plate Tests in London Clay. *Géotechnique* **27** No. 2 pp 2l7-243.

MAIR, R.J. and WOOD, D.M. (l987)
Pressuremeter Testing. Methods and Interpretation. Construction Industry Research and Information Association Project 335. Publ. Butterworths, London. ISBN 0-408-02434-8

MANASSERO, M. (1989)
Stress-Strain Relationships from Drained Self Boring Pressuremeter Tests in Sand. *Géotechnique* **39**, No.2.

MUIR WOOD, D. (1990)
Strain dependent soil moduli and pressuremeter tests. *Géotechnique*, **40**, pp 509-512.

NEWMAN, R.L., CHAPMAN, T.J.P. and SIMPSON, B. (1991)
"Evaluation of pile behaviour from pressuremeter tests". Proc. Xth European Conference on Soil Mechanics and Foundation Engineering, Florence, May 1991

PALMER, A.C. (l972)
Undrained plane-strain expansion of a cylindrical cavity in clay: a simple interpretation of the pressuremeter test, *Géotechnique* **22** No. 3 pp 45l-457.

RANDOLPH, M.F. and WROTH, C.P. (l978)
An analytical solution for the consolidation around a driven pile. Int. J. Numer. Anal. Methods in Geomech.

ROBERTSON, P.K. and HUGHES, J.M.O. (1985)
"Determination of Properties of Sand from Self-Boring Pressuremeter Tests ". The Pressuremeter and Its Marine Applications, Second International Symposium.

ROWE, P.W. (1962)
"The Stress Dilatancy Relation for Static Equilibrium of an Assembly of Particles in Contact". Proceedings of the Royal Society. Vol. 269, Series A, pp 500-527.

WHITTLE, R.W. and DALTON, J.C.P. (1990)
Discussing 'Experience with the self boring rock pressuremeter'. *Ground Engineering*, Jan/Feb, pp 30-32.

WHITTLE R.W, DALTON J.C.P and HAWKINS P.G. (1992)
Shear Modulus and Strain Excursion in the Pressuremeter Test. Proc. Wroth Memorial Symposium, Oxford, July 1992.

WHITTLE R.W, HAWKINS P.G and DALTON J.C.P (1995)
The view from the other side - lift-off stress and the six arm self boring pressuremeter. The Pressuremeter and its New Avenues, Proc.4th International Symposium 17-19 May 1995.

WHITTLE R.W (1993)
Discussing 'The assessment of in situ stress and stiffness at seven overconsolidated clay and weak rock sites'. *Ground Engineering*, Sept 1993, pp 19-20.

WHITTLE R.W (1999)
Using non-linear elasticity to obtain the engineering properties of clay. Ground Engineering, May, vol. 32, no.5, pp 30-34.

WITHERS, N.J., HOWIE, J., HUGHES, J.M.O. and ROBERTSON, P.K. (1989)
Performance and Analysis of Cone Pressuremeter Tests in Sands, *Géotechnique* **39**, No. 3, pp 433-454.

WINDLE, D. (l976).
In situ testing of soils with a Self-boring Pressuremeter, PhD Thesis University of Cambridge

WINDLE, D. and WROTH, C.P.(l977)
The Use of a Self-boring Pressuremeter to determine the Undrained Properties of Clays. *Ground Engineering*, September.

WOOD, D.M. and WROTH, C.P. (l977)
Some laboratory experiments related to the results of pressuremeter tests. Internal Report No. CUED/C Soils TR 32, Cambridge University Engineering Department, also published in *Géotechnique* **27**, pp l8l-20l

WROTH, C.P.(1982)
British Experience with the Self Boring Pressuremeter in Proceedings of the Symposium on the Pressuremeter and its Marine Applications, Paris April l982. Editions Techniq. 75737 Paris Cedex l5.

WROTH, C.P. (1984)
"The Interpretation of In Situ Soil Tests". Twenty Fourth Rankine Lecture, *Géotechnique* **34**, No. 4, pp 449-489